THE COGNITIVE MAP AND COMPARTMENTALIZED SPACE

Neural Representations of Surface Cue Boundaries

by

Chia-Hsuan Wang

A dissertation submitted to Johns Hopkins University in conformity with the requirements for the degree of Doctor of Philosophy

Baltimore, Maryland
May, 2019

Abstract

It is important for us to adjust our behaviors and responses when the same stimulus is received under different environmental contexts. For example, hearing the thunder outdoors, you will probably start looking for a shelter; on the other hand, you may do nothing particular if you hear the thunder from home. The ability to encode and recognize an environment is thus critical for survival. It is believed that the hippocampus is responsible for generating a mental representation, or a 'cognitive map', of the current environment.

While the information encoded by the cognitive map is assumed to be in accord with the real world, accumulating evidence suggests inconsistencies between physical space and its mental representation. For example, the mental distance between two locations can be perceived as longer than the true physical distance if the locations are separated by a boundary. While the neural representation of a compartmentalized environment has been examined in a series of rodent studies, these studies focused on whether similar spatial firing patterns would be observed across perceptually similar compartments. Hence, the physiological basis of the perceptual distortions caused by environmental boundaries is not well understood.

This current dissertation work focused on the neural representation of

environmental boundaries constructed by flat surface cues, and of the space segregated by these boundaries. Concentrations of place field edges recorded from dorsal CA1 and CA3 were observed near the surface boundaries, and the population vectors of firing rates changed more rapidly near the boundaries. We demonstrated that this phenomenon is observed in both 1D and 2D environments, and can be triggered by transitions between surface textures or tape line markings. In the 2D environments, we further showed that the rapid decorrelation of neural signal is observed along the direction perpendicular to, but not in parallel with, the surface boundaries. These results suggest that the locations of the boundaries were encoded by an enhanced decorrelation of the neural representations of locations across the boundaries, which might further explain the distortion effect observed in humans.

Thesis committee: James J. Knierim (advisor), Ernst Niebur (chair), Kechen Zhang (reader), Cinthia F. Moss, and David Foster (prior)

Acknowledgements

One of my childhood ambitions was to write a book, maybe a novel about legends, magic and imaginary creatures. Little did I know the very first book I wrote in my life would be about a tiny part of a rat, based on scientific facts and numbers, and not even in my native language. Although quite different from what I had imagined, writing a book is one of the few childhood ambitions I have fulfilled so far, and it would be impossible for me to accomplish this without the assistance of my advisor, Dr. Jim Knierim. When I first joined the Neuroscience program, the US was completely foreign to me and I had little neuroscience and experimental background back then. Jim has been very patient and investigated a lot of time on me to help me catch up. He equipped me with the necessary knowledge and the right mindset for becoming a competent PhD. There has been a lot of uncertainties and anxiety in graduate school, but because of Jim I was able to overcome those and finish my thesis.

The guidance from my thesis committee was also indispensable. I would like to thank Dr. David Foster, Dr. Cindy Moss, Dr. Ernst Niebur, and Dr. Kechen Zhang for their wisdom and critical advices about the current project, my graduate study and future career. I would like to especially thank Kechen for being the second reader of

the thesis and helping me improve it in great details. Also, I would like to thank Ernst for the mentoring and guidance he provided during my rotation.

I would not be able to collect and analyze the experimental data without the help from the other lab members. They taught me from scratch how to train and record from a rat, how to make hyperdrives, and every single things I need to know to gain data. I would like to thank my colleagues for the academic supports, and more importantly, for their emotional supports which have made the Knierim lab a warm and delightful place. They made me feel that I had got companies fighting the same war during those late working nights. I am lucky to have the chance to work with them and I really appreciate it.

Finally, I would like to thank my family. My mother has been taking good care of herself and enjoying her life since I, her only child, left Taiwan, and hence I could focus on the graduate school. When I was about to give birth to a baby, she flew to and stayed in a foreign country for months so her daughter could keep working on her thesis. She bore with my anxiety and bad temper after labor and took care of the baby and the housework when I was overwhelmed. Same did my husband who took a long parental leave and moved to a foreign country to take care of the family when the baby came. His constant emotional company has always been one of the largest supports that get me through graduate school.

More and more names jumped out and memories flashed back as I was writing the acknowledgement. I wish I had enough time and space to thank all of them but I do not. For those who have shaped and supported me, I would like you to know that you are deeply thanked in my heart even if your names are not listed here.

Table of Contents

List of Figures

Chapter 1: General Background

Our understanding of ourselves, others, and the world are largely based on accumulating memories of events. You would never consider yourself a sentimental man if you forgot how hard you cried over that movie. You would not realize how reliable your friends are if you forgot how they helped you get through the hardest time. You would not know how magnificent nature can be if you forgot your trip to the Grand Canyon. Memories connect us to others and to the world in that no relationships can be built up if memories do not last. However, one can eternally lose the ability to remember an event if a brain structure named the hippocampus is seriously damaged. In the following chapter, we will discuss what the hippocampus is, how it is related to memory, and what other functional roles the hippocampus might play.

1.1 The hippocampus is a phylogenetically primitive cortical area

In mammals, most of the cerebral cortex possesses a six-layered structure with columnarly organized processing modules (Mountcastle, 1997). This six-layered cortex is only seen in mammals. It is called the neocortex since it is more recently developed evolutionarily compared to other parts of the cortex of the mammalian

brain. In contrast, a small proportion of the mammalian cortex has different laminar structures with fewer layers. These atypical cortical areas margin the neocortex and are named allocortex. The neocortex and the allocortex derive from the dorsal and medial pallium respectively. While the embryonic pallial subdivisions are homologous among developing amniote vertebrates, the structures which arise from the medial pallium in different species vary in their morphologies and connectivity. On the other hand, the structures differentiated from the dorsal pallium are relatively conserved across species (Striedter, 1997; Tosches et al., 2018). In other words, the mammalian allocortex is phylogenetically primitive compared to other parts of the mammalian cortex and resemble the corresponding cortical areas of non-mammals. One would guess that the homologous allocortex might be strictly necessary for survival in that it was relatively exempted from evolutionary renovation. This assumption leads to the following questions: what functional role does the allocortex play, and is it true that its homologous correspondents exhibit similar functions across species?

The hippocampus, as an essential part of the allocortex, has received especially extensive attention from researchers of different fields. The hippocampus is a collective term for a set of neighboring cortical areas. However, the term is inconsistently defined and its constituents vary in different literatures. In this thesis

work, as proposed by Amaral & Lavenex (2007), I reserve the word for the Cornu Ammonis (CA) regions. The hippocampus and its surrounding cortices, namely the dentate gyrus (DG), subiculum, entorhinal cortex, presubiculum, and parasubiculum, are collectively named the hippocampal formation because they are anatomically interconnected and functionally interrelated with each other.

1.2 The anatomy of the hippocampal formation

The gross anatomy of the hippocampal formation is similar across mammals. In primates, the hippocampal formation is buried deep in the medial temporal lobe and lies in the floor of the temporal horn of the lateral ventricle. It is an elongated, c-shaped structure aligned rostrocaudally. In rodents, the hippocampal formation is more curved and vertically oriented compared to primates, and it extends from near the septal nuclei, bending over and behind the thalamus, into the temporal lobe (septotemporally) (Figure 1-1). Different areas of the hippocampal formation can be envisioned as adjacent bands extending along the longitudinal axis of the structure (the rostrocaudal axis of primates and the septotemporal axis of rodents).

On the transverse plane, different components of the hippocampal formation are aligned in a signature interlocking fashion (Figure 1-2). The molecular and granule cell layers of DG are folded into a “U” or “V” shape, clinching one end of the hippocampus, which extends outside of the DG blades, bends around the upper

blade, and transitions to the subiculum. Along the cell layer of the hippocampus (the transverse axis), the site closer to the DG is considered more proximal, while the site closer to the subiculum is more distal. From distal to proximal, the hippocampus comprises a series of cytoarchitectonically distinct *Cornu Ammonis* (CA) subfields:

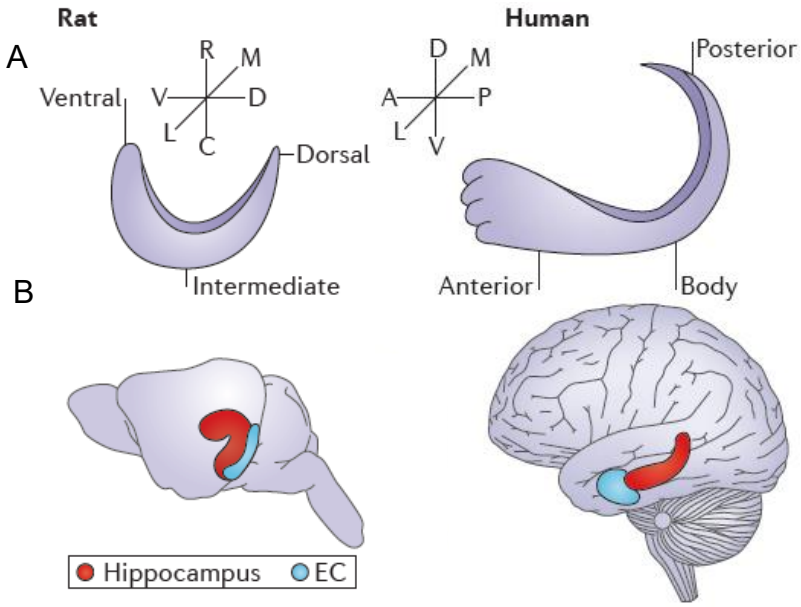

Figure 1-1 Schematics of the orientation of the hippocampus

(A) The shapes and orientations of the rodent and human hippocampi. (B) The relative locations and orientations of the hippocampi and the entorhinal cortices in human and rodent brains. This figure is modified from Strange et al. (2014).

CA1, CA2, and CA3, as named by Lorente de No (1934).

The DG and the CA share the typical characteristics of the allocortex in that they both are tri-laminar structures, and the layers are named distinctively based on the unique compositions of cell types and fibers contained in the layer. In DG, the principal cell type is the granule cell, and thus the principal cell layer is called the granule cell layer. The molecular layer lies superficially to the granule cell layer, and

these two layers encompass a cellular region which is the third layer, the polymorphic cell layer, or the hilus. A granule cell only extends its dendrites superficially to the molecular layer and forms a characteristic cone-shaped dendritic tree there. In the hippocampus proper, the principal cell type is the pyramidal cell, and the pyramidal cell layer is intervened between two plexiform layers, which are further subdivided into several laminae. Deep to the pyramidal cell layer are the stratum oriens and the alveus. Superficial to the pyramidal cell layer are the stratum lucidum, stratum radiatum, and the stratum lacunosum-moleculare. However, the stratum lucidum is distinct to CA3, and the stratum radiatum is immediately superficial to the pyramidal cell layer in CA1 and CA2. The pyramidal cell extends its basal dendrites to the stratum oriens and its apical dendrites to different laminae of the superficial plexiform layer. The inputs to the pyramidal cells are laminae-specific, in that the pyramidal cell receives segregated inputs from different sources or fibers in these different laminae, and the details will be discussed later. Since the layers of the hippocampus proper bend upside-down and wrap around the upper blade of DG, in contrast to other cortical areas, the superficial layers of CA1 and CA2 are farther from the brain surface compared to the deep layer.

The laminar structure is generally similar across the CA fields. However, clear boundaries can be defined (at least in rodents) between different CA fields based on

their cell morphology, intrinsic and extrinsic connectivity, chemoarchitectonic features, and gene-profiles. For example, the size of the pyramidal cell is smaller in CA1 compared to in CA2 and CA3, and the CA2 field appears to have the most compact and narrow pyramidal cell layer along the hippocampus proper. The hallmark of CA3 is the strong recurrent network observed in both the stratum oriens and stratum radiatum. Another characteristic is the existence of the stratum lucidum, which contains the mossy fibers (the axons of the granule cells) conveying information from DG to CA3.

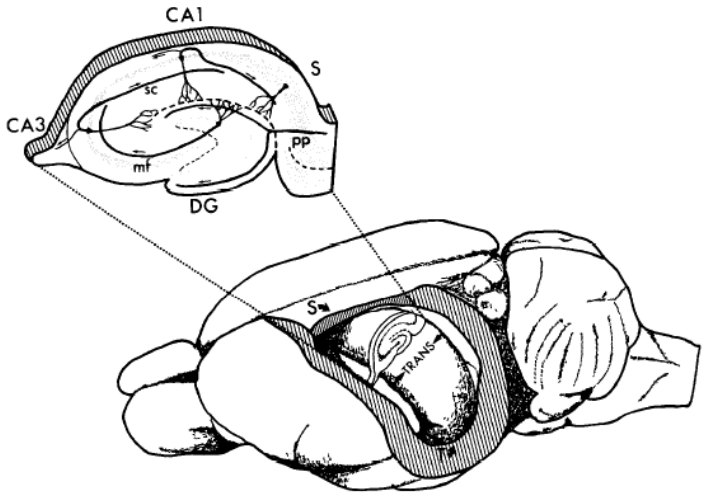

Figure 1-2 Schematic of the gross anatomy of the hippocampus

The bottom right shows the position of the hippocampus in the rat brain. The neocortex overlying the hippocampus is removed in the figure to reveal the hippocampus. The inset is an example transverse plane section and demonstrates the trisynaptic circuit. mf: mossy fibers, pp: perforant path, S: subiculum, sc: Schaffer collaterals. Figure is copied from Amaral & Witter (1989)

1.3 Characteristics of the hippocampal formation

The hippocampus is a unique cortical area not only because it preserves the

ancient cytoarchitecture, but also because the internal information flow is largely unidirectional. While reciprocal connections are usually observed between different cortical areas (Felleman & VanEssen, 1991), unidirectional projections are prevalent within the hippocampus. The DG receives inputs from the entorhinal cortex (EC) through the perforant pathway, and projects outputs to CA3 through the mossy fibers; CA3 further innervates CA1 via the Schaffer collaterals. These three pathways construct the "trisynaptic circuit" (Figure 1-2) (Andersen, 1975). Although accumulating evidence has shown that such one-way circuitry oversimplifies the connectivity within the hippocampus (for example, a small number of CA3 cells project back to the DG; Kneisler & Dingledine, 1995), the strong unidirectionality is still a crucial feature of the hippocampus.

Besides the internal unidirectional circuit, the connectivity between the hippocampal formation and other cortical areas further distinguishes the hippocampus from the other parts of the brain. The hippocampus receives information from and sends information back to all the major association areas of the cerebral cortex through the EC. In contrast to the primary sensory areas, the outputs of the association areas are highly-processed. For example, while neurons in the primary visual cortex are tuned to basic visual elements such as oriented line segments, neurons in the association areas are triggered by more sophisticated

stimuli, like faces or objects. The major input to the hippocampal formation thus contains highly processed information in different modalities. Such information is transferred to the superficial layers of the EC, and the processed information is transmitted primarily to the DG. The CA1 projects the major hippocampal outputs to the subiculum and the deep layers of the entorhinal cortex, from where reciprocal feedback is sent to the source cortical areas.

Another characteristic of the connectivity of the hippocampal formation is that the projections are topographically and laminarly organized. The lateral entorhinal cortex (LEC) projects to the superficial third of the molecular layer and the medial entorhinal cortex (MEC) projects to the middle third of the molecular layer of DG, while the interneurons in the polymorphic cell layer receive inputs from and send feedback to the granule cells. For the CA areas, the EC directly innervates the stratum lacunosum-moleculare, while the CA3-CA3 recurrent network and the CA3-CA1 Schaffer collateral connections reside in the stratum oriens and the stratum radiatum, and the DG-CA3 mossy fiber ends in the stratum lucidum. The distal CA3 receives DG inputs mostly from the upper blade of DG, and projects to the proximal CA1, which relays the outputs to the distal subiculum and MEC; while the proximal CA3 receives outputs from both the upper and lower blades of DG, and projects to the distal CA1, which relays the outputs to the proximal subiculum and

LEC. Such connectivity patterns imply that there might be parallel processing streams within the hippocampal formation, and the information from different cortical sources might not be entirely intermixed during the processing procedure.

1.4 Different functions of the hippocampal formation suggested by studies in different species

The evolutionally conservative nature and the characteristic connectivity of the hippocampal formation imply that it is anatomically positioned for the generation of memory: Memory can involve information in all types of modalities; the hippocampus is the confluence of the processing streams of different sensory systems, and thus provides a platform for information in different modalities to be integrated. Memory is believed to be stored among the cerebral cortices in a distributed way (Attneave & Hebb, 1950; Lashley, 1950); the neocortex-hippocampus-neocortex circuitry routes the sensory information back to the cortical source after being processed by the hippocampus. Physiologically, the synapses in almost all the major pathways within the hippocampus are highly plastic in their configurations and transmission efficacy. The ability of these synapses to be modified swiftly upon receiving a high-frequency stimulus train can assist recording and retaining new information. Furthermore, when it comes to experiences in life, memory can be formed without a repetitive learning process. As a potential

underlying physiological mechanism, potentiation of neural activity in CA1 and CA3 has been found to be triggered by a single trial event (Bittner *et al.*, 2015; Monaco *et al.*, 2014). These characteristics suggest that the hippocampus may play a crucial role in memory formation, and direct proof of such correlation comes from human amnesia studies.

Memory deficiencies were observed in patients with impaired hippocampi. H.M. is the earliest and the most influential case which directly demonstrated the connection between memory and the medial temporal lobe (MTL) in humans (Scoville, 1954). H.M. underwent bilateral resection of MTL for epilepsy treatment. Although the surgery successfully relieved his epilepsy, he was unable to form new memory about facts and episodes experienced after (anterograde amnesia) and right before (anterograde amnesia) the operation, even if his memory long before the surgery remained intact. He could remember materials for a short period, but the memory vanished once he got distracted. His memory deficit was regardless of sensory modality or mode of response. Also, there was no obvious change in his personality, general intelligence, or sensory perception (Corkin, 1984; Milner *et al.*, 1968; Scoville & Milner, 1957). Interestingly, he was able to obtain new skills even though he could not remember himself learning the task. His performance was comparable to normal subjects when trained to draw lines along the contours of

complex figures by looking at the images of the figures in the mirror (Milner, 1962), or to recall primed words (Postle & Corkin, 1998) or images (Gabrieli *et al.*, 1990). Similar amnesia has been observed in other MTL resection patients if the hippocampus was removed. These studies suggest that under certain circumstances, the human hippocampus is required for the development of long-term declarative memory (i.e., memory that can be brought to consciousness and verbally described, such as memory of an event or general knowledge of facts) (Ryle, 1949).

These pathological studies stimulated neuroscientists to produce animal models for amnesia by lesioning the hippocampal areas. Surprisingly, the early attempts to replicate the amnesia results on nonhuman animals failed, in that in many cases the lesioned animals were able to perform tasks that appeared to be memory-dependent. For example, in discrimination tasks where one pair of stimuli (e.g. brightness, objects, visual pattern, or tactile stimuli) was presented simultaneously, with only one of the stimuli associated with reward, the lesioned monkeys were capable of remembering the valence of the stimuli and selecting the rewarded stimulus (Orbach *et al.*, 1960). Even William Beecher Scoville, who performed the resection of MTL on H.M., failed to obtain consistent results when he replicated the same operation on monkeys (Correll & Scoville, 1965a, 1965b). Similar discrepancies were also observed in the rat literature (Kimble, 1963). The inconsistency leads to the question

of whether human and nonhuman hippocampi are functionally equivalent or similar, and if not, what the function of the nonhuman hippocampus might be.

In parallel with the lesion studies, a series of spatial units had been found within the rodent hippocampal formation. In 1971, O'Keefe and Dostrovsky discovered place cells in rat hippocampus. These neurons are activated whenever the animal is within a preferred location (the place field) in a given environment, and such activity is not tied to individual sensory cues in the environment (O'Keefe, 1976). The head-direction cells were subsequently discovered in presubiculum and related areas (Taube *et al.*, 1990). The head-direction cell fires whenever the animal's head is pointing in the preferred direction. Such direction tuning is allocentric, that is, the angle is defined based on the environmental frame, and the preferred directions at different locations of an environment are parallel rather than converging with each other. The grid cells were discovered in the MEC in 2005 (Hafting *et al.*, 2005). These cells have a unique hexagonal firing structure in that their firing fields construct the vertices of a regular grid of equilateral triangles. Finally, the boundary-vector cells found in the subiculum (Lever *et al*., 2009) and the border cells in MEC (Savell *et al.*, 2008; Solstad *et al.*, 2008) fire at a fixed distance and direction to orientation-specific environmental boundaries such as platform edges and internal walls. Similar neural correlates have also been found in humans

(Ekstrom *et al.*, 2003; Horner *et al.*, 2016; Jacobs *et al.*, 2013; Lee *et al.*, 2018). These findings reveal the spatial function of the hippocampal formation and imply that the hippocampal formation might be integral for spatial representation and navigation.

1.5 Concerns about methodology when comparing the results across species

The discovery of the spatial units suggested a new candidate function of the hippocampus: the rodent hippocampus, unlike human hippocampus, is dedicated to processing spatial information(Hartley *et al.*, 2014; Moser *et al.*, 2008). There are anatomical and physiological differences between the human and rodent hippocampi, and it is plausible that such evolutionary differences have translated into functional differences. However, as mentioned previously, the human and rodent hippocampi are homologous structures, and are in general similar in their architectures. Also, the physiological properties of individual neurons inside the hippocampal system are comparable in these two species. Multiple possibilities have been proposed to explain the discrepancy between the human amnesia and rodent lesion studies, presuming a functional consistency across species.

One potential confound causing the discrepancy is that the lesion locations in rodents did not accurately correspond to the damaged areas of amnesia patients. The

hippocampal formation is composed of a group of functionally related subareas. While the resection of H.M. removed all of these subareas completely or in part, the lesion sites of some of the rodent studies were limited to certain subareas. It has been shown that damage to different subareas within the hippocampal formation can cause different components of the amnesia seen in H.M. while leaving the rest intact (Zola-Morgan *et al.*, 1989). The inconsistency in lesion locations across different rodent studies thus accounted for some of the incongruity observed between the human and rodent data.

The second possibility lies in the dissimilarity in the task design. Since nonverbal animals cannot follow instructions nor state the content of their memory, it is necessary to design comparable behavioral tasks that are ostensibly similar to the tasks applied to humans. Even if the behavioral tasks taken by animals appear to be counterparts to the nonverbal tests for humans, the strategies used by the animal to solve the tasks might be substantially different, and thus the demands placed on memory by the tasks would be different. Take the discrimination task performed on monkeys (Orbach et al., 1960, described on p. 18). Gaffan pointed out that the ability to gradually learn an association between a stimulus and a reward or a response through many trials is more like 'habit' learning (Gaffan, 1972). Such learning depends on the basal ganglia (Malamut *et al.*, 1984; Teng *et al*., 2000) rather than

hippocampus and is spared in amnesia patients with impaired hippocampus. On the other hand, the ability to recognize a stimulus from prior experiences is generally impaired in the amnesia patients. Gaffan argued that the task should directly examine whether the animal is aware of the prior occurrence of a stimulus, and proposed using the 'delayed matching to sample (DMTS)' task with a large pool of object samples to study amnesia (Gaffan, 1974).

The proposed DMTS task contains two phases: the sample phase and the choice phase. In the sample phase, the monkey is presented with a novel object on its own, and the monkey needs to displace the object to retrieve reward. The choice phase follows after a variable delay, after which a second novel object is presented simultaneously with the one just seen in the sample phase. Again the monkey needs to displace the object displayed in the sample phase to retrieve reward. While the DMTS task seems to resemble the task used in amnesia patients, the matching rule can be confusing in that the monkey needs to displace the 'novel' object in the sample phase but the relatively 'familiar' object in the choice phase. Mishkin and Delacour (1975) thus developed the 'delayed nonmatching to sample (DNMTS)' task in which the monkey learns to displace the 'novel', or the 'nonmatching', object in the choice phase instead. Although controversial results have also been reported (Ringo, 1991), both monkeys (Alvarez *et al.*, 1994; Overman *et al.*, 1990) and

rodents (Clark *et al.*, 2001) with lesion sites similar to H.M. are seriously impaired in learning the DNMTS task, and this task soon emerged as the benchmark task for studying such type of amnesia.

The work by O'Keefe and Conway (O'Keefe and Conway, 1980) also showed how subtle changes of the experimental parameters could alter the experimental results and the corresponding interpretation. In their task, rats were trained to retrieve food rewards at the end of the goal arm of a plus maze. The maze was surrounded by a set of distal cues for orientation. The hippocampus-lesioned rats can perform the task normally when the distal cues were centered at the goal arm, thus acting as "beacons" to the rewards, but they had impaired performance when the cues were dispersed in the environment, even if the compositions of the cue sets of these two configurations were exactly the same. Therefore, modifications of experimental parameters which seem irrelevant to the problem being examined may lead to controversial conclusions.

1.6 A unitary view of the function of the hippocampal formation

Multiple hypotheses of the function of hippocampus focus on features being examined under different task designs and try to bridge the human and rodent work based on the substantial differences in the demands placed on memory by different

tasks. The case study of H.M. showed that despite the serious impairment of memorizing facts and events, his abilities to learn new skills and form habits were intact. The selectivity of the impairment in amnesia patients such as H.M. inspired the development of the multiple memory system theory (Squire, 2004). The theory proposed that memory is not unitary, and there are parallel memory systems in humans dealing with different types of memory (Figure 1-3). Memory that can be verbally expressed is classified as declarative memory (the 'what' memory), which includes semantic memory (memory about facts) and episodic memory (memory about events). Memory that is not describable are non-declarative memory ('how' memory), such as skills and habits. The declarative memory theory suggests that the hippocampal formation supports only declarative, but not non-declarative, memory

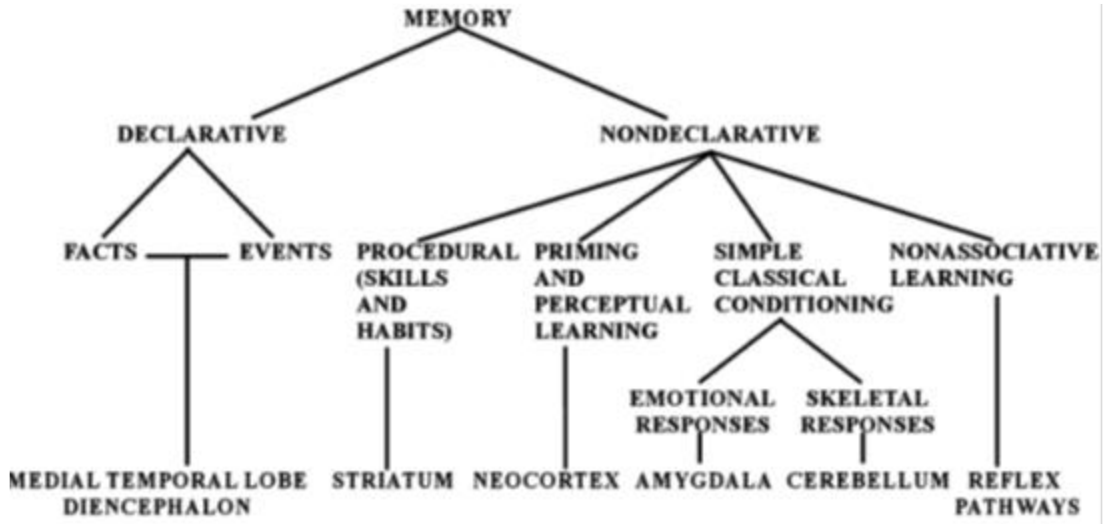

Figure 1-3 Categories of long-term memory

The hierarchical structure of the classifications of different types of long-term memory. Copied from Squire, 2004.

(Squire, 2004).

Eichenbaum and Cohen took this point of view and further generalized it to a 'relational network' model which can also be applied to rodents (Cohen & Eichenbaum, 2008). They proposed that both the human and rodent hippocampal formations are very similar systems, if not the same. The function of the hippocampal formation in both species is to rapidly form associations between its inputs based on the relations between them. Such associations can be flexibly modified, combined, and used in the future, under contexts similar with or different from the condition when the associations were created. The association procedure can be visualized by a graph, on which the nodes denote features, items, events, concepts, or any entities to be associated with other entities, and the nodes are connected based on the relations. Nodes can be linked into chains if there is a sequential relationship, and chains can be merged into networks if there are common

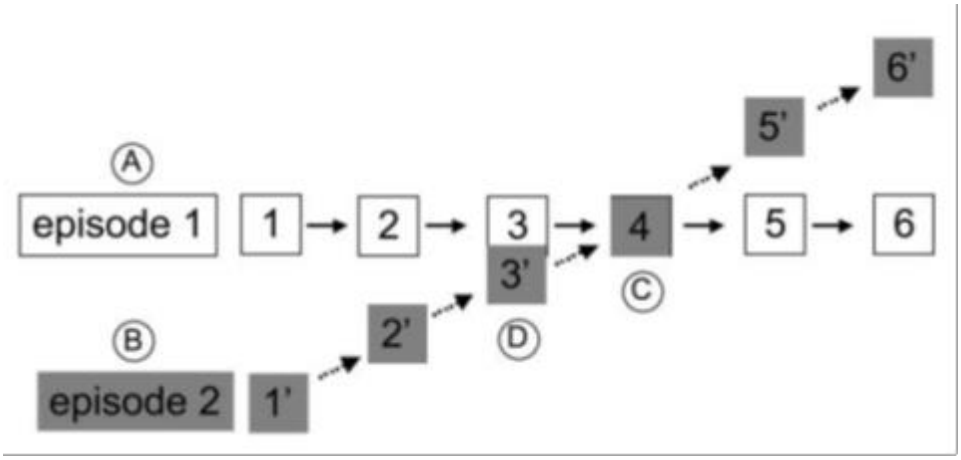

Figure 1-4 Schematics of a relational network example

The figure depicts how two events can be stored based on the relational network hypothesis. Different components of each event are nodes that are chained into a list, and the common elements across different events can be merged and form a network. Figure copied from Eichenbaum, 2004.

elements between different chains (Figure 1-4).

As direct evidence supporting the relational network theory, the work from Bunsey and Eichenbaum (1996) demonstrated that animals are capable of flexibly using associations between arbitrarily-paired stimuli, and such ability is hippocampus-dependent. In their experiment, the rats were exposed to an odor in the sample phase, and in the following choice phase, an 'associate' odor and an unrelated odor were presented simultaneously. The rats needed to learn the odor-odor associations and select the corresponding odor to retrieve food rewards. Both hippocampus-lesioned and control rats were able to form odor-odor associations. However, the control rats were capable of drawing transitive inference (ex: the rat would select odor C after cued by odor A if the association pairs A-B and B-C were learned and odor B was not presented in the choice phase), and symmetric inference (selecting odor A if cued by odor B once the A-B association was learned) from learned associations, while the lesioned animals failed to do so.

To explain the amnesia observed in the hippocampus-impaired patients, the relational network theory proposes that the content of the episodic memory can be represented by chains of events, and the semantic memory can be derived from the common elements shared by multiple episodic memory chains. Since the ability to construct flexible associations is necessary to generate both types of memory, the

hippocampal formation is required for the formation of declarative memory. A similar theory, the configural association theory, also suggests that the hippocampus is responsible for creating associations (Rudy & Sutherland, 1995). However, different from the relational network, it hypothesized that the hippocampus only helps combining related stimuli into a compound stimulus when the specific stimulus configuration is required to stimulate a response. For example, if a rat can achieve rewards when signaled by either a tone or a light , but would get penalty if it responded when the tone and the light are present simultaneously, it cannot solve the task by directly associating either tone A or tone B with the response to receive rewards. Instead, the association between rewards and the tone A-tone B stimulus needs to be created. The configural association theory hypothesizes that the hippocampus is dedicated to constructing such compound stimuli.

The relational network theory suggests that the ability to perform some memory tasks was spared in the hippocampus-lesioned rodents because such tasks did not involve creating flexible associations between entities. As for the O'Keefe and Conway experiment, the hippocampus-lesioned rats were able to find the rewards when the global cues centered near the goal arms, because in such experiments the rats did not need to learn the relationships between the global cues, or the relationships between the cue configurations and the reward location. Instead, the

rats were trained for a stimulus-response learning such that a rigid link was constructed between the locations of some or all of the global cues and the retrieval of food rewards.

Another dominant theory of the function of the hippocampus is the cognitive map theory proposed by O'Keefe and Nadel (O'Keefe & Nadel, 1978). Based on the observation that rats can take novel short-cuts, Tolman suggested that an organism would construct a 'cognitive map' which represents its surrounding environment in an allocentric way, and could be used to devise flexible solutions to variable cognitive tasks (Tolman, 1948). O'Keefe and Nadel extended the idea and further hypothesized that the cognitive map is instantiated by the hippocampal system. According to their theory, there are two information-processing systems in the brain: the locale system and the taxon system. The locale system depicts a physical or abstract space by rendering a coordinate system to define arbitrary locations in the space, and allows the insertions and editions of information on top of the system. It generates a map to represent the space of interest and defines the possible routes that can be taken in the space. On the other hand, the taxon system is responsible for generating instances to be attached to specific locations on the map, and for creating inflexible links connecting instances to form 'routes' on the map. They recognized the hippocampal formation as the essential element of the locale system, and the

taxon system is considered to reside in other brain areas. The ‘cognitive map’ is one of the maps produced by the locale system, and it represents the surrounding physical space at different moments in humans. Since spatial and temporal components are substantial for episodic memory, impairment of the hippocampus would lead to deficits in episodic memory.

O’Keefe and Nadel believed that although the mapping systems and the functions of hippocampus are similar across species, the cognitive map is purely a ‘spatial map’ in rodents. For a task to be hippocampus-dependent, there must be spatial elements involved for rodents, while the same statement is not true for human, and thus comes the discrepancy. Their explanation for the O’Keefe and Conway experiment is that when the global cues were dispersed in the environment, the rats need to learn the locations of the goal arm with respect to the cue configurations. Therefore, the locale system needs to be activated to build a map of the environment for the animal to locate themselves, the global cues, and the goal arm. When all the global cues were clustered near the goal arm, the task is not different from a beacon-learning task; the rat only needs to learn to move towards the clusters of global cues to earn rewards. Such goal-directed routing is implemented by the taxon system, and thus hippocampus is not required for the process.

The indexing theory (Teyler and DiScenna, 1986) further accounts for the

storage and retrieval of episodic memory. This theory assumes that the sensory stimuli involved in a specific episode would establish a memory trace by triggering a specific neocortical firing pattern. Such memory trace activates a subset of the hippocampal neurons, and the co-occurrence of these sensory inputs would strengthen the synaptic connections between these co-activated neurons in the hippocampus. The active set of hippocampal neurons thus serves as a 'memory index' which can project back and reactivate the memory trace recorded in the neocortex in a pattern-completion manner when sensory stimuli related to the episode is reexperienced in the future.

1.7 Comparisons between the dominant theories explaining the function of the hippocampal formation

Apart from the potential confound of lesion loci, both the relational-network and the cognitive map theories suggest that the lesion studies were inconsistent with the amnesia studies not because the functions of hippocampus in rodents and human are fundamentally different, but because the hippocampus is only required for certain types of memory. Imprecise experiment designs do not recruit the hippocampus-dependent memory system and thus lead to dubious interpretations. Both theories suggested that species differences in hippocampal functions reflect differences in the available inputs to the system, but not in the underlying structure

or computational function of the system. Nevertheless, unlike Eichenbaum and Cohen's emphasis on the consistency across species, there are disparities between the human and rodent hippocampal functions proposed by the cognitive map theory. The major difference was mentioned previously that the temporal information is incorporated in the cognitive map in human but not in rodents. Furthermore, the repertoire of the available manipulations over the instances embedded on the map includes more complex and flexible operations in human. O'Keefe and Nadel also suggested that the left human hippocampus serves as a semantic map which is the underlying deep structure of language and is not seen in nonhuman hippocampus. However, none of these differences implicates a substantial difference between the human and rodent hippocampi.

Another major difference between these two theories is that O'Keefe and Nadel suggested that the axes of the cognitive map are purely spatial in rodents, while the relational network is a more generalized model which can be applied to other types of information. The discoveries of hippocampal cells responsive to elapsed time (the time cell, MacDonald *et al.*, 2011) or to tone frequencies (Aronov *et al.*, 2017) suggest that the rodent hippocampal cells can represent a non-spatial axis in a analogous manor to how the place cells represent the spatial axis. The accumulating results are converging towards the direction that the rodent cognitive map is not

merely spatial-based. However, although O'Keefe and Nadel expressed explicitly that the cognitive map only represent things with spatial or spatiotemporal contents, the semantic map proposed in the same theory implies that the mapping system can be generalized and built based on coordinates which are more abstract.

Although the output of the hippocampus would be a network of elements with defined relationships between them according to both theories, the output networks are constructed in distinct ways. In the relational network theory, the hippocampal system is a structure which creates associations: the relational connection between instances are explicitly constructed and combined by the system. In contrast, in the cognitive map theory, the hippocampus is a coordinate system which generates the underlying map and incorporates non-spatial instances (e.g. different objects, landmarks) onto the map. The relationships between the instances are implicitly inferred from the absolute coordinates, but are not explicitly created by the system.

The similarities and differences between these two theories become obvious when one pictures how a physical space with scattered objects would be represented by the hippocampus according to both theories. The relational network suggests that the hippocampus would organize the sensory inputs associated with the abstract concepts, such as 'location A', 'location B', or 'object A', 'object B', into instances, and connect these instances into a network based on their relationships. For example,

‘location A’ would be linked with ‘object A’ by the relationship ‘at’ if object A is located at location A. On the other hand, the cognitive map theory suggests that the hippocampus would generate a coordinate system which paves the space, receives the abstract concept of object instances created by the taxon system, and attaches the instances to the corresponding locations on the map. While in both cases the space is represented by a network, the generation processes are distinct.

The existence of a spatial coordinate system hypothesized by the cognitive map theory is widely accepted in the field nowadays. However, whether the hippocampus only constructs spatial-specific coordinates in rodents (spatiotemporal-specific in human) has been challenged. Since the outputs of the hippocampus suggested by both theories are very similar, it is difficult to examine the correctness of each theory based on current literature. In this thesis work I reserve the term 'cognitive map' for the neural representation of the physical space created by the hippocampal formation. However, one should bear in mind that none of the theories has been verified to elaborate the exact function of hippocampus.

1.8 Anchoring the cognitive map based on the environmental sensory cues

While it is thought that the hippocampus generates a map-like representation of the surrounding environment, an organism does not receive an input that clearly

indicates the absolute spatial ‘coordinates’ of itself, or objects and landmarks in the environment. It is crucial to understand how an organism could manage to infer its current location based on its own idiothetic cues and the environmental sensory cues. In order to understand whether the cognitive map would realign corresponding to systematic changes of the environmental cues (e.g., cues shifting or rotating in the same direction), the firing locations of place cells have been widely examined under different manipulations of different types of environmental cues. The environmental cues can be classified as global or local depending on whether the animal has physical access to the cue; global cues are usually salient visual cues that animals see from a distance, while the local cues are usually the apparatus boundaries or sensory cues placed on the apparatus, and animals can see, touch, sniff, and taste these cues. One issue in the literature has been to understand whether the place field locations would be controlled by the local or global cues, and which one dominates when the cue configurations conflict with each other.

The discussion started when the place cells were first identified by O’Keefe and Dostrovsky (1971). They trained rats to run on an open platform with a homogeneous surface texture, and rotated the platform between sessions to examine whether these cells are encoding a high-level cognitive representation of ‘space’ rather than driven by a particular local sensory stimulus. Since there were minimal

local cues the place cells can react to, and the place fields did not rotate with the apparatus, the authors thus concluded that they are ‘place cells’. The subsequent work from the same lab further demonstrated that place fields were not affected when the arms of a T-maze were interchanged or when the apparatus alone was rotated, but they rotated correspondingly when the apparatus and the global cues rotated together (O’Keefe & Conway, 1978). Similar results were found by Kubie and Ranck (1983) that rotation of a radial eight-arm maze did not change the locations of the place fields. These results imply that the local cues cannot be the sole element affecting the spatial selectivity of place cells, and suggest a dominant role played by the global cues.

However, whether the animal can have physical access to the cues does not seem to be the determinant of whether it can control the orientation of the place cell map. When the animal was placed in a high-walled circular chamber, with a cue card decorated on the apparatus wall polarizing the environment, the locations of the place fields are controlled by the rotation of the chamber (Muller & Kubie, 1987). Besides cue cards on the wall, it has also been shown that objects placed near the periphery of a high-walled circular chamber can control the orientation of the place cell map, but the influence was gone when the objects were placed near the center of the apparatus. These results hold even when the compositions and relative positions

between objects remained the same in both 'peripheral' and 'center' cases (Cressant *et al.*, 1997). These findings suggested that rather than the physical accessibility of the cues, whether the cues are at the edges of the environment area is the key feature distinguishing the 'global' and 'local' cues.

Consistent with this idea, it has been shown that the geometry of the apparatus, which is defined by the apparatus boundaries, can also control the orientation of the place cell map. For example, the rotation of a walled rectangle chamber can lead to place field rotations (Kubie & Ranck, 1983). Behaviorally, a large literature on the "geometric module" demonstrated that human children and other animals use the geometric features of an environment to reorient themselves. When asked to find hidden rewards in a high-walled rectangular environment, human children tended to search at both the correct and the geometrically equivalent locations (Figure 1-5) even when these two locations can be distinguished by non-geometric features such as different visual patterns on the wall (Hermer & Spelke, 1994; Lee & Spelke, 2011). Similar results have also been observed on rodents (in which the phenomenon was first described; Cheng, 1986; Julian *et al.*, 2015; Keinath *et al.*, 2017), birds (Lee *et al.*, 2012; Pecchia & Vallortigara, 2012), and fish (Lee *et al.*, 2013). When place cell activities were recorded during such a task, it was observed that in different trials, the firing locations of place cells coherently switched between geometrically

equivalent locations, and the behavior of the rat (searching for rewards at the correct or the geometrically equivalent location(s)) can be predicted by the orientation of the place cell map (Keinath et al., 2017). Although a series of studies argued that this phenomenon disappeared when examined in a larger environment (Learmonth, Nadel, &Newcombe, 2002; Learmonth, Newcombe, &Huttenlocher, 2001), the geometric module studies suggested that under certain situations, the orientation of the cognitive map seems to be controlled by the environment geometry, or the apparatus boundary.

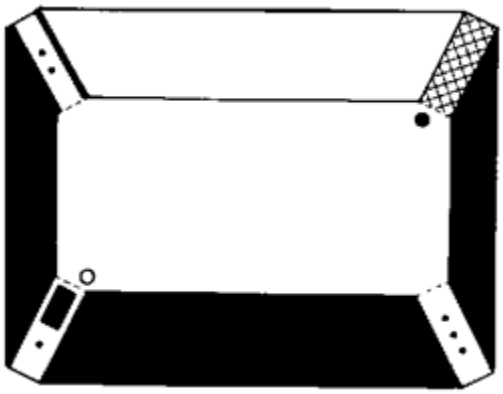

Figure 1-5 Schematics of an example geometric module apparatus
The rats tended to made systematic mistakes at the geometrically-equivalent location (white circle) of the reward location (black dot), even when the four corners of the rectangle box are decorated by distinct non-geometric features. Copied from Cheng, 1986.

Before the 90s, it was thus commonplace to assume that the cognitive map is dominantly controlled by the global cues (or the peripheral cues) compared to the local cues. However, this perspective omitted the fact that the amount and saliency of the local cues had been deliberately diminished in the early studies, and did not

address the inequality in the perceptual saliencies between the global and local cues. Young *et al.* (1994) identified the issue and recorded place cells from a plus maze that had disparate surface texture inserts on each arm as local cues and was placed in an environment with no prominent global cues. The rats were trained to retrieve rewards from the ends of the arms in random order until all differently-textured arms had been experienced exactly once, after which the second bout started. The surface texture inserts of the arms were interchanged immediately after the rat visited any of the arms. Unlike previous studies in which the animals were trained to visit differently-located arms in sequence, this task had no explicit requirement for spatial memory since the rats were trained to memorize the surface cues, instead of the locations of the arms. Young found similar proportions (1/5) of the place cells fired only with respect to the cues or to the locations of the arms, while the majority of cells were controlled both by the conjunction of locations and surface textures. This study suggests that the local cues also exert a substantial influence on the place cells when there were no salient global cues polarizing the environment.

Such surface texture cues were used in following work to examine whether the place cells would be controlled by the local cues or the global cues when both types of cues are equivalently salient and conflict with each other. In order to make legitimate comparisons between the global and the local cues, a series of double

rotation tasks have been conducted in which salient local and global cues coexist in the environment and are rotated in opposite directions in the probe sessions (Brown & Skaggs, 2002; Knierim, 2002; Lee *et al.*, 2004; Shapiro *et al.*, 1997; Tanila *et al.*, 1997). In these tasks, either a plus-maze or a circular track was used, with different surface textures stably occupying different subareas of the apparatus as local cues, and salient visual objects at fixed locations as global cues in each session. Across experiments, a mixture of results has been found: some place fields followed the local cues, some followed the global cues, and some remapped because of the change of the cue configuration. While the heterogeneity and the complexity of the behaviors of place cells make it hard to interpret how the underlying cognitive map is being aligned with the environmental cues in the probe sessions, these results clearly indicate that the local cues can control the orientations of the place fields as strongly as, or even stronger than, the global cues.

Besides the inequality in saliency, the way in which the environmental cues were manipulated might also have affected the interpretation of the relative influence of the global and local cues. Based on the assumption that the influence of the environmental cues over the cognitive map should not be altered by how the cues were manipulated, most experiments examined the influence by rotating, scrambling, or deleting the cues. However, to understand how the cognitive map is anchored to

the environment, it is important to know not only how the map is oriented when the environmental cues rotate, but also whether the cognitive map shifts accordingly when the environmental cues shift. Studies showed that when the apparatus was moved vertically (Knierim & Rao, 2003) or horizontally (Siegel *et al.*, 2008) to different locations within the same room, the locations of the place fields followed the apparatus-based frame, or were dominantly controlled by the local cues. A model proposed by Knierim and Hamilton (2011) further suggested that both the global and local cues affect the firing locations of the place cells, but in different manners. The global cues affect the orientation of the cognitive map, while the local cues decide the translation and scale of the map.

1.9 Conclusions

In this chapter, we reviewed the major literature about the anatomy and the function of the hippocampal formation. We first described that the hippocampal formation is different from the rest of the cortical areas in many aspects. These distinct features of the hippocampal formation make it a prime candidate to be the formation site of long-term memory. The pathological studies of H.M. and other amnesia patients further support the idea. However, the attempt to create an animal model for amnesia failed and different hypotheses have been raised to explain the discrepancies between the human and non-human animal studies regarding the

functions of hippocampus. The arguments have been converging that one of the cross-species functions of the hippocampus is to create a mental representation of space, and people have been studying how the representation of space can be affected by systematically manipulating the environmental cues. In the following chapter, we will focus on a specific type of sensory cues – the boundaries, and introduce the questions to be addressed in this dissertation.

Chapter 2: Specific Background

The discovery of the place cells and the subsequent hypothesis that the hippocampus constructs a 'cognitive map' to represent the physical world raise a series of questions of the encoding mechanism: Among the overwhelming sensory details one can perceive in an environment, what environmental features would be selectively represented by the cognitive map, how is the information represented, and why is the information represented in that way? While diverse sensory features can be observed in different environments, boundaries are one of the few sensory cues that are constantly present in various environments. Boundaries define the realm and the geometry of an environment, and construct the skeleton of a scene. There are even neural correlates dedicated to represent environmental boundaries (Lever *et al.*, 2009; Savelli *et al.*, 2008; Solstad *et al.*, 2008). Therefore, there has been wide interest in how the boundary can affect the cognitive map, the perception of space, and navigation behavior. It is essential to understand how the environmental boundaries are represented by the cognitive map to answer these questions.

However, typical experimental boundaries are barriers that cause discrepancies in the behavior and the visual field of an organism when it is near versus away from

the boundary. Thus it would be hard to dissociate the neural representation of a boundary from any alternations of the neural signal caused by these discrepancies. To deal with this issue, a boundary that is not obstructive and causes minimum change in an animal's behavior and visual field needs to be used, such as a painted line or other flat surface cues. Nevertheless, this leads to another substantial question of whether the obstructive nature is an essential component that constitutes a boundary. In the following chapter, we will review how different types of boundaries can affect the neural representation, perception, and behavior. While boundaries constructed by flat surface cues can distort the perception of space like traditional boundaries, the underlying physiological mechanism is still unknown and it has not been reported yet how a surface boundary might be represented in the cognitive map. The current dissertation work suggests that the surface boundaries are represented by the concentration of place field edges and starts the first step of bridging the gap.

2.1 Peripheral boundaries determine the topography of the cognitive map

The peripheral boundaries that enclose an environment, such as the side walls of a chamber or the curtains surrounding an open platform, play a crucial role in modulating the cognitive map. It was briefly mentioned in the first chapter that sensory cues placed near these boundaries, such as object arrays or cue cards,

dominate in controlling the orientation of the cognitive map. More direct evidence demonstrating the influence of the peripheral boundaries was observed when the same place cell was recorded in environments with different geometries, which were defined by the boundaries. Cases were shown that the spatial relations between place fields and specific boundaries remained the same across a series of rectangular environments (O'Keefe & Burgess, 1996). For example, a place cell that fires at the southwestern corner of a square box could also fire at the southwestern corner of a rectangle box; the distances between the place field and the southern or western walls remained similar in both boxes, as if the firing location of the cell was determined by the locations of the side walls.

Similar results were replicated on the grid cell map (Barry *et al.*, 2007), in that the phase of the grid pattern (the x-y displacement of the grid pattern) was set by the locations of the boundaries. Also, when the environment dilated or compressed, the scale of the grid pattern (the distance between two neighboring peaks) altered correspondingly. Such modulation could be inhomogeneous across the x and y dimension if the environment only rescaled in one dimension. In a tapered environment (e.g., a trapezoid), inhomogeneous grid scale was observed along the tapered direction corresponding to the decreasing width of the environment (Krupic *et al.*, 2015). It was further shown that the grid pattern could be locally distorted

when a small part of the boundaries changed locations and the environment morphed locally (Krupic *et al.*, 2018). While the argument has been raised that the scale changes of the grid pattern reflects overlapping of multiple identically-scaled grid-cell maps anchored to different boundaries (Keinath *et al.*, 2018), the determinant role of the boundaries was not questioned. There is also neurophysiological and neuroimaging evidence suggesting that humans and rodents encode the locations of task-related objects based on their distances to the nearby walls in virtual environments (Doeller &Burgess, 2008; Hartley *et al.*, 2004).

2.2 The neural correlates of boundaries

The Boundary-vector-cell (BVC) model hypothesized how the environmental boundaries might affect the firing location of a place cell (Barry *et al.*, 2006; Hartley *et al.*, 2000; O'Keefe & Burgess, 1996). The model proposed the existence of the BVC, whose firing pattern can be simulated by integrating a series of Gaussian functions. Each Gaussian function corresponds to an environmental boundary extending in the preferred direction, and describes how the firing rate of the BVC would be modulated by the specified boundary in the perpendicular direction. The BVC would fire optimally when the animal was at a fixed distance to an environmental boundary with specified orientation. A place cell may receive feedforward excitatory inputs from multiple BVCs, and its place field would reflect

the intersection zone of the firing fields of the BVCs. The location and scope of the place field can thus be predicted based on the BVC inputs that the place cell receives and the locations and orientations of the environmental boundaries. As strong supporting evidence to the model, the BVC was subsequently discovered in the subiculum (Lever *et al.*, 2009), and the border cell was found in the MEC (Savelli *et al.*, 2008; Solstad *et al.*, 2008). These cells responded to specifically-oriented boundaries regardless of their characteristics (e.g., both high walls and vertical drops could trigger BVC activity) and other environmental cues as predicted (Lever *et al.*, 2009). The majority of BVCs and the border cells observed tended to fire immediate to the boundaries, which is consistent with the findings that place fields tended to concentrate near the edge of a chamber (Hetherington & Shapiro, 1997).

2.3 Internal boundaries segregate space and modulate the cognitive map

Interestingly, the BVC can also be triggered by boundaries in the interior of an environment. For example, a new BVC field would appear upon the insertion of an internal wall if it is placed in the preferred orientation. Also, multiple BVC fields could be observed at a fixed distance and direction to all the specifically-oriented boundaries when an environment is segregated (Lever *et al.*, 2009). These results predict that when parallel internal boundaries segment an environment into multiple

compartments, a place cell might also develop multiple fields at the geometrically corresponding locations within each compartment. Indeed, repetitive place fields were observed in a series of studies that investigated whether and how rodent place cells distinguish similar, connected spatial compartments. The animals were trained to navigate in a segmented environment with perceptually similar or identical compartments, and a significant number of place cells repeated their firing patterns as predicted (Fuhs *et al.*, 2005; Grieves *et al.*, 2016; Nitz, 2011; Singer *et al.*, 2010; Skaggs & McNaughton, 1998; Spiers *et al.*, 2015). Analogous repeating firing patterns were also seen in grid cell maps when rats ran through hairpin mazes (Derdikman *et al.*, 2009) or on early exposure to an environment consisting of two visually identical boxes connected by an external corridor (Carpenter *et al.*, 2015). In these studies, the spatial segregation is represented by periodic elements of the cognitive map, potentially triggered by the BVC system because of the geometrical similarity across compartments. It is unclear whether segmentation information would still be embedded in the cognitive map even when the compartments were not highly repetitive.

2.4 Internal boundaries modulate the perception of space

In the human literature, it has been shown that spatial segregation can exert a strong effect on the memory of the environment. The ‘location-updating’ effect

demonstrates that when human subjects are roaming between different rooms, the memory of objects encountered in the current room decreases when the subjects move to another room (Horner *et al.*, 2016; Lawrence & Peterson, 2016; Radvansky & Copeland, 2006; Radvansky *et al.*, 2011; Radvansky *et al.*, 2010). Also, people were less accurate in distinguishing objects located in geometrically analogous locations across different rooms than distinguishing objects within the same room when tested in virtual environment (Marchette *et al.*, 2017). It was suggested that the mental representation of a segregated space is fragmented, and people need to switch between different local maps in order to load the correct information about the current environment when walking into a different spatial segment.

Spatial segregation can also alter the perception of the environment. Although real-world space (at least locally) is isotropic, with distance varying regularly along each of 3 dimensions, the psychological space can be anisotopic as it is distorted by compartmentalization of an environment. When requested to memorize the locations of objects or landmarks in a compartmented environment, people tended to underestimate distances between targets within the same spatial compartment, and overestimate distances if the targets were in different compartments (Allen, 1981; Hirtle, J; Jonides, 1985; Kosslyn *et al.*, 1974; McNamara, 1986; McNamara *et al.*, 1989; Newcombe & Liben, 1982). Reconstructing the spatial distributions of the

objects based on the estimated distances between objects led to a distorted map of the space (Kosslyn *et al.*, 1974). Similarly, judgment errors in relative spatial relationships increased when two objects were located in different spatial compartments (Greenauer & Waller, 2010; Han & Becker, 2014). These systematic errors imply that the psychological space is not an accurate replica of the physical space. While repetitive spatial compartments are known to trigger periodic spatial firing, whether there is a relationship between the periodicity of the cognitive map and the distortion of the mental representation is still unclear, not to mention how the distortion might be generated by perceptually disparate compartments.

2.5 What essential features constitute a boundary?

Yet another pending question related to these studies is what constitutes a boundary that perceptually segregates an environment. Despite the obvious importance of the environmental boundaries suggested by the previous discussion, little is known about the characteristics that define a boundary. When the BVC was discovered, it was shown that the cell reacts to boundaries with disparate multi-modal features, such as high walls with different surface textures, vertical drops, and a short rim followed by vertical drops (Lever *et al.*, 2009). However, no conclusion has been made whether there is a substantial feature for an object, a flat surface cue, an intersection between surfaces, or any other sensory cue to be

recognized as an effective boundary.

Typical boundaries used in behavioral experiments are opaque barriers which prevent the animal from crossing or seeing through them. There has been wide interest investigating whether the nature of being obstructive, physically or visually, is the decisive feature which distinguishes boundaries from other non-boundary sensory cues. Different types of sensory cues have been shown to be 'effective' boundaries depending on the purpose of the boundary and the exact task performed. If a sensory cue is considered as a boundary based on whether it activates the BVC, then neither the obstruction of movement nor of sight of the animal is essential. For example, the BVC responds to gaps between platforms that the rat could jump over (Lever *et al.*, 2009). Also, the phase of the grid pattern can be reset by transparent walls (Derdikman *et al.*, 2009), and periodic place fields were observed on a spiral track separated by short walls (Nitz, 2011). Nevertheless, these boundaries still altered the movement or the visual field of the animal, and it has not been examined yet whether cues which provide no impediment to navigation, such as 2-dimensional surface marking, can be recognized as a boundary by the BVC.

Even though an environmental cue triggers the BVC system, it does not necessarily mean that the organism is using the boundary to perceptually segregate the environment. Conceptually, objects, local contexts, or any other sensory cues

which can serve as demarcations can be used to perceptually segregate the environment into distinct compartments. For example, a road could be segmented by the locations of the street trees, and different tiling on the floor could define the realm of a kitchen and distinguish it from an abutting dining area. However, in practice, the systematic error in judging the relative distances between pairs of objects was not observed universally. While human children were biased when either low wooden fences or opaque hanging rugs were used to segregate the same environment, human adult subjects were affected only when the boundaries were opaque (Kosslyn *et al.*, 1974). These results suggest that not all the boundaries can be used to perceptually segregate an environment, and the opacity of the barrier might be essential for human adults. Similar results were replicated when the direct distance of each object was estimated (Newcombe & Liben, 1982). However, contrary results have also been reported, in that strings attached to the ground can trigger the distortion effect on human adults regardless of whether the subjects were requested to treat the string boundaries as a physical barrier to movement or not (McNamara, 1986). Therefore, while for human children neither opacity or obstruction seems to be a critical factor determining the perception of spatial segregation, the importance of opacity is still controversial for human adults. The fact that human children and adults can be affected differently by such ‘transparent

walls' also suggests that there might be a developmental factor involved.

Similar questions have been investigated by the geometric module studies. As mentioned previously, the geometric cues of an environment can override the non-geometric cues when human children and animals need to reorient themselves. In the same task, when the walls were replaced by small curbs, the boundaries (i.e., curbs) no longer defined the perceptually and navigationally available environment. Nonetheless, human children and birds still used the geometry of the segment to solve the task (Lee & Spelke, 2011; Lee *et al.*, 2012), suggesting that the spatial segment was recognized as an isolated part of the environment and possessed geometric features. In other words, the curbs were used to segregate the environment. However, when the environments were segregated by a luminance contrast on the floor (e.g., a black rectangle painted on a white floor), human children and chickens no longer made systematic errors at the geometrically equivalent location (Lee & Spelke, 2011; Lee *et al.*, 2012). Consistent with these findings, a human fMRI study indicated that the scene-selective cortices, namely, the parahippocampal place area (PPA) and the retrosplenial cortex (RSC), showed weaker responses when flat surface cues were used to construct the boundaries of a virtual scene, compared to when the boundaries extended into the z axis (Ferrara & Park, 2016). One might conclude from these results that whether the boundary

extends vertically might be a crucial element deciding whether it would be used to segregate the environment. However, information about the presence of geometric boundaries may be dissociated from the use of this geometric information for orientation. The reported inability of organisms to reorient to geometric boundaries defined by flat surfaces does not necessarily imply that the space is not segregated by such boundaries.

2.6 Questions to be answered

To understand whether 2-dimensional surface cues are encoded by the cognitive map, and whether there are signs showing that these cues might be used to segregate the environment, we trained rats to forage on surfaces with perceptually distinct regions demarcated by floor textures or tape line markings. Such 2-dimensional surface cues have been used as local cues to understand how the cognitive map is aligned based on the environmental cues, and it has been shown that scrambling, deleting, or rotating these surface cues can lead to corresponding changes in the cognitive map (Brown & Skaggs, 2002; Knierim, 2002; Lee *et al.*, 2004; Shapiro *et al.*, 1997; Tanila *et al.*, 1997). However, it is still unclear whether surface cues can also serve to construct environmental boundaries. Our results demonstrated that the edges of place fields recorded from dorsal CA1 and CA3 concentrated near the boundaries, resulting in a swift change in the population vectors of firing rates near

the boundaries. We thus concluded that surface cue boundaries caused inhomogeneity of place field maps, and the locations of the boundaries were encoded by an enhanced decorrelation of the neural representations of locations across the boundaries.

Chapter 3: General Methods

In the current chapter we describe the experiment-related details of the subject animals, and the general methodologies used to collect and preprocess tetrode recordings. For task-specific experimental details and analyses please see *Chapter 4:* and Chapter 5: .

3.1 Subjects and surgery

A total of 49 adult male Long-Evans rats were used in this study: 41 rats participated in the double rotation task, 6 rats in the complex-board forage task, and 3 rats in the simple-board forage task (see below for task descriptions). Separate groups of rats were used in different tasks except for one rat that underwent both the complex-board forage task and the simple-board forage task. The double rotation data were previously collected and published for other purposes (Lee *et al.*, 2015; Lee & Knierim, 2007; Lee *et al.*, 2004; Lee *et al.*, 2004; Monaco *et al.*, 2014; Joshua & Knierim, 2014; Yoganarasimha *et al.*, 2006; Yu *et al.*, 2006). The rats were housed individually on a 12/12-h light/dark cycle and all experiments took place during the dark phase of the cycle. The rats had free access to water but were food restricted such that their body weights were maintained at 80-90% of the *ad libitum* level.

For surgical implantation of a microdrive array, the rat was injected with ketamine (60 mg/kg) and xylazine (8 mg/kg), followed by isoflurane inhalation to produce a surgical level of anesthesia. A craniotomy was made on the right hemisphere, and the microdrive array was placed at the center of the craniotomy targeting the dorsal hippocampus. For post-operative analgesia, the rat was administered ketoprofen (5 mg/kg) or meloxicam (1 mg/kg) subcutaneously, or 1 cc of oral acetaminophen (Children's Tylenol liquid suspension, 160 mg) right after the surgery. Further analgesia was either provided on the following two days by meloxicam administered orally or blended in food (Metacam, 1~2 mg/kg), or provided on the following day by a second injection of ketoprofen or by access to diluted acetaminophen in drinking water as needed. All implanted rats received 0.15 ml of enrofloxacin (Baytril, 2.27%) and 30 mg of Tetracycline blended in food daily until termination. All animal procedures complied with U.S. National Institutes of Health guidelines and were approved either by the Institutional Animal Care and Use Committee at Johns Hopkins University or by the Institutional Animal Care and Use Committee of the University of Texas Health Science Center at Houston.

3.2 Electrophysiology and recording electronics

Microdrive arrays that contained 6-20 independently adjustable tetrodes were built for extracellular recordings. Each tetrode was composed of four 12 or 17 μm

nichrome wires, or four 17 μm platinum-iridium wires, twisted together. The tips of the nichrome wires were individually gold-plated to reach 200-500 kΩ impedance measured at 1 kHz. After at least four days of recovery from surgery, each tetrode was advanced gradually per day over 20-40 days until its tip arrived at the hippocampal CA1 or CA3 layers and activities of pyramidal cells were observed while the rat rested on a pedestal.

During recording, the neural signal was buffered by a unity-gain preamplifier and filtered between 600 Hz and 6 kHz by the data acquisition system (Neuralynx, Bozeman, MT). Whenever the electrophysiological signal passed a threshold between 50-70 μV, a 1 ms segment was extracted at 32 kHz and stored as a spike waveform. To track position, the head stage was equipped with protruding arms extending backwards or to the sides of its head. Red and green light emitting diodes (LEDs) were attached to the arms to track head position and direction, captured at 30-60 Hz by cameras mounted on the ceiling.

3.3 Single-unit isolation

Single units were isolated offline with customized spike-sorting software (Winclust, Knierim). For each tetrode, the putative spikes were displayed as points in a multidimensional waveform parameter space, and the points were manually clustered primarily based on the relative spike amplitudes and energy simultaneously

recorded from individual wires of the tetrode. The isolation quality was subjectively rated on a scale of 1 (very good) to 5 (poor), representing the extent to which a spike cluster could be separated from other clusters and noise. The ratings were completely independent of any spatial or behavioral correlates of the unit. Units categorized as 4 (marginal) or 5 (poor) were excluded from analyses.

To ensure that we did not artificially inflate the sample size by repetitively sampling the same units across multiple sessions, for each tetrode we only included the day with the largest number of place fields recorded. When repeated sessions were presented in the same day, we only included the cell-session with the highest within-field mean firing rate of the day in our analyses.

3.4 Histology

After the experiments were complete, the rats were anesthetized with 1 cc of Euthasol and were transcardially perfused with saline followed by 4% formalin. In some rats, a subset of tetrodes was selected to pass current and create marker lesions 24 h before perfusion. After perfusion, the cranium was partially opened and the brain was exposed to formalin for at least 4 h with the tetrodes in place to preserve the tracks of the tetrodes. The brain was extracted and soaked in formalin for 12 h before transfer to a 30% sucrose formalin solution (wt/vol). After the brain was frozen, it was sectioned at 40 μm in the coronal plane and stained with 0.1% cresyl

violet. Recording locations of the tetrodes were assigned by matching the identified tetrode tracks on the brain slices against the known configurations of the microarrays and marker lesions, if any. For the tetrodes targeting the CA1 and CA3 layers on different recording days, depth reconstruction of the tetrode tracks was performed for each recording session to identify the brain region from which the units were recorded.

Chapter 4: Representation of Surface Boundaries in a 1-D Environment

A large number of tetrode recordings had been collected in previous studies from our laboratory (for the methodologies used please see Section 3.2 *Electrophysiology and recording electronics*) as the rats foraged on a circular track covered with different surface texture patches. In order to investigate how a compartmentalized environment is represented by the cognitive map when the separation was defined by flat surface cues, we analyzed these previously collected and published data, and observed that place field edges concentrated near the surface boundaries. The concentration of field edges further enhanced the decorrelation between neural representations of space across the surface boundaries. These results suggest a novel neural coding mechanism in representing environmental boundaries.

4.1 Methods

4.1.1 Double rotation protocol

Forty-one rats were trained to run clockwise on a circular track (76 cm O.D., 10 cm wide) to collect food pellet rewards placed at arbitrary locations on the track. On average, the rats obtained ~2 rewards/lap, but this varied across rats and sessions as

needed to promote good performance. The recording sessions started after the rats learned to continuously run on the track with few pauses (~1-2 weeks of pretraining). Before the recording session, the rat was disoriented (by being placed in a covered box and walked a number of cycles around the apparatus) and placed at an arbitrary starting location on the track. The same food reward schedule was used as in the training sessions and the session ended after the rat finished ~15 laps around the track. In both training and recording stages, whenever the rat turned around and moved counterclockwise, the experimenter would block its path with a piece of cardboard until it turned back and resumed the clockwise movement. The experimenter also discouraged grooming behavior by snapping fingers or activating a hand-held clicker when the rat paused to groom.

The quadrants of the circular track were covered by differently textured surfaces which served as local cues, starting from 12 o'clock and in the clockwise direction: a gray rubber mat with a pebbled surface, brown medium-grit sandpaper, beige carpet pad material and gray duct tape with white tape stripes (Figure 4-1, Knierim, 2002). The track was placed in a circular, curtained environment (2.7-m diameter) in which six distinct objects were present either on the floor or on the curtain as global cues. For the standard (STD) sessions, the local and global cue configuration was maintained as during training. For the mismatch (MIS) sessions,

the global and local cues were rotated clockwise and counterclockwise, respectively, to achieve total cue mismatches of 45°, 90°, 135° or 180°. Each day of recording consisted of either 5 sessions, with three STD sessions interleaved with two MIS sessions, or 6 sessions, identical with the 5-session day except for an additional STD session at the start. The mismatch angle for each MIS session was pseudo-randomly selected such that each angle was experienced once during the first 2 days and once again during the second 2 days. For most of the rats there were four days of recording, but for a small proportion of rats there were over 10 recording days. We used only the first four days of recording of each rat to balance the data.

Figure 4-1 Double rotation task

Top-down schematics of the double rotation experiment sessions. Local textures on the track are denoted by the different patterns of the inner ring. Global cues are denoted by shapes on the black outer ring representing the black curtains surrounding the track. In this example, 180° (session 2) and 45° (session 4) mismatch sessions were interleaved with 3 standard (STD) sessions.

4.1.2 Spatial cell filtering

A linear classifier based on the average firing rate and spike waveform width was applied to units with isolation qualities in category 1 to 3 (See *Chapter 3*

Single-unit isolation) to select and exclude the putative interneurons, which have narrower waveforms and higher mean firing rates than principal cells. Units that were identified as interneurons by the experimenter during spike sorting were also excluded. The remaining cells were classified as putative pyramidal cells, and they were included in quantitative analyses if they fired at least 30 spikes during forward movement. For all analyses (unless noted otherwise), data were discarded when the rat's speed was less than 10°/s, in order to prevent contamination of the results by nonspatial firing that occurs during immobility.

The standard Skaggs spatial information measure (Skaggs *et al.*, 1992) tended to produce false negative errors when applied to 1-dimensional data (Monaco *et al.*, 2014), and thus we also incorporated the Olypher spatial information score (Olypher *et al.*, 2003) to compensate for the Skaggs measure (Monaco *et al.*, 2014). The statistical significance of both Skaggs and Olypher measures were computed by temporally shifting the spike trains to construct the control distribution. Since the rats were trained to run continuously on a circular track, the temporal sequences of the rat positions were quasiperiodic, and thus we additionally reversed the spike trains before the time-shifting procedure to break the regularity and prevent creating false negative results (Monaco *et al.*, 2014). For the putative pyramidal cells with enough spikes, cells were further analyzed if the Skaggs score was larger than 1.0

bits per spike or the Olypher score was larger than 0.4 bits, and the score was > 99% of the scores from the shuffled data.

4.1.3 Place field detection

The average firing rates were calculated as the spike counts divided by the occupancy durations within each track-angle bin (1°), and the firing rate vectors were circularly smoothed with a Gaussian kernel with standard deviation 4.3°. Putative place fields were isolated by thresholding the smoothed firing-rate vectors at 10% of the unit's maximum firing rate and grouping the contiguous bins with firing rates larger than the threshold. Putative fields separated by only 1 track-angle bin were merged. After merging, the fields that had maximum firing rate > 1.5 Hz and that were 15°–330° long were included in the following analyses. The large upper bound was chosen based on the observation that a small number of putative pyramidal cells fired almost all over the track but they were silent within a small gap. The median place field size was 60° with interquartile range (IQR) 38° (Q1 = 42° and Q3 = 80°) for CA1 fields, and was 73° with IQR 62° (Q1 = 44° and Q3 = 106°) for CA3 fields; only two fields were larger than 270° (Figure 4-2). The starting and ending edge location of the place fields were defined as the starting and ending track angle bins, respectively.

4.1.4 Cross-correlograms

We constructed population firing rate cross-correlograms to visualize the similarities between the place cell population activity recorded at different track locations. Place cells were identified and their firing-rate vectors were calculated and smoothed as described in the 1D place field construction section. Vertically stacking the transposed firing-rate vectors formed an N-by-360 population firing rate matrix, where N is the number of units used to construct the matrix. The i^{th} row of the matrix was the firing-rate vector of the i^{th} unit, and the j^{th} column of the matrix was the population vector (PV) of firing rates at the j^{th} track-angle bin. The term PV has been used to describe the resulting vector sum of the preferred movement directions of individual cells in previous studies (Georgopoulos *et al.*, 1986), and each element of the PV represents one of the three dimensions of a physical space, However, for here and throughout this thesis, PV refers to the vector of neural activities, with each element representing the average firing rate of a neuron. The cross-correlogram was constructed by calculating the Pearson correlation coefficients between pairs of PVs. The (i^{th},j^{th}) element of the cross-correlogram was the correlation between the i^{th} and j^{th} column of the population firing rate matrix (Lee *et al.*, 2004; Neunuebel *et al.*, 2013). To balance the activity strengths across different units, we reported the normalized cross-correlograms in which the firing-rate vectors of individual units

were divided by their maximum firing rates before being stacked together.

4.1.5 Place field edge distribution

To examine whether the place field edges concentrated near the local-cue boundaries, we defined 30° wide zones centered on the local cue boundaries as the local-cue windows and calculated the proportions of place field edges located within the windows. Both field shuffling and bootstrap techniques were used to test whether the proportions were significantly higher than chance level.

For the shuffling test, the place field locations were randomly rotated while the field sizes remained the same. For each field the rotation angle was randomly selected from [0°, 360°) and the in-window field edge proportion was calculated based on the rotated field edge locations across the population. This shuffling procedure was performed 1000 times. The distributions of the shuffled in-window field edge proportions simulate the expected distributions assuming the fields were randomly scattered on the track. The result was significant if the percentage of the shuffled samples that were larger than or equal to the observed in-window field edge proportion was smaller than 0.00625 (significance level $\alpha = 0.05$, two tailed with Bonferroni correction for 4 comparisons).

To bootstrap the data, we randomly resampled with replacement the same number of place fields as the original set 1000 times. In each trial the bootstrapped

in-window field edge proportion was calculated to construct the bootstrap distributions. The observed in-window field edge proportions were then compared against the confidence intervals of the bootstrap distributions.

4.1.6 Control for head-scanning and pausing behavior

To verify that the field edge concentration effect was not a result of head-scanning or pausing behavior interfering with the place field detection algorithm, we excluded nearby data when a scan or pause was detected (see Monaco *et al.*, 2014) near or within a place field. For each place field a window that was 15° wider than the field on both sides was defined. If a scan or pause started within the window, we removed the behavior and spiking data of that traversal through the window. After the same removal process was performed on every field, we excluded the cell-sessions if, for any part of the track, no data were left after the deletion. We detected place fields and constructed the field edge distributions based on the filtered data following the same procedures described in the previous sections.

4.2 Results

4.2.1 Place field edges coincided with the local cue boundaries

We collected extracellular tetrode data from the CA1 and CA3 pyramidal cell layers of the hippocampus while rats moved clockwise around a circular track in a double rotation task (Figure 4-1). The quadrants of the track surface were covered by different texture patches (local cues), and objects were placed on the surrounding curtains or on the floor (global cues) (Knierim, 2002). For both standard (STD) and cue-mismatch (MIS) sessions, place fields covered the entire track with no obvious tendency to concentrate at specific locations (Figure 4-2), and no obvious changes of population average firing rates was observed near the local-cue boundaries (Figure 4-3).

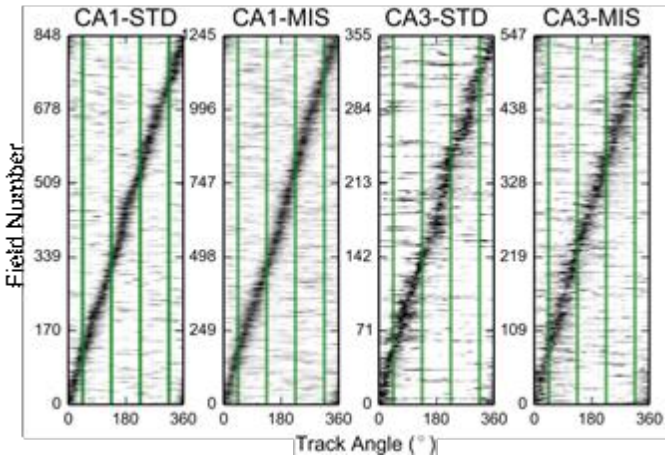

Figure 4-2 Sorted firing-rate maps of all the place fields included in the analyses

The abscissa of the map is the track angle (in degree) and each row of the map is the firing-rate map of a unit. The locations of the local-cue boundaries are denoted by the green lines. The rate maps were normalized by the peak firing rates of each unit and were sorted by the circular centers of mass of the fields. The same rate map is included in the figure multiple times if the place cell had multiple place fields.

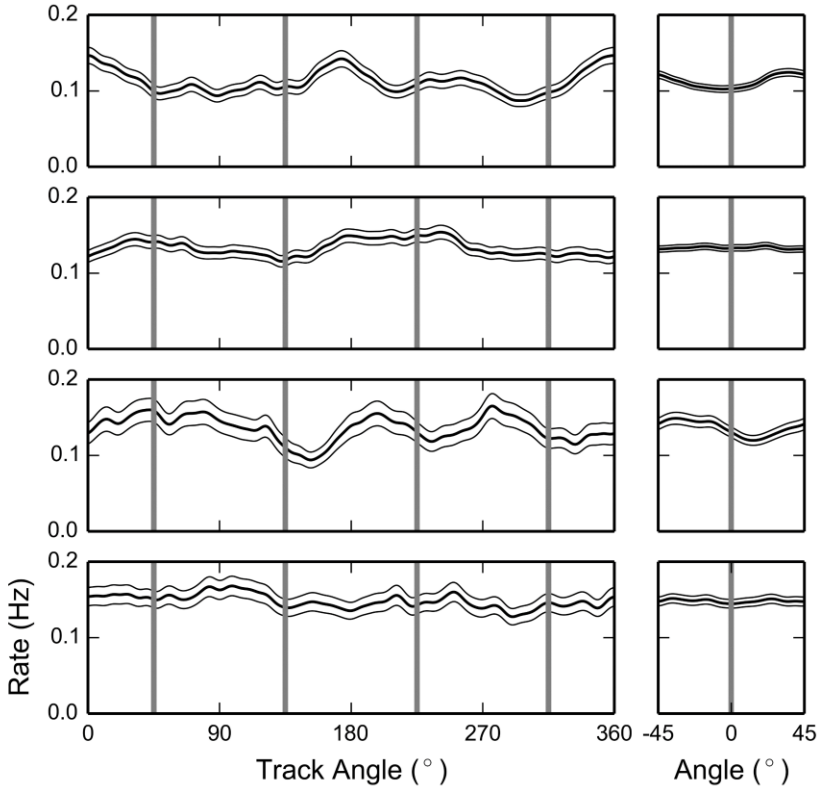

Figure 4-3 Population firing rates did not change robustly near the local-cue boundaries
(A) The population firing-rate maps. The smoothed firing-rate maps of different units were normalized by the peak firing rate of each unit and stacked together. The mean firing rates across units were calculated and denoted by the thick black curve, and the standard errors denoted by the thin curves. The abscissa of the map is the track angle (in degrees). The gray lines indicate the locations of the local-cue boundaries. There is no clear evidence of changes in mean firing rates at the local-cue boundaries. (B) Local population firing-rate maps near the local-cue boundaries. To further examine whether the population firing rates consistently increased or decreased near the local-cue boundaries, the behavior and spike data were binned based on their relative locations to the closest boundaries, and the mean firing rates were calculated. The abscissa of the map is the relative location to the local-cue boundary (in degrees), and the mean firing rates were denoted by the black curves. The gray lines label position 0.

Although many place fields crossed local-cue boundaries or fired at a distance

from them, there appeared to be a disproportionate number of fields with edges near the local-cue boundaries (Figure 4-4). To illustrate this phenomenon, we constructed cross-correlograms of the population vectors (PVs) of firing rates (Figure 4-5). The width of the diagonal band reflects the distance the animal has to travel before two locations are represented by uncorrelated population activity. The diagonal bands became narrower near the locations of the local-cue boundaries (especially in CA3), indicating a more rapid change in the population activity near the boundaries.

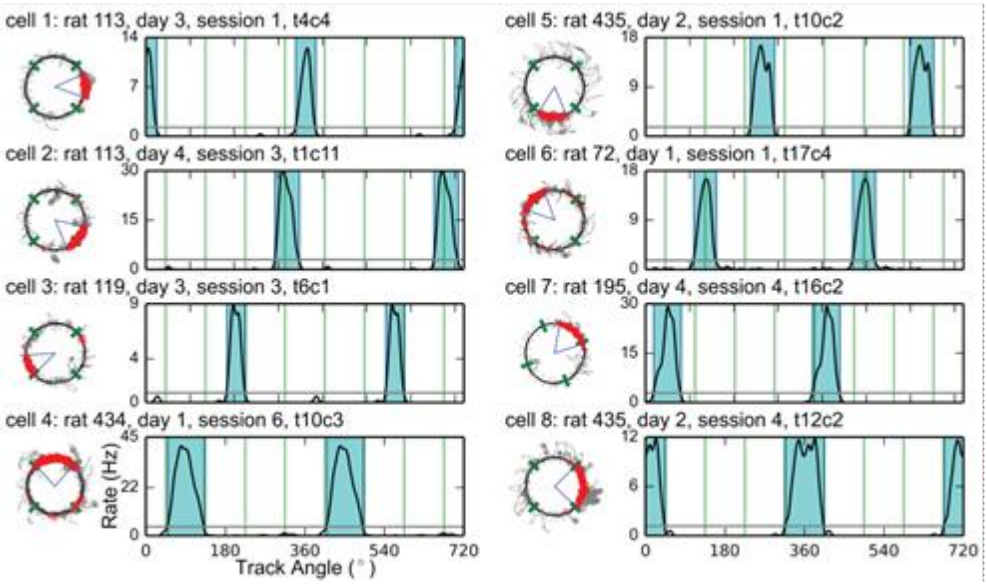

Figure 4-4 Examples of different types of place fields

The trajectory-spike plots and the linearized firing-rate maps of the example place fields observed in CA1 (left, cell 1–4) and CA3 (right, cell 5–8). The blue-shaded areas represent the range of the place field, and all rate maps are duplicated and concatenated in order to show fields crossing 0°. The local-cue boundaries are labelled by green lines in both plots. Fields confined within a texture quadrant (cell 1 and 5) or fields crossing local-cue boundary(ies) (cell 2 and 6) could have no edges close to any of the local-cue boundaries and seemed irrelevant to the boundaries. However, many fields had edges located near the local-cue boundaries. The fields either had only one edge near the boundaries, spanning across multiple quadrants or confined within one quadrant (cell 3 and 7), or occupied one or multiple quadrant(s) and had both of their edges near the boundaries (cell 4 and 8).

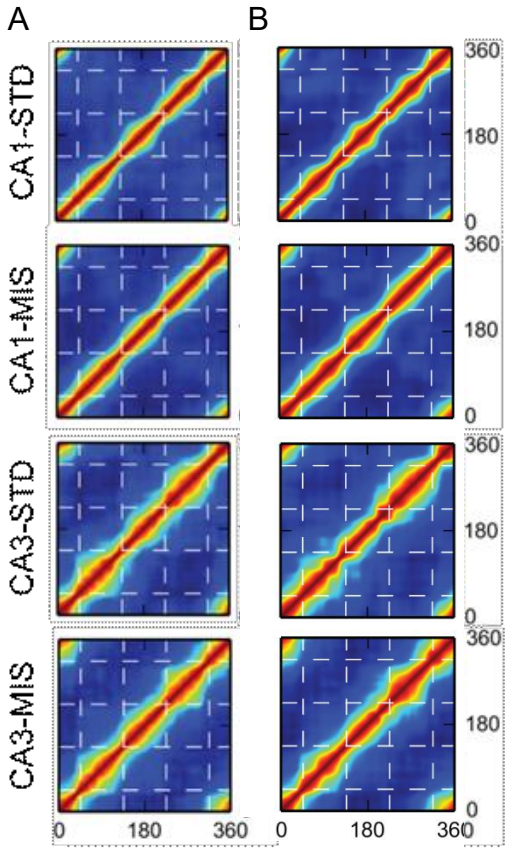

Figure 4-5 The cross-correlograms of the PVs (A) The narrowed pinch points of the diagonal band near the local cue-boundaries (dashed lines) shows that the PVs changed more rapidly across the boundaries than across similar distances within a texture quadrant. The firing-rate maps were normalized by the peak firing rates before constructing the cross-correlograms. (B) The same as A except that the firing-rate maps were not normalized.

To statistically determine whether more place field edges than expected by chance were located near the local-cue boundaries, we created histograms of the locations of the field edges (Figure 4-6, left column). The proportions of field edges located ± 15° from the local-cue boundaries were significantly greater than shuffled distributions (Figure 4-6, middle column, for all session types, $p < 0.05$, two-tailed, Bonferroni corrected for 4 comparisons). To provide further support, we performed a bootstrap analysis by randomly resampling the fields with replacement and calculating the field edge proportion of the re-sampled fields for each bootstrap trial. Since the local-cue windows occupied 1/3 of the track area, we expected to see bootstrapped distributions centered near 1/3 under the null hypothesis of a

homogeneous distribution. However, all the bootstrapped field edge proportions were greater than 1/3 (Figure 4-6, right column, bootstrap confidence intervals with significance level $\alpha = 0.05$, Bonferroni corrected for 4 comparisons: CA1-STD, [0.338, 0.396]; CA1-MIS, [0.352, 0.396]; CA3-STD, [0.353, 0.438]; CA3-MIS, [0.371, 0.436]). Both starting and ending edges of place fields tended to concentrate near the local-cue boundaries (Figure 4-7A, starting edges. Middle column, shuffling test, $p < 0.05$ for all but the CA1-STD session, two-tailed, Bonferroni corrected for 4 comparisons. Right column, bootstrap confidence intervals with significance level $\alpha = 0.05$, Bonferroni corrected for 4 comparisons: CA1-STD, [0.329, 0.411]; CA1-MIS, [0.357, 0.420]; CA3-STD, [0.350, 0.482]; CA3-MIS, [0.333, 0.432]. Figure 4-7B, ending edges. Middle column, shuffling test $p < 0.05$ for CA3-MIS, two-tailed, Bonferroni corrected for 4 comparisons. Right column, bootstrap confidence intervals with significance level $\alpha = 0.05$, Bonferroni corrected for 4 comparisons: CA1-STD, [0.326, 0.410]; CA1-MIS, [0.327, 0.391]; CA3-STD, [0.307, 0.435]; CA3-MIS, [0.376, 0.482]), although the statistical evidence was weaker than the combined analysis (Figure 4-6). The proportions were not significantly different comparing CA1 to CA3. In contrast to the local-cue boundaries, field edges did not appear to concentrate near the global-cue boundaries (Figure 4-8, middle column, shuffling test, $p >= 0.05$ for all datasets, two-tailed,

Bonferroni corrected for 4 comparisons. Right column, bootstrap confidence intervals with significance level $\alpha = 0.05$, Bonferroni corrected for 4 comparisons: CA1-STD, [0.368, 0.420]; CA1-MIS, [0.395, 0.441]; CA3-STD, [0.374, 0.461]; CA3-MIS, [0.351, 0.422]).

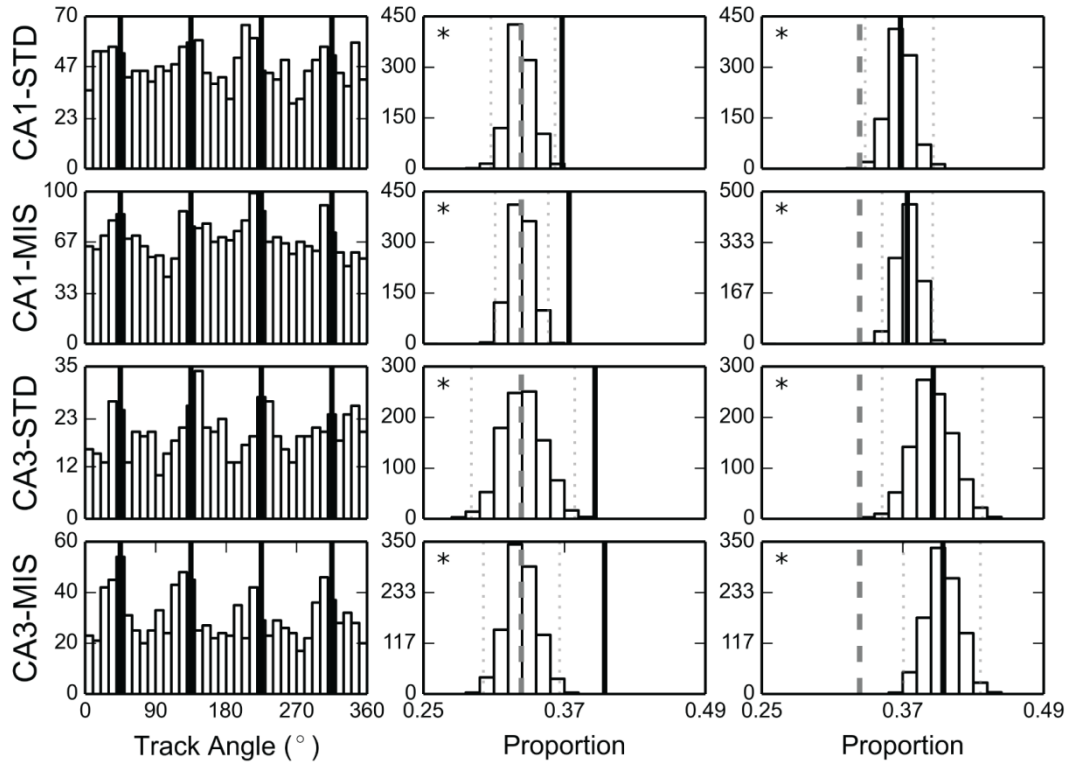

Figure 4-6 Place field edges coincided with local-cue boundaries

(Left) The distributions of place field edges peaked near the local-cue boundaries (denoted by the black lines). The abscissa of the map is the track angle and the ordinate is the number of field edges observed within the corresponding spatial bin. (Middle) The random shuffling control distribution of the proportion of field edges observed within the local-cue windows. The experimentally observed value (thick black line) is outside the 95% confidence intervals (dotted lines) of the shuffled distributions. (Right) The bootstrapped distributions of the field edge proportion. The chance level (0.33) is denoted by the dashed line. The solid represents the observed value. *, $p < 0.05$, Bonferroni corrected for 4-comparisons.

Figure 4-7 Both the start and end of place fields tended to happen near the local-cue boundaries

The distributions of the field edges with respect to the local-cue boundaries (left), of the shuffling test (middle), and of the bootstrap test (right) for the (A) starting and (B) ending edges. Although the ending edges showed a trend to be preferentially located at the local-cue boundaries, in most cases this tendency did not survive the Bonferonni-corrected statistical tests. (Middle)

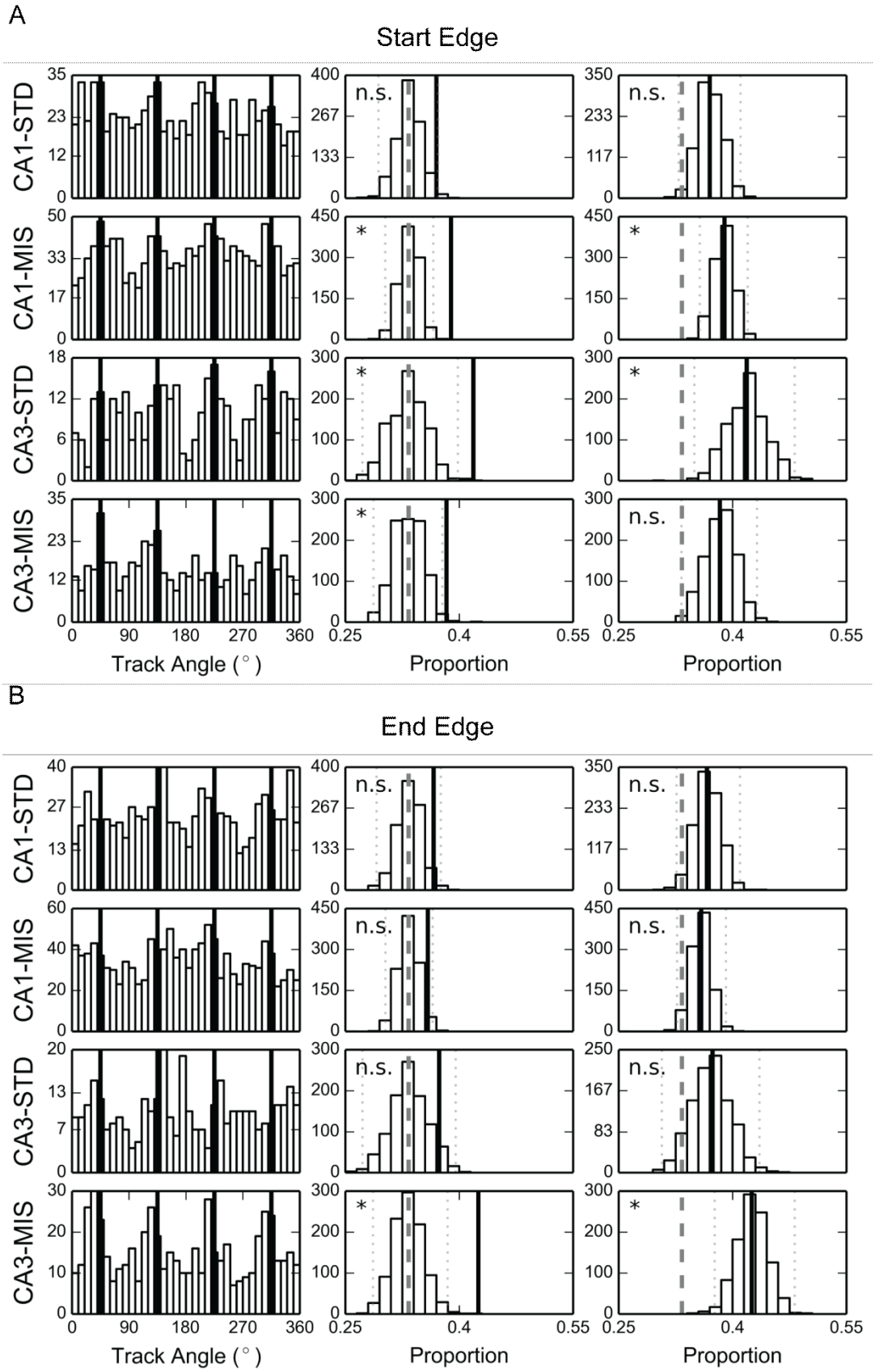
A
Start Edge
CA1-STD
CA1-MIS
CA3-STD
CA3-MIS
n.s.
*
Track Angle (°)
Proportion
Proportion
B
End Edge
CA1-STD
CA1-MIS
CA3-STD
CA3-MIS
n.s.
*
Track Angle (°)
Proportion
Proportion

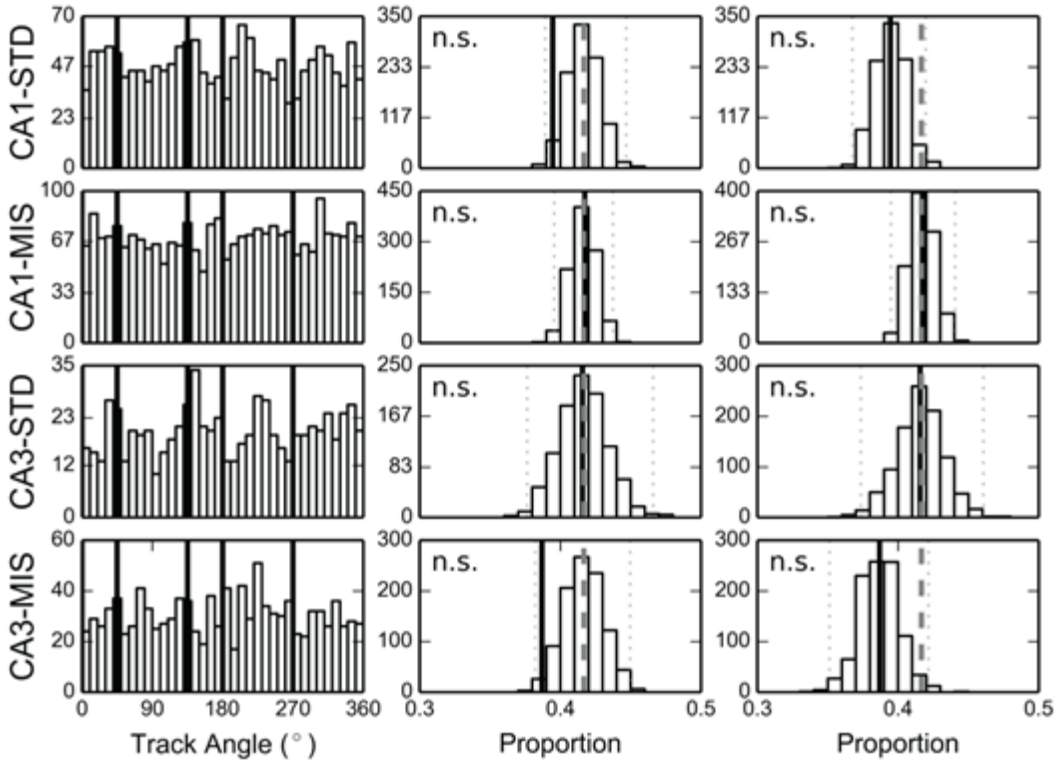

Figure 4-8 Place field edges did not concentrate near the global-cue boundaries

The distributions of the place field edges with respect to the global-cue boundaries (denoted by the solid lines) (left), of the shuffling test (middle), and of the bootstrap test. Two local-cue boundaries located at 45° and 135° and overlapped with the global-cue boundaries.

4.2.2 The concentration of place field edges was not an artifact caused by behavioral biases

At times during the double rotation task, the rats spontaneously slowed down and then paused to investigate the surrounding environment by performing a head-scanning behavior (Monaco *et al.*, 2014). Head-scanning was more likely to happen near the local-cue boundaries. Since low-velocity epochs were filtered out before rate map construction (see Section 4.1.2 *Spatial cell filtering*), the decreased velocity associated with head scanning could have forged artificial place field edges near the local-cue boundaries because of the removal of spikes. To eliminate this

possibility, we repeated the analysis without the velocity filter, and the distributions of the field edges still peaked near the local-cue boundary locations (Figure 4-9A, middle column, shuffling test, $p < 0.05$ for all session types, two-tailed, Bonferroni corrected for 4 comparisons. Right column, bootstrap confidence intervals with significance level $\alpha = 0.05$, Bonferroni corrected for 4 comparisons: CA1-STD, [0.354, 0.408]; CA1-MIS, [0.351, 0.402]; CA3-STD, [0.342, 0.439]; CA3-MIS, [0.351, 0.423]). Another potential speed-related artifact is the known modulation of place cell firing rates by running speed. The place cell firing rate can decrease with declining velocity near the local-cue boundaries, and if the firing rate drops below the place field detection threshold, field edges might artificially develop near the boundaries (even if the rat's speed is still above the velocity threshold). To control for this possibility, we discarded the data collected from all laps in which the animal paused or scanned near a place field and created new rate maps. The place field edges still concentrated near the local-cue boundaries for all but the CA1-MIS session (Figure 4-9B, middle column, shuffling test $p < 0.05$ for all but the CA3-STD sessions, two-tailed, Bonferroni corrected for 4 comparisons. Right column, bootstrap confidence intervals with significance level $\alpha = 0.05$, Bonferroni corrected for 4 comparisons: CA1-STD, [0.336, 0.393]; CA1-MIS, [0.358, 0.405]; CA3-STD, [0.327, 0.425]; CA3-MIS, [0.348, 0.420]).

A

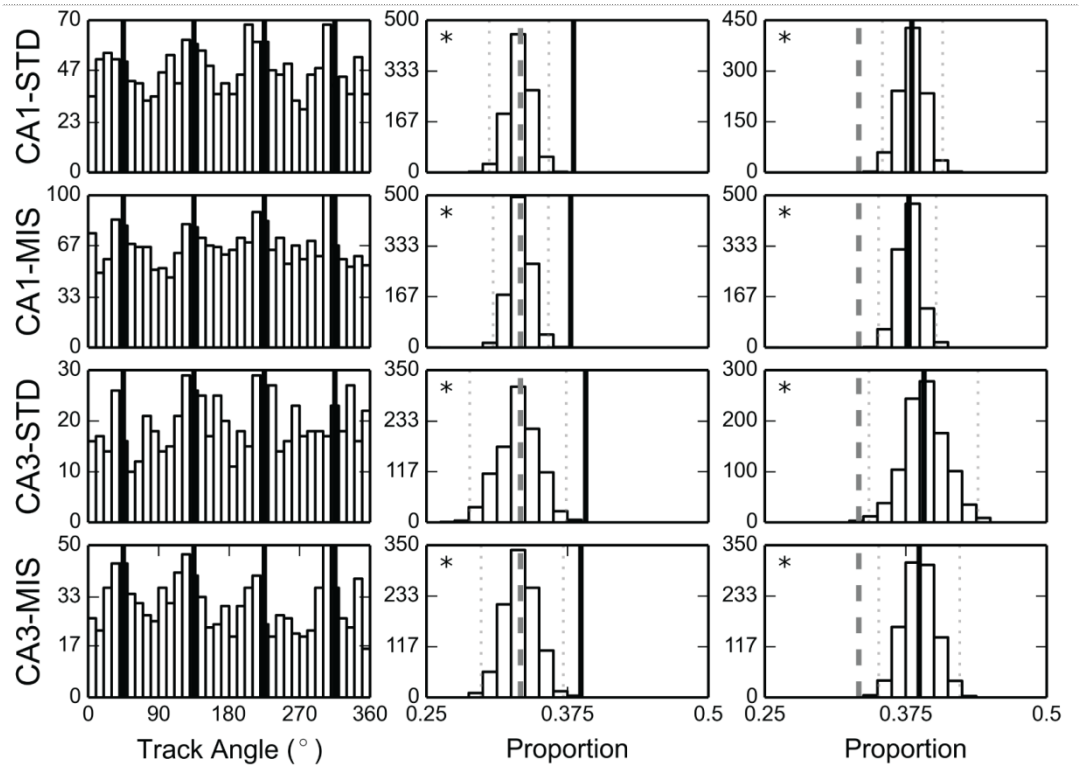
CA1-STD
CA1-MIS
CA3-STD
CA3-MIS
*
Track Angle (°)
Proportion
Proportion

B

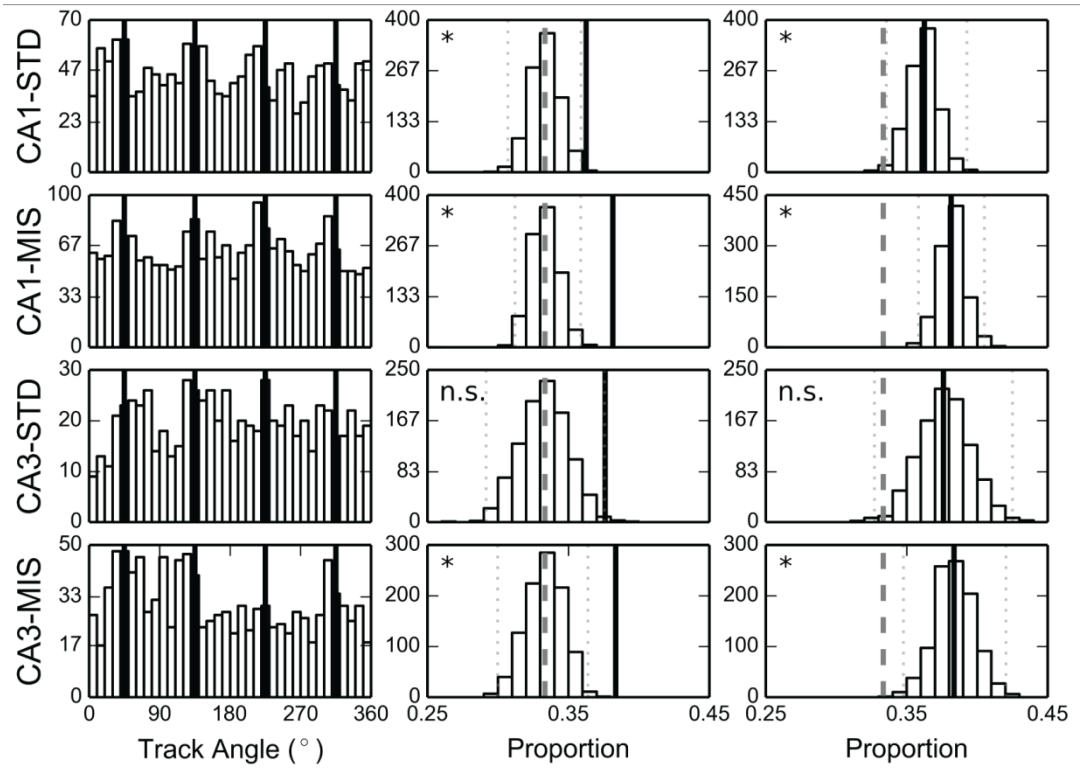
CA1-STD
CA1-MIS
CA3-STD
CA3-MIS
*
n.s.
Track Angle (°)
Proportion
Proportion

Figure 4-9 The prevalence of place field edges near local-cue boundaries was not a speed-related artifact

(A) The distributions of the place field edges with respect to the local-cue boundaries (left), of the shuffling test (middle), and of the bootstrap test, based on the raw data which were not velocity-filtered. (B) The distributions of the place field edges with respect to the local-cue boundaries (left), of the shuffling test (middle), and of the bootstrap test, after excluding the data segments contaminated by non-forward movements. These results suggest that the field edge concentration effect was not an artifact resulting from animal slowing down near the local cue boundaries.

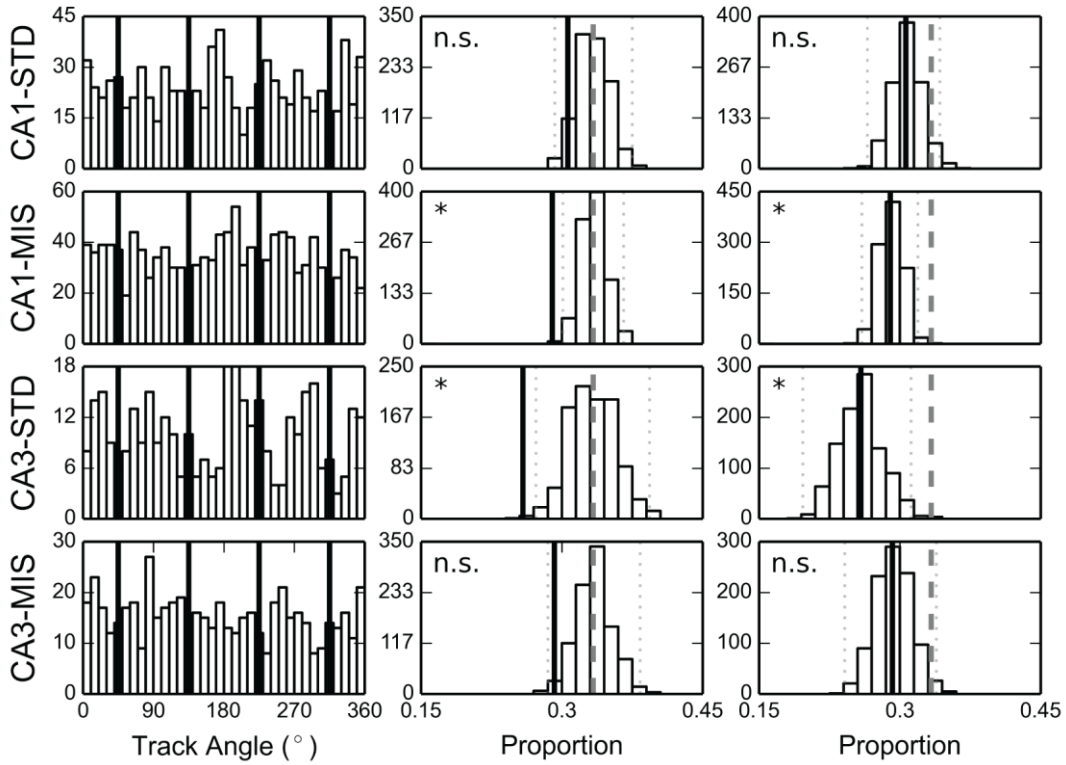

Figure 4-10 Local-cue boundaries were not over-represented by field COMs

The distributions of the place field COMs with respect to the local-cue boundaries (left), of the shuffling test (middle), and of the bootstrap test. Low prevalence of COMs is observed near the local-cue boundaries for all session types.

The head-scanning behavior is also known to trigger place field formation near the scanning location when the place cell fires more than expected during scanning (Monaco *et al.*, 2014). Preferential head-scanning behavior near the local-cue boundaries could thus result in accumulation of place fields and increase the number

of field edges observed near the boundaries. Consistent with the visual inspection of the population rate maps (Figure 4-2), however, the observed proportions of circular centers of mass (COMs) (Monaco et al., 2014) were significantly fewer than (or trended in that direction) from the shuffling results (Figure 4-10, middle column, shuffling test, $p < 0.05$ for CA1-MIS and CA3-STD, two-tailed, Bonferroni corrected for 4 comparisons) or the uniform distribution chance level (Figure 4-10, right column, bootstrap confidence intervals with significance level $\alpha = 0.05$, Bonferroni corrected for 4 comparisons: CA1-STD, [0.265, 0.343]; CA1-MIS, [0.259, 0.319]; CA3-STD, [0.197, 0.312]; CA3-MIS, [0.241, 0.339]). This underrepresentation of field COMs near the local-cue boundaries might be explained by the sizes of place fields. Given that 70% of the CA1 and CA3 place fields were 33°-103° in length and the local-cue boundaries were at 90° intervals, most fields that started or ended near the local-cue boundaries would have their COMs away from the local-cue boundaries. The high prevalence of place fields with edges near the local-cue boundaries would therefore lead to a low prevalence of COMs near the boundaries.

In (Monaco *et al.*, 2014), the associated scanning behavior of a scanning-triggered place field could be located near the start or end of the field. As a result, the field COMs could be distant from the scanning locations for large fields,

even as the edges of the same fields were located near the boundaries. To further examine whether the field edges were concentrated near the local-cue boundaries because of inhomogeneous scanning distributions, for each rat we calculated the proportion of head-scanning that started within the local-cue windows, and compared that to the proportion of field edges detected within the windows. There was no correlation between how often a rat scanned near the local-cue boundaries and how often its place fields started or ended near the local-cue boundaries (Figure 4-11, CA1-STD: $r^2 = 0.046$, $p = 0.337$; CA1-MIS: $r^2 = 0.020$, $p = 0.491$; CA3-STD: $r^2 = 0.018$, $p = 0.637$; CA3-MIS: $r^2 = 0.002$, $p = 0.868$). These results suggested that the concentration effect cannot be fully explained by scanning-triggered field formation during recording. However, the animals had been trained in the STD environment for many days before recording, and thus it is possible that the inhomogeneous distributions of the field edges were shaped by head-scanning behavior during training.

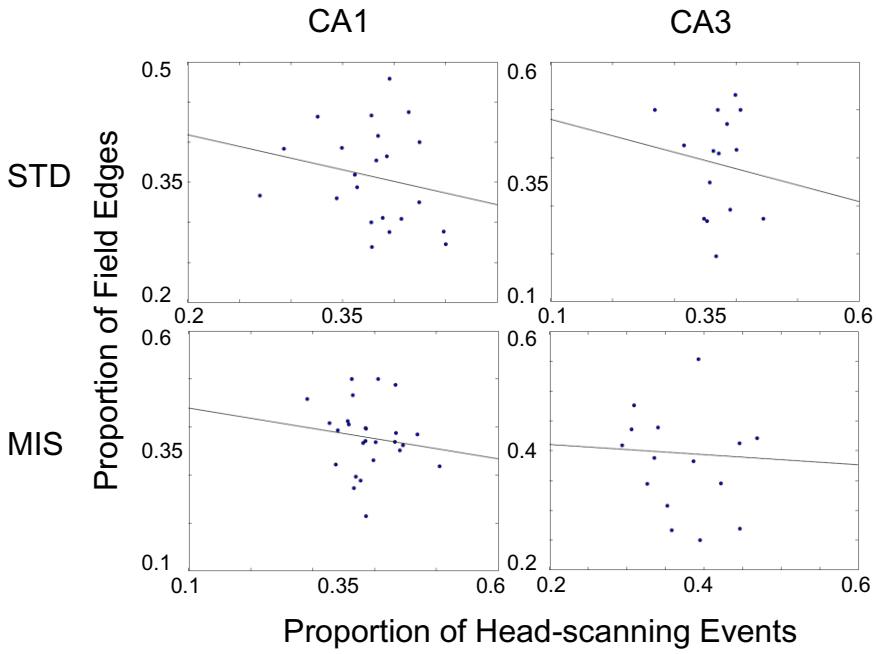

Figure 4-11 The prevalence of place field edges was not predicted by the prevalence of head-scanning events near the local-cue boundaries

The scatter plots of the proportions of head-scanning events observed within the cue windows and the proportions of field edges observed within the cue windows. Each data point comes from an animal.

Chapter 5: Representation of Surface Boundaries in 2-D Environments

Place field properties can be different when rats run stereotyped trajectories on one-dimensional (1-D) circular or linear tracks, compared to when they perform more irregular foraging on two-dimensional (2-D) open fields or platforms (Markus *et al*., 1995). We thus examined whether place field edges concentrate near surface texture boundaries in 2-D environments. We started the 2-D experiments with a board which has a complicated geometric pattern on the surface. However, the same place field could react differently to different surface boundaries (i.e., it respected some of the boundaries while it crossed the others), and no robust consistency was observed across different cells. While anecdotal observations from the complex board supports the idea that place field edges tend to coincide with surface cue boundaries, we performed the quantitative analyses and statistical tests on data collected from boards with simple surface patterns in order to quantify the concentration effect accurately. We demonstrated that the field edge concentration effect was also observed on the simple boards. Also, the neural representation of space changed more rapidly across the boundaries than far away or along the boundaries. For locations near the cue boundary, the strongest change in neural

representation was observed in the direction perpendicular to the boundary. In addition to transitions between different surface texture patches, we also examined the potential influence caused by tape line markings as a second type of surface cue boundary, and a weaker effect was observed when the boundary was defined by the tape line. These results suggest that surface boundaries are also encoded in the cognitive map in 2-D environments.

5.1 Methods

5.1.1 Complex board protocol

Five rats were trained to search for chocolate pellets placed at arbitrary locations on an open field with a homogeneous surface texture located in or outside of the experiment room. The recording experiments started after the rats learned to continuously run on the platform with few pauses. In each recording session, either a textured board with a complex surface pattern (the *complex board*) or a plain board with a uniform surface texture (the *plain board*) was placed at the center of a circular, curtained environment with no deliberate salient global cues. The rats performed the same foraging task for 20 min on the board. For three of the rats, 1-3 *complex board* sessions were performed each day, followed by one *plain board* session in some cases. The other two rats experienced two *plain board* sessions

followed by one complex board session per day. There was a minimum of two days of recording for each rat.

The *complex board* was 1-by-1 m and its surface was composed of a complex pattern of geometric shapes demarcated by different texture patches and tapes (Figure 5-1). The upper left half of the platform was covered by different surface textures: a grey rubber mat with a pebbled surface shaped as a rectangle and a small triangle, white sand paper shaped as a square and brown cork mat shaped as a large triangle. The lower right half of the platform was uniformly painted black with yellow tape labeling borders 180° rotationally symmetric to the upper left half. The *complex board* was novel to the rats on the first day of recording. The *plain board* was a 1.1-by-1.1 m wooden board and its surface was uniformly painted black.

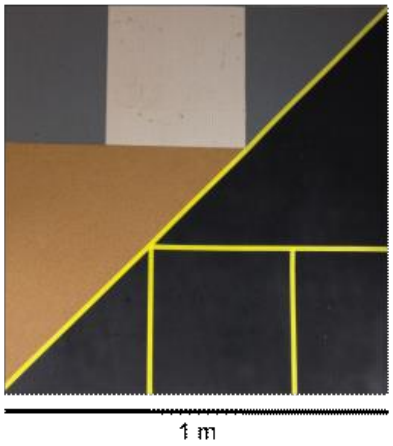

Figure 5-1 Photo of the complex board

5.1.2 Simple board protocol

The same training procedure as described in the *Complex board protocol*

section was used to train three rats to forage in an open field. For each 20 min recording session, the rats performed the same foraging task on a textured board with a slanted linear boundary crossing the surface. The board was placed at the center of a circular, curtained environment with no deliberate salient global cues.

Four different boards were used in the *simple board forage task*: *leather-standard*, *leather-shift*, *tape-standard*, and *tape-shift*. The brown smooth wooden surface of each leather board was partially covered by a black, synthetic leather patch, and the boundary between the two surface textures was an oblique line crossing the board. For the leather-standard board, the separation line passed the bottom edge of the board at the center, and the top edge at 25 cm from the top-right corner. For the leather-shift board, the separation line shifted 20 cm to the left. The brown wooden surface of each tape board was labeled by an oblique white tape line crossing the board. The geometric patterns of the tape boards were 90° rotated mirror images of the leather boards (Figure 5-2).

There were two days of recording for each rat, and the rats foraged on the leather boards for one day and on the tape boards for the other day. For two out of three rats the leather boards came first. During each recording day, the rat experienced two *standard* sessions, followed by a *shift* session and back to the standard session. The rat was brought out of the experiment room for 5-10 min

between sessions to rest and was provided access to water on a pedestal. All four boards were novel to the rats before the first recording session of the board, and for two rats the simple boards were the first experiment apparatus with inhomogeneous surfaces (the other rat performed the complex board foraging task before the simple board foraging task). The data collected from the *plain board* (See *Complex board protocol*) were used as the control data for the simple board forage task.

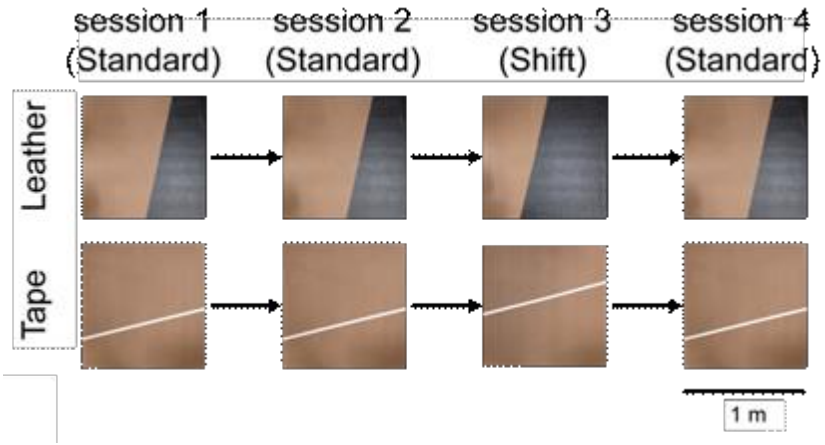

Figure 5-2 Photos of the simple boards and schematics of the simple board foraging task protocol

5.1.3 Firing rate map construction

The experiment boards were divided into small spatial bins and the average firing rate at each bin was smoothed (see below) to construct the firing rate map. We binned the experiment boards in different ways as described in the corresponding sections depending on the purposes of the analyses. The average firing rates were calculated as the spike counts divided by the occupancy duration within each spatial bin. Only running activities with velocity > 5.76 cm/sec (to match the velocity filter

used in our double rotation task) were included in spatial cell analyses. The results were similar when 4 cm/sec or 10 cm/sec velocity filters were applied (not shown).

The Gaussian filter is widely accepted as a rate map smoothing method in place field studies. However, this filter blurs high-contrast transitions and can distort the edges in images (e.g., by smoothing sharp corners) which might interfere with our

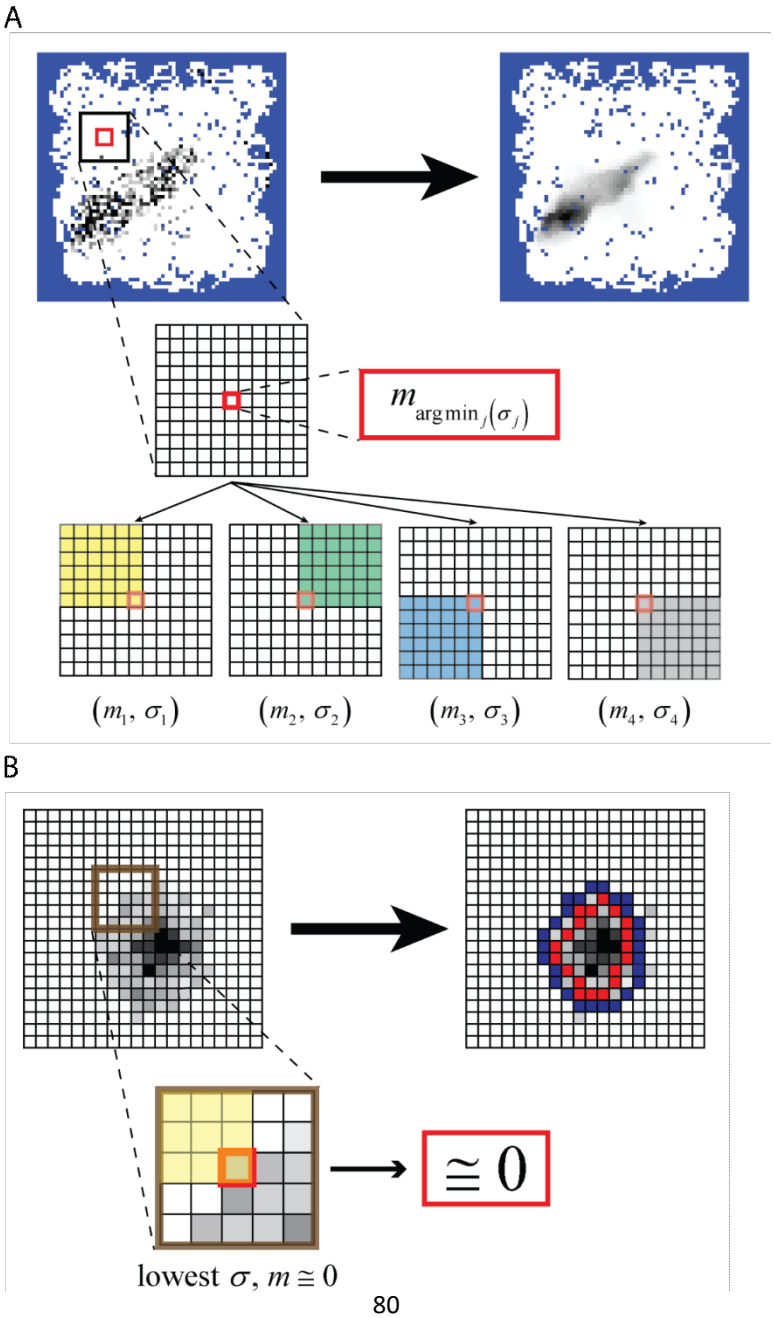

Figure 5-3 Kuwahara smoothing method

(A) Schematics of the Kuwahara kernel and the smoothing process. The Kuwahara filter generated a smoothed firing rate at each bin with an 11-by-11 bin sliding window (black square). The window was centered at the bin of interest (red square) and was equally divided into four sub-windows each located at a corner of the larger window (labeled in different colors on bottom row). The sub-windows were 6-by-6 bins and overlapped with adjacent sub-windows either by one column or one row of bins. The mean and the standard deviation of the average firing rates from each sub-window were calculated, and the smoothed firing rate for the bin of interest was defined as the mean firing rate (m_i) of the sub-window that has the lowest standard deviation (σ_i). If multiple sub-windows had the same standard deviation, we compared the means from the candidate sub-window, and the mean closest to the average firing rate at the bin of interest was selected as the smoothed firing rate.

(B) The constant-0 firing rate of the silent area can lead to exclusion of the outskirts of a place field. The standard Kuwahara filter has been widely used in image processing. However, when applied to place cell recordings, necessary modifications were required to compensate for the inherent inequality in the firing rate distributions between the preferred locations and the non-preferred locations. A standard place cell tends to remain silent when the animal is outside of its place field, as shown in the upper left cartoon firing-rate map. For a spatial bin near the edge of the place field (the red square in the insert), the sliding window (brown square) could cross the field edge and have both sub-window(s) inside and outside of the field. For the sub-window exterior to the field, the firing rates could be nearly all-zeros and the standard deviation of the firing rates would be very close to zero. In contrast, when a sub-window was interior to the field, the standard deviation of the firing rates would rarely be as low. In this case, the standard deviation and the mean of the firing rates within the sub-window would be the lowest when the sub-window covers mostly the silent area (like the yellow-shaded sub-window of the insert). Therefore the smoothed value would be close to 0, and the silent area eroded the place field(s) after smoothing (the red squares in the upper right panel represent the field edges, which do not overlap with the optimistic field edges (the blue squares)). To solve this problem, we fabricated numbers for the bins with zero firing rates while calculating the standard deviations and thus artificially increased the standard deviations outside of the preferred location. For each cell-session, we calculated the median firing rate r of the non-zero bins of the rate map, and substituted a chess board pattern of interleaving 0s and rs for the zeros bins when computing the standard deviations. With the substitution, we prevented artificially shrinking the place fields due to the low standard deviation of the silent zones.

examination of whether sharp firing rate changes reflected the locations of the cue boundaries. Thus, we instead used edge-preserving smoothing algorithms to retain the undistorted, sharp changes. A Kuwahara filter (Kuwahara *et al.*, 1976) was

applied to the preprocessed average firing rate maps (Figure 5-3), followed by a median filter.

The Kuwahara filter could also create “block artifacts”, (i.e., artificial discontinuities between regions) and thus we further applied a median filter (Tukey, 1977) with a 3-by-3 bin kernel to improve the smoothness. The median filter is another widely used edge-preserving smoothing algorithm, and it smoothed data by taking the median of the data inside of a sliding window. The smoothed firing-rate maps were then used in the quantitative analyses.

5.1.4 Spatial cell filtering

For the analyses restricted to place cells, the isolated units were scrutinized as described above to exclude putative interneurons. The spike trains of the units were considered reliable only if the isolation quality was at category 3 or better (see Section 3.3 *Single-unit isolation*), and there were at least 50 running spikes recorded in the session. The Skaggs spatial information scores (Skaggs *et al.*, 1992) were calculated for the qualified cell-sessions to examine whether their firing activities were spatially tuned. For each cell-session, the experiment board was partitioned into a matrix of 2-by-2 cm spatial bins. The smoothed average firing rate for each bin was calculated as described in the firing-rate map construction section, and the spatial information and the p value were calculated based on the smoothed firing-rate maps.

To pass the spatial-cell criteria, the cell-session must have spatial information greater than or equal to 0.6, at a significance level of 0.01.

5.1.5 Cross-correlograms

In order to compare the population neural activities of the place cells across the cue boundaries, we binned the simple boards with grids that were aligned with the cue boundaries (not orthogonal to the board edges) (Figure 5-4A). To maximize available data without including the out-of-platform area, a rotated square area inscribed in the platform rim was used for the analysis. The rotated square was ~ 82.5 by 82.5 cm^2 and was divided into a 42 x 42 matrix with each bin ~ 4 cm^2.

For each cell-session, the averaged firing rates of the spatial bins were calculated as the spike counts divided by the occupancy durations, and the firing-rate maps were smoothed as described in the *Firing rate maps construction* section. Each column of the firing-rate map corresponded to a band parallel to the cue boundaries (Figure 5-4A). The m^{th} columns of the firing-rate maps from different units were stacked to construct the population firing-rate matrix of the m^{th} parallel band (Figure 5-4B). For the normalized correlograms, the firing-rate vectors of individual units were divided by the maximum firing rates before being stacked.

The correlograms were composed of the averaged correlation between pairs of population firing-rate matrices. The Pearson correlation was calculated between the

same columns from the i^{th} and j^{th} population firing-rate matrices, and the correlations from each column were averaged and became the (i^{th}, j^{th}) element of the correlogram (Figure 5-4C) Each bin of the correlograms represented the averaged correlation between two parallel band areas.

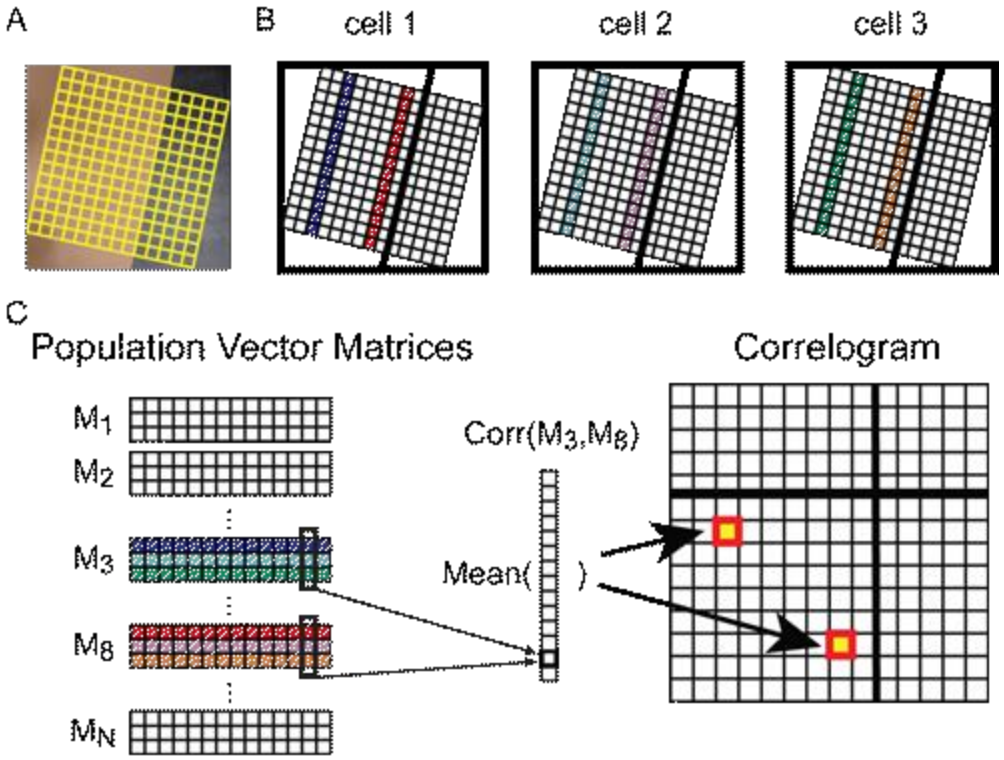

Figure 5-4 Constructing cross-correlogram of the simple board

(A) The spatial binning of the simple board. The firing-rate map was constructed based on binning (denoted by the yellow grid) aligned with the surface boundary. (B)(C) The construction of the cross-correlogram. Assuming there were only three cells (denoted by the squares in (B)), the firing rates of the third columns of the grids from each cell (the purple, cyan, and green stripes in (B)) were stacked together and formed the third population vector matrix (PVM) (M_3 in (C)), and the 8^{th} columns (the red, pink, and orange stripes in (B)) formed M_8, etc. For each element of the cross-correlogram, the Pearson's cross-correlation coefficients were calculated between the corresponding columns of the selected PVMs, and the mean correlation was calculated across the columns.

5.1.6 Place field detection

For each cell-session collected in the simple board or the plain board sessions

that passed the spatial cell filter (see the *Spatial cell filtering* section), place field edges were detected for an area extending 30 cm beyond each side of the experiment board. These detection areas were 1.6-by-1.6 m for the simple boards and 1.7-by-1.7 m for the plain board. To construct the place fields, each area was partitioned into a matrix of 2-by-2 cm spatial bins, and the smoothed average firing rate for each bin was calculated as described in the *Firing rate map construction* section.

We binarized the firing-rate maps with floor-thresholds that were independently calculated for each cell-session. The spatial bins with firing rates larger than the thresholds were selected, and each connected group of bins was classified as a putative place field. The thresholds were set to maximize the differences between the mean firing rates within and outside of the place field(s), to minimize the variance of the firing rates outside of the place field(s), and to minimize the total size of the place field(s) (this last term was required to prevent all bins being included in the place field). In practice, we defined an error function of the threshold and optimized the error function with the *minimize_scalar* function under the *Scipy optimize* package (https://docs.scipy.org/doc/scipy/reference/generated/scipy.optimize.minimize_scalar.html) to find the best threshold θ that minimized the error function. The tolerance level was set at 10^{-7}.

The error function was empirically defined as

$$err(\theta) = [m_{below}(\theta) - 0.1 \cdot m_{above}(\theta)] + 10 \cdot v_{below}(\theta) - 1.3 \cdot a_{below}(\theta),$$

where $m_{below}(\theta)$ was the mean firing rate of the bins with non-zero firing rates ≤ the current threshold θ, $m_{above}(\theta)$ was the mean firing rate of the bins with firing rates > θ, $v_{below}(\theta)$ was the firing rate variance of the bins with non-zero firing rates ≤ θ, and $a_{below}(\theta)$ was the number of bins with non-zero firing rates ≤ θ, divided by the number of bins with non-zero firing rates. The search range for θ was limited to positive numbers ≤ the peak firing rate of the cell-session.

Since the same error function was used for different cell-sessions, some normalization for the means and variances of the firing rates across cell-sessions was necessary. For each cell-session, we first removed the firing rate outliers by calculating the quartiles and the interquartile range (IQR) of the non-zero firing rates, and truncated the firing-rate map at $Q_1 - IQR$ and $Q_3 + IQR$, where Q_1 and Q_3 were the first and third quartiles of the non-zero firing rates. For any element of the firing-rate map with non-zero value smaller than $Q_1 - IQR$ or larger than $Q_3 + IQR$, the firing rate was re-assigned as $Q_1 - IQR$ or $Q_3 + IQR$, respectively. We then normalized the truncated firing-rate map with the following rules: for the bins

with non-zero firing rates, the truncated firing rates were transformed into the standard scores, and the normalized firing rates were defined as the standard scores + 5; for the bins with zero firing rates, the normalized firing rates were still zero. The constant term (+5) was included to artificially differentiate the silent bins and the bins with non-zero firing rates. This preprocessing procedure was taken before optimizing the error function. Once the thresholds were determined based on the preprocessed firing-rate maps, the preprocessing procedure was reversed to recover the threshold, and the place fields were detected by binarizing the original firing-rate maps at the recovered threshold.

The connected bins with firing rates above threshold were grouped as putative place fields, and the contours of the putative place fields were then smoothed by opening and closing operations used in image processing. An opening operator with a 3-by-3 bin square kernel was first applied to the putative fields to trowel small protrusions, followed by a closing operator with a 3-by-3 bin square kernel to grout the small dents, and finished with a second opening operator with a cross-shaped kernel to eliminate any artificial protrusions created during the closing operation (Figure 5-5). After smoothing, the grouping of bins and putative field assignments were updated as above. Putative fields smaller than 35 bins, with peak firing rate < 0.1 Hz, or with no more than 30 in-field running spikes, were discarded, and the

remaining qualified putative fields were labeled as place fields. For each spatial bin within a place field, we examined whether any of its adjacent bins (the bins above, below, to the left of, or to the right of the bin of interest) did not belong to the place field. If so the bin was labeled as belonging to the contour of the place field.

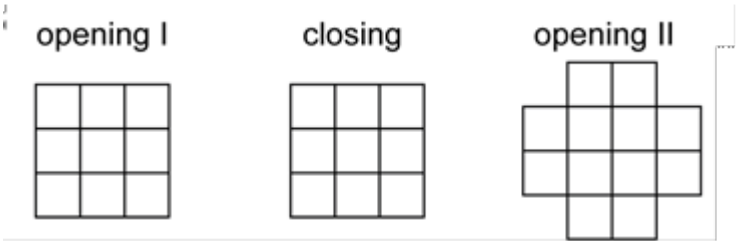

Figure 5-5 The opening and closing operators

The shapes of the kernels used in smoothing the place field contour. The kernels of the opening and closing operations are sliding matrices, and each element within the matrix can either be 0or 1. Each group of squares represents the nonzero part of the kernel. For example, the first opening operator was a3 x 3 matrix with all 1s and thus it is denoted by 3 x 3 squares. For the opening operation, an erosion operation was applied to the data followed by a dilation operation. During the erosion operation, the zero part of the firing rate map erodes the nonzero part within the sliding kernel if the nonzero part of the kernel overlaps with spatial bins with zero firing rate, while during the dilation operation, the nonzero part of the firing rate map expands if the same situation happens. For the closing operation, the order of the erosion and dilation operations is reversed.

5.1.7 Boundary preference index (BPI) analyses

The spatial binning of the experiment boards and the construction of place field edges were described in the *Place field detection* section. For each simple board we examined whether more field edges concentrated near the cue boundaries than expected by chance, by calculating the differences between the field edge density near and far away from the cue boundaries and comparing the observed differences to the control data collected from the plain board.

To calculate the field edge densities, the simple boards were partitioned into the boundary zones and the non-boundary zones based on the distance to the boundary. The boundary zones were bands aligned with the cue boundaries, extended to the board edges and expanded 10 cm wide on each side of the cue boundaries. For each spatial bin within the boundary or non-boundary zone and far from the board edges, we counted the number of fields with edges that overlapped with the bin. The field edge density was defined as the sum of the field edge counts from each bin divided by the total number of bins within the zone. The zone boundaries were defined by linear equations, and a spatial bin could thus partially belong to the boundary and non-boundary zones simultaneously. For the spatial bins segregated by the zone boundaries, the field edge counts and bin counts were assigned to each zone proportionally based on the bin area within each zone. Since the place fields would be forced to end near the board edges, we excluded any spatial bin with center less than 10 cm from any of the board edges to avoid including place field edges that were not meaningful contributors to the analyses of surface cue boundary effects.

We calculated the boundary preference index (BPI) $\frac{d_b - d_{nb}}{d_b + d_{nb}}$ for each *simple board*, where d_b was the field edge density within the boundary zone and d_{nb} was the field edge density within the non-boundary zone. The chance level of the density difference was determined by projecting the boundary and non-boundary zone

demarcations from the simple boards onto the plain board, and calculating the density difference of the data collected from the plain board accordingly. For all four simple boards, the same plain board and the same set of data recordings were used to calculate the control field edge density difference. The plain board (1.1-by-1.1 m) was slightly larger than the simple boards (1-by-1 m), and therefore we rescaled the plain board data to fit the sizes of the simple boards.

To test whether the observed BPI was significantly higher than the control BPI, we separately and independently bootstrapped the place fields collected from the simple boards and the plain board 1,000 times. Each time N place fields were randomly resampled from the specified board with replacement, where N was the number of actual place fields collected from the board. The BPIs were calculated, and the difference between the observed and the control BPI (observed - control) was recorded in each trial.

Based on the results obtained from the double rotation and the complex board data, we designed the simple board foraging task with the *a priori* prediction that field edges would concentrate near the cue boundaries, thus producing an observed BPI larger than the control BPI. The statistical significance was obtained by examining whether 95% of the bootstrapped BPIs was greater than 0.

We also performed a permutation test to examine whether the BPI difference

was significant. For each trial, the source labels of the place fields were shuffled and the fields were randomly reassigned to the simple board or the plain board. The BPI difference was calculated based on the shuffled field labels and the same process repeated 1,000 times. The observed BPI was considered significantly larger than the control BPI if the observed BPI difference was larger than or equal to the 1.25 percentile (significance level $\alpha = 0.05$, one-tailed and Bonferroni corrected for 4 comparisons) of the shuffled distribution of the BPI difference.

5.1.8 Gaussian-band matching analyses

If field edges tended to concentrate near the cue boundaries on the simple boards, the field edge density should peak near the boundary and decrease when moving away from the boundary. We modeled such a trend with a Gaussian-band template and quantified how well the field edge density map was described by the model by calculating Pearson's correlation coefficient between them.

The section of the template is a Gaussian function when sliced perpendicular to the cue boundary, and a constant function when the section is parallel with the cue boundary. The standard deviation of the Gaussian function was set to be 5 cm such that the template would be strongly correlated with the field edge density map if most field edges were observed within the boundary zone. Since we do not expect to see field edge density affected by the distance to the cue boundary for areas far from

the boundary, the template is set to be zero for points that were at least 20 cm from the cue boundary.

Similar to the methodology described in the previous session, the correlations between the template and the field density maps of the simple boards were compared to the plain board control. The significances of the differences in correlations were examined by the bootstrap and permutation methods.

5.1.9 Population vector direction of change analyses

In order to compute the maximum population vector (PV) of firing rates difference and the corresponding movement direction for each location, the experiment boards were binned and the smoothed mean firing rate at each spatial bin was calculated as described in the *Firing-rate map construction* section. Since the binned rate maps allow calculation of movement angles in only 8 directions, none of which necessarily corresponded to the angle of the cue boundary, interpolation of the PV difference at arbitrary movement direction is thus necessary. The PV representing arbitrary location (not restricted by the empirical binning) can be depicted by a continuous multivariate function $r(x, y)$ which can be complex and implicit. Nevertheless, the tangent plane of $r(x, y)$ can be estimated based on the binned rate maps even though $r(x, y)$ itself is unknown. Taking each spatial bin as the reference point, we linearly approximated $r(x, y)$ by its tangent plane $T(x, y)$ and

calculated the change of PV from the reference point to any neighboring locations. We quantified the difference between two PVs by the Euclidean distance between them and computed the movement direction ω with the largest PV difference (Figure 5-6, also see Appendix Afor mathematical derivation of this procedure).

There are some noteworthy implicit rules applied to the searching of ω based on the linearity of the tangent plane. First, walking away from the same location at the same speed but in opposite direction on the tangent plane would lead to the same amount of translocation on the plane. In other words, if the maximum PV difference was perceived at movement direction ω, the same amount of change would be observed at movement direction ω+180°. We therefore restricted ω to range from 0° to 180° while theoretically ω can range from 0° to 360° (0° is defined as parallel with the cue boundary for simplicity). Second, if the PV difference is only observed in the x (y) direction on the empirical binned rate map, ω would be the x (y) direction; if the PV difference is also observed in the y (x) direction, ω diverges from the x (y) direction. That is, the movement direction with the largest change would be perpendicular to the direction with the minimum change. If the direction with the largest change was perpendicular to the cue boundary, it also implied that the change was the smallest when the animal moved along the boundaries.

After the movement direction ω was calculated for each spatial bin, the

direction vectors (unit vector with angle ω) within the boundary zone (or non-boundary zone) were concatenated and the lengths were divided by the cell number to construct the mean direction vector of the boundary zone (or non-boundary zone). The mean vector length was then defined as the length of the mean direction vector.

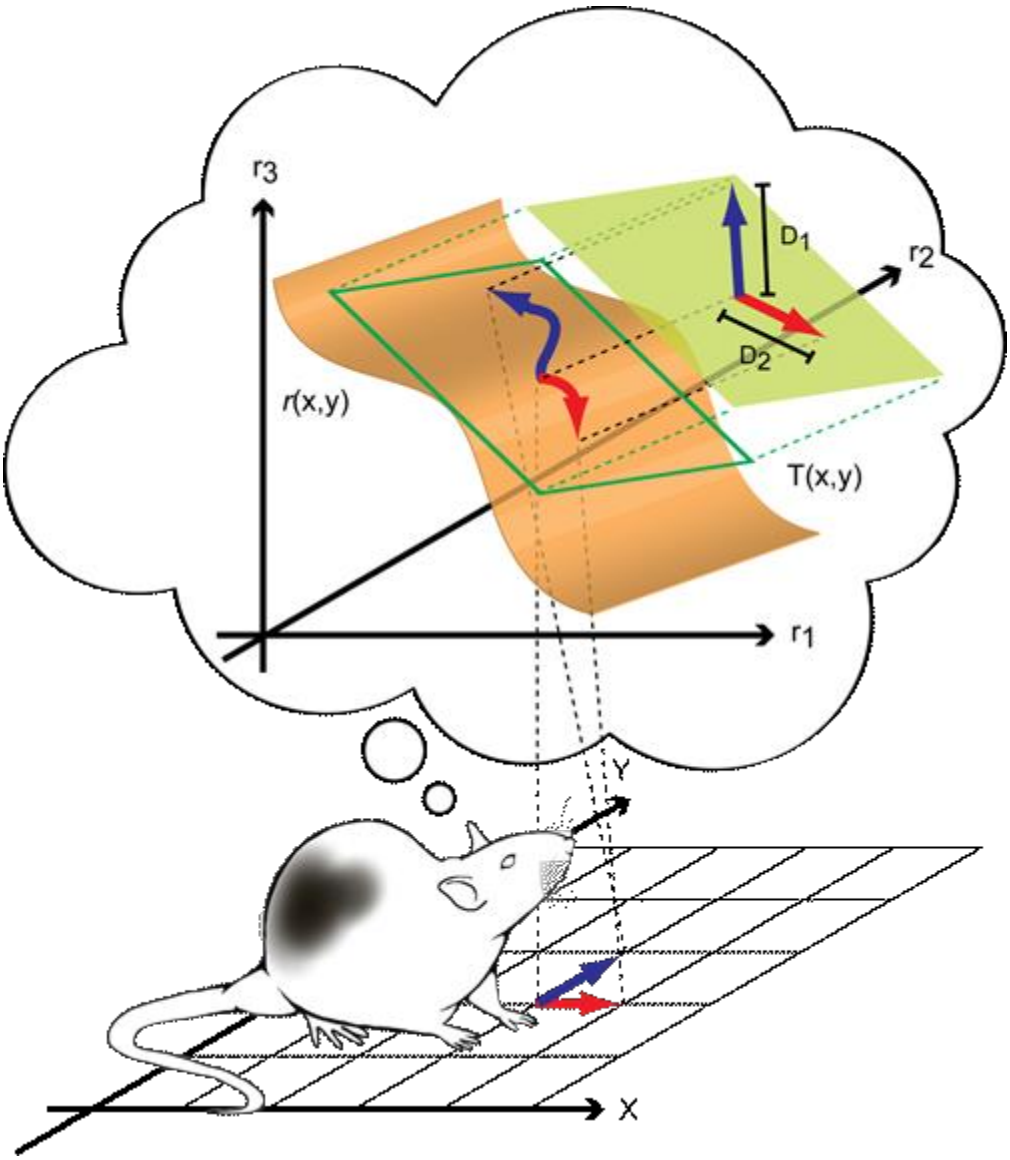

Figure 5-6 Interpolation of PV

A linear approximation method was used to interpolate the PV differences. On the experiment platform (represented by the x-y plane at the bottom), the PV can be empirically calculated for any spatial bin. These PVs are discrete samplings of the continuous function *r*(x, y) (the orange surface) which defines the PV at arbitrary location. In order to examine the differences between PVs at all possible movement directions, for every spatial bin, we computed the tangent plane T(x, y) (the green plane) of r(x, y) and interpolated the PV for arbitrary location. The red and blue angles denote two orthogonal movement directions in the physical world, and their corresponding PV changes in the neural space. D_1 and D_2 are the resulting PV differences (defined as the Euclidean distances) for these two different movement directions.

5.2 Results

5.2.1 Firing rate maps are modulated by surface boundaries in 2-D environments

We first trained 5 rats to forage on a *complex board* with a complicated surface pattern composed of geometric shapes constructed from different texture patches and tape lines (Figure 5-1). Anecdotal observation showed that some place field edges were aligned with a subset of the cue boundaries and corners (Figure 5-7). These examples suggest that the place field edges respect the local texture boundaries on the platform, similar to the circular track. However, a number of place fields crossed some boundaries, even as they were aligned to other boundaries; thus, the fields were not always contained within a single boundary region. The complexity and heterogeneity of place field edges relative to the patterns on the board made it difficult to analyze the results quantitatively. Thus, to make the analyses tractable, we further explored this question by collecting data from 3 rats foraging on *simple boards* with a single cue boundary.

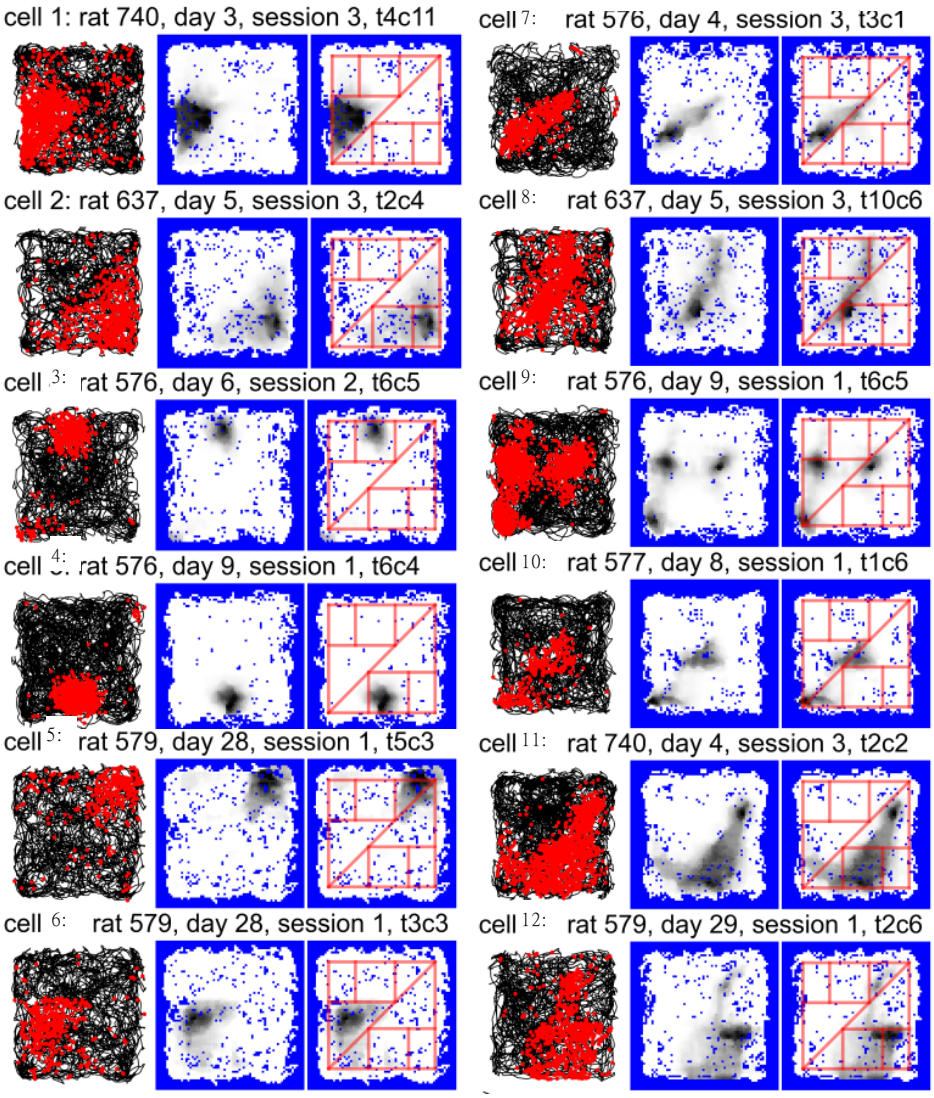

Figure 5-7 Place field edges modulated by surface boundaries on the complex board

Examples of CA1 place fields modulated by the surface boundaries. For each cell the trajectory-spike plot (left), the smoothed firing-rate map (middle), and the smoothed firing-rate map with cue boundaries labeled by red lines (right) are presented. The cue boundaries appeared to modulate the edges of the place fields, Cells 1-6 occupied a geometric shape defined by the surface boundaries, and developed triangular, rectangular, or complex-shaped fields. Cells 7-8 fired along the surface boundary and had elongated, stripe-like fields. The cue boundaries also seemed to affect the locations of the place fields. For example, cell 9 developed multiple fields at the intersections of the cue boundaries defining a triangular shape, and cell 10 fired at the bottom-left vertices of the triangular patches. Cell 11-12 showed complex behavior that appeared to be controlled by the surface boundaries.

The simple board experiments contained two types of boards. For the *leather boards*, the cue boundary was formed by the contrast between a leather surface patch

and a wooden texture; for the *tape boards*, a white tape line divided the board into two sections (Figure 5-2). The surface patterns of the leather and the tape boards were 180°-rotated, mirror images of each other. Therefore any possible field edge concentration effect observed in the latter board could not be explained by the effect generated in the preceding board. Place fields were distributed over the entire surface of the simple boards and a subset of the fields appeared to be modulated by the boundaries (Figure 5-8).

To visualize whether the field edges were modulated by the cue boundaries at the population level, we partitioned the simple board into equally-spaced stripes parallel to the cue boundary and calculated the similarities between the population activity vectors of the stripes (Figure 5-4). The widths of the diagonal hot band of the normalized cross-correlograms decreased near the cue boundary locations for the leather boards, but they remained relatively homogeneous along the diagonal lines for the tape boards (Figure 5-9A). Similar results were obtained for non-normalized correlograms, although some inhomogeneity of the diagonal band width started to appear for the tape boards (Figure 5-9B). Furthermore, the diagonal hot band of the leather-shift board became narrower at the cue boundary location of both the leather-shift and the leather-standard boards, which suggests a memory trace of the prior location of the boundary. These results indicated that the place cell population

activities changed more rapidly near the cue boundaries for the leather boards, while the effect was much weaker for the tape boards.

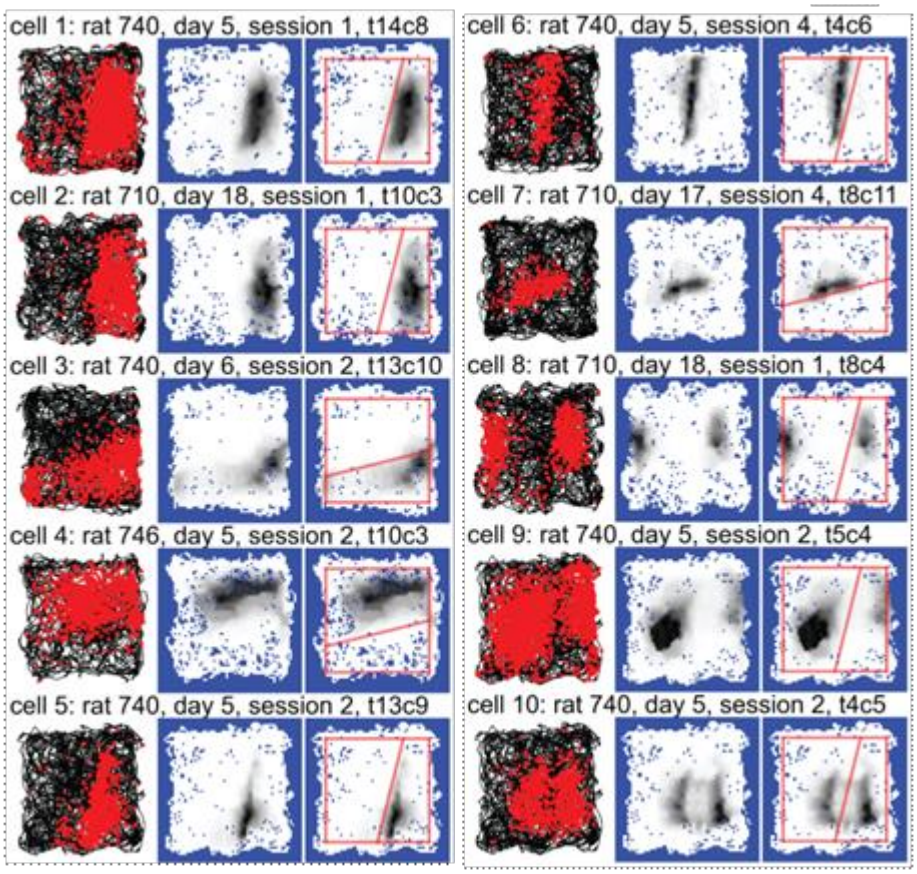

Figure 5-8 Place field edges modulated by surface boundaries on the simple boards

Examples of CA1 place fields modulated by the cue boundaries. Similar to the complex board, we observed place fields that occupied a geometric shape defined by the cue boundary and the edges of the experiment board (cells 1-4), and elongated fields extending along the cue boundary (cells 5-7). Some of the neural correlates near the cue boundary were similar to those near walls or other traditionally defined boundaries reported in previous studies. Cell 8 resembled boundary cells in that it developed multiple fields at corresponding locations with respect to the cue boundary and the board edge. Cell 9 seemed to have two fields intersecting with each other along the cue boundary. Cell 10 showed two parallel fields along the cue boundary, as if its firing activity was inhibited by the cue boundary.

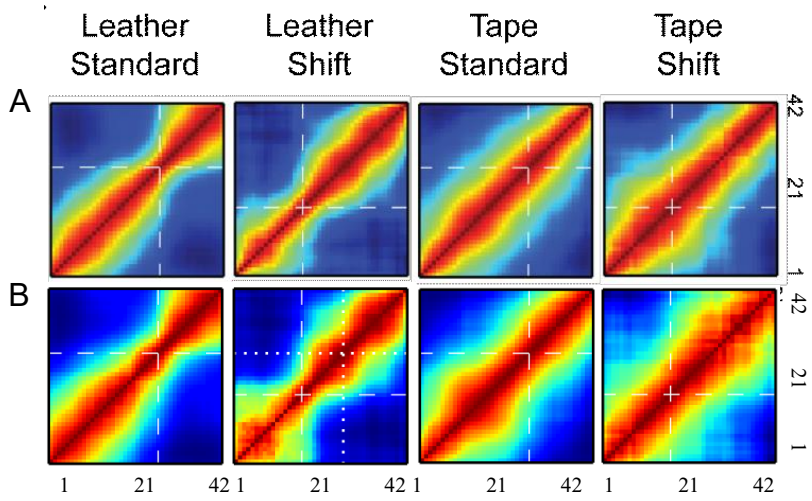

Figure 5-9 Surface boundary enhances neural decorrelation

(A) The cross-correlograms of the PVs. Along the direction perpendicular to the surface boundary, the correlation dropped more rapidly near the surface boundaries (denoted by the white dashed lines) for the leather boards. The firing-rate maps were normalized by the peak firing rates before constructing the cross-correlograms. (B) The same as A except that the firing-rate maps were not normalized.

5.2.2 Place field edges concentrated near the boundaries on the simple boards

To determine whether place field edges concentrated at the leather or tape boundaries, similar to the texture-cue boundaries on the circular track (Figure 4-1), we created 2-dimensional field-edge density maps for the 4 types of boards. Hot spots along the cue boundaries were observed for the leather and tape standard boards (Figure 5-10A), demonstrating a trend for the field edges to concentrate near the cue boundaries (as well as near the perimeters of the boards). To quantify whether field edges were more frequently observed near the cue boundaries than

away from the boundaries, we calculated boundary preference indices (BPIs) between locations that were ≤ 10 cm from the cue boundary (the "boundary zone") and locations that were > 10 cm from both the cue boundary and from the periphery of the board (the "non-boundary" zone).

For each board we randomly resampled the place fields with replacement to create a thousand bootstrapped samples of place fields, from which a BPI was calculated for each sample. Concurrently, we projected the boundary versus non-boundary zone partitions of the simple board onto a board with a plain surface, and calculated the BPI of the data collected from the *plain board* accordingly. By randomly pairing observed and control bootstrapped samples, we calculated the BPI difference between the selected samples (observed – plain control).

The BPI differences were significantly larger than zero for all but the tape-shift board (Figure 5-10B, top row; a one-tailed test was used because we had a strong, *a priori* prediction based on the results of the circular track experiment; one-tailed cut-off value of the bootstrapped distribution with significance level $\alpha = 0.05$, Bonferroni corrected for 4 comparisons: leather-standard, 0.002; leather-shift, 0.008; tape-standard, 0.033; tape-shift, -0.174). This result implied that for all conditions but the tape-shift board, the field edges were more concentrated near the cue boundaries than expected by chance. A permutation test showed similar results,

although the leather-shift test lost statistical significance while retaining the same trend (Figure 5-10B, bottom row; for the standard boards, $p < 0.05$, two-tailed, Bonferroni corrected for 4 comparisons).

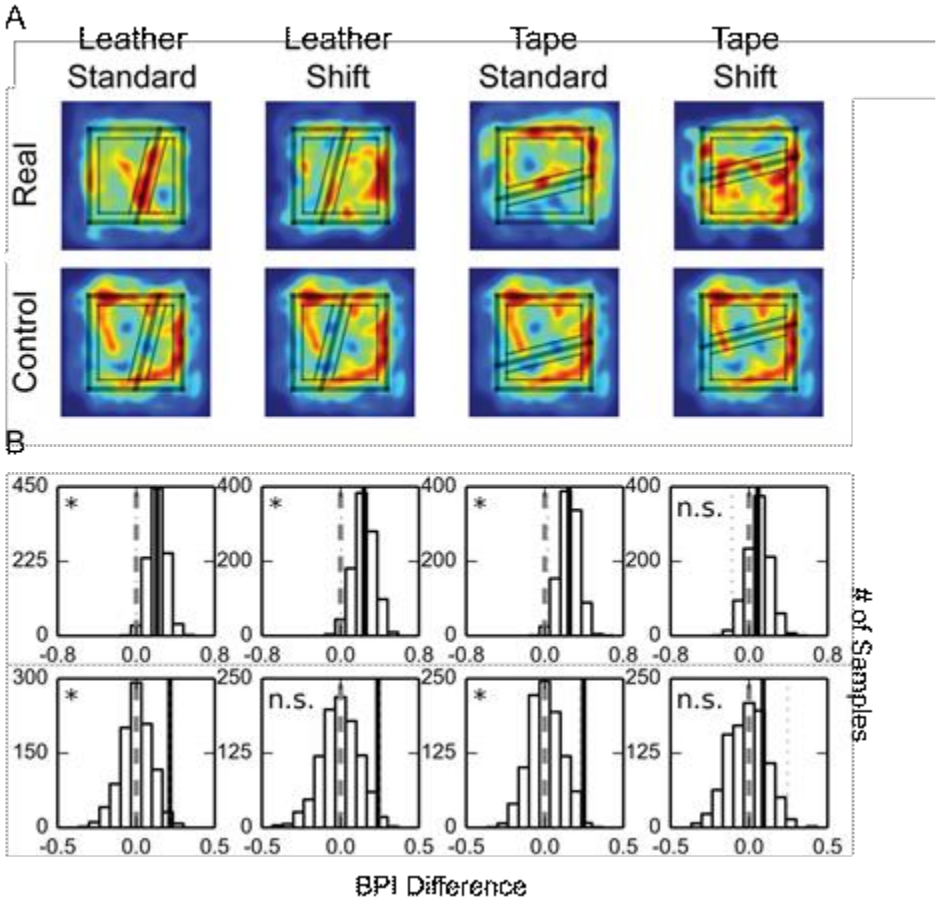

Figure 5-10 Place field edges concentrated near the surface boundaries

(A) The place field edge density maps of the simple boards (top) and the control plain board with zone markings from the corresponding simple boards (bottom). The rim of the platform and the cue boundary are labeled by thick solid lines, and the thin solid lines demarcate the boundary and non-boundary zones used in the analyses. (B) The bootstrapped distributions (top) and the permutation distributions (bottom) of the BPI difference. The details of the lines are as described in Figure 4-7.

As a final test, we predicted that the field edge density would peak near the cue boundary and decrease as a normal distribution as a function of distance to the boundary. Therefore we calculated the correlation between the field edge density

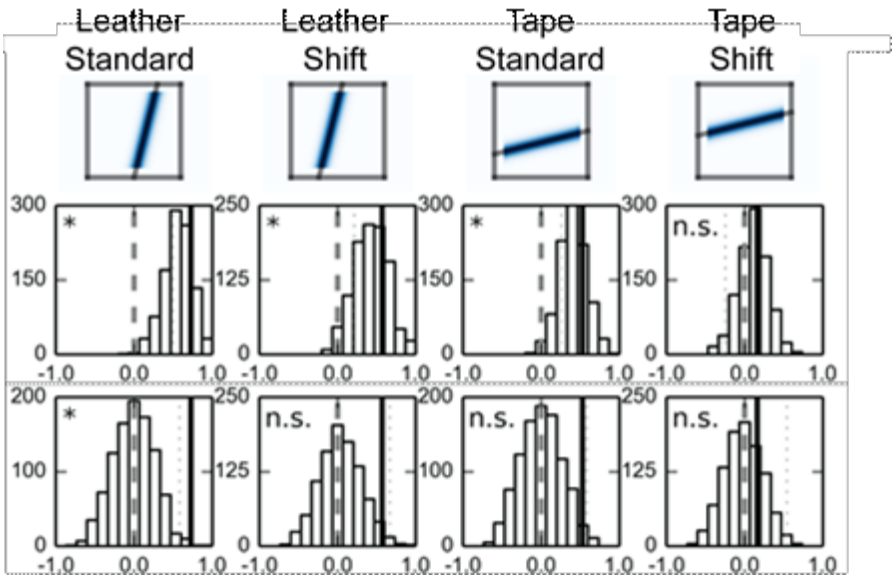

Figure 5-11 The field edge distributions near the cue boundaries on the simple boards were better described by a Gaussian-band than on the plain board

The Gaussian-band templates (top row), the bootstrapped (middle row) distributions of the correlation coefficient differences, and the permutation distributions (bottom row) of the correlation coefficient differences. The figure denotations are as described in Figure 4-10. The bootstrapped distributions were ased in that they did not center at the observed values. In order to adjust for the bias, the BCa cut-off value instead of the basic cut-off value was calculated. The significance remained the same when the basic cut-off was used (The one-tailed basic cut-off values: leather-standard, 0.533; leather-shift, 0.203; tape-standard, 0.251; tape-shift, -0.216.).

map and a Gaussian-band model (Figure 5-11, top row), and compared the correlations between the simple boards and the plain board control. The results were consistent with the BPI analyses (Figure 5-11, middle row, the one-tailed bias-corrected and accelerated (BCa) (Buckland *et al.*, 2006) cut-off value was calculated because the bootstrap distributions were not centered at the observed values, with significance level $\alpha = 0.05$, Bonferroni corrected for 4 comparisons: leather-standard, 0.498; leather-shift, 0.213; tape-standard, 0.264; tape-shift, -0.245. Bottom row, for the standard boards, $p < 0.05$, two-tailed, Bonferroni corrected for 4

comparisons.). The fact that the concentration effect was observed on the tape-standard board suggests that the effect was not merely a reflection of putative surface-texture-driven place fields, since the surface textures were the same on both sides of the tape-line boundary.

5.2.3 Adjacent place fields extended along the cue boundaries

The field edge concentration effect can be a result of (a) a disproportionate number of fields neighboring the cue boundary, (b) elongated field edges along the cue boundary, or (c) a combination of these possibilities (Figure 5-12). For all simple boards, the cue boundaries were not over-represented by the place field centers of mass (COMs) (Figure 5-13). Furthermore, the proportions of fields that had edges overlapping with the boundary zones on the simple boards were not significantly different from the plain-board control except for the tape-shift board (two-tailed χ^2 test with d.f.=1: leather-standard, χ^2= 0.0914, p=0.762 (n.s.); leather-shift, χ^2= 0.329, p=0.567 (n.s.); tape-standard, χ^2= 0.997, p=0.318 (n.s.); tape-shift, χ^2= 7.109, p=0.008 (*). α=0.05 with Bonferroni correction for 4 comparisons). The results were further verified with permutation tests (Figure 5-14A, only for the tape-shift sessions, $p < 0.05$, two-tailed, Bonferonni corrected for 4 comparisons).

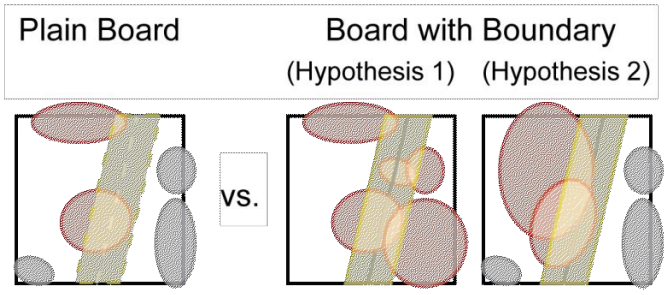

Figure 5-12 Hypothetical place field Potential Hypothesis

Schematics of different hypotheses explaining why the field edge density difference between the boundary and non-boundary zone was larger on the experiment boards than on the plain board. The place fields are denoted by colored circles, while the red ones represent the fields which increase the field edge density within the boundary zone. Hypothesis 1 suggests that more place fields overlapped within the boundary zone on the simple boards than on the plain board. Hypothesis 2 suggests that place fields tended to extended along the cue boundary on the simple boards but not on the plain board. These hypotheses are not mutually exclusive and it is possible that both phenomena are observed in the data.

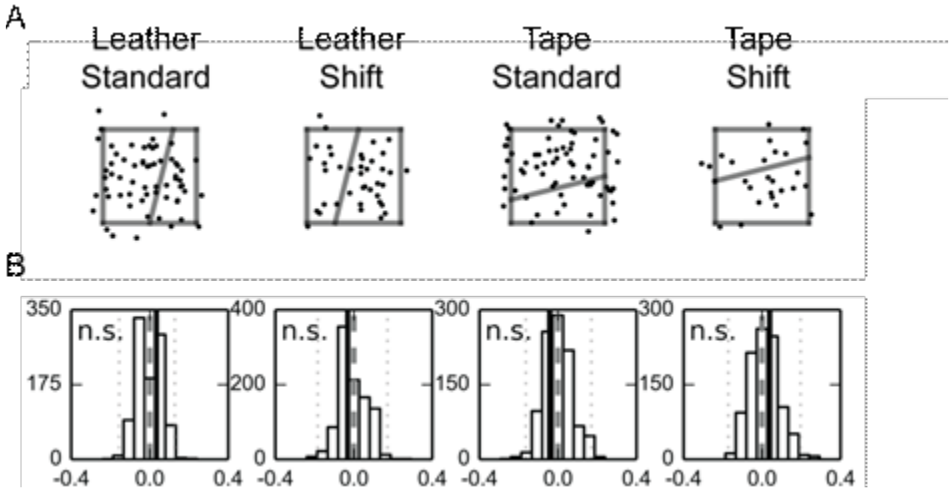

Figure 5-13 Cue-boundary was not over-represented by place field COMs

(A) The distributions of place field COMs. Each dot represents the COM of a field. The proportions of fields that had edges overlapping with the boundary zones on the simple boards were not significantly different from the plain-board control (B) The permutation distributions of the differences of COM proportions. The denotations are as described in Figure 5-10B.

On the other hand, the average edge lengths within the boundary zones, defined as the average number of spatial bins within the boundary zones containing a field edge, were significantly greater than the plain-board control except for the

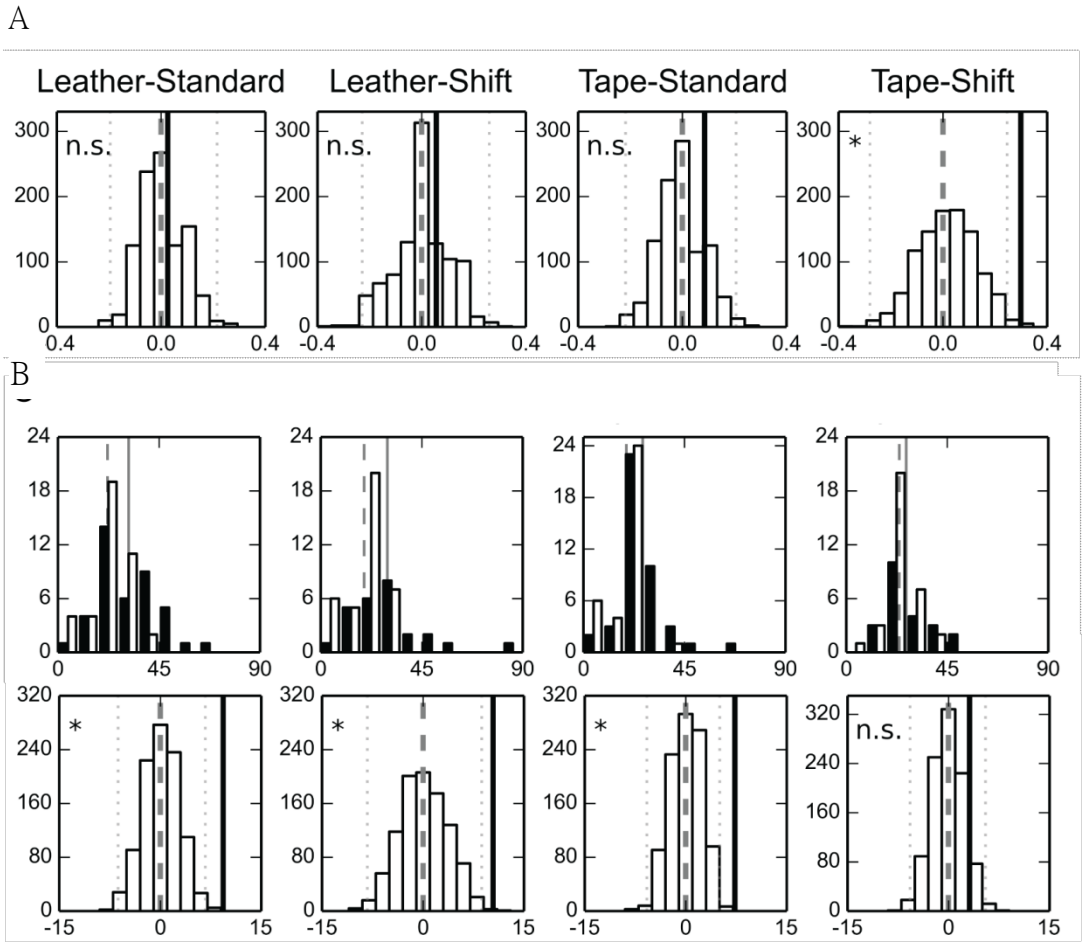

Figure 5-14 Adjacent fields extending along the surface boundaries

(A) Similar proportions of place fields overlapped with the boundary zone on the simple boards as on the plain board control except for the tape-shift session. (B) Longer field edges were found near the surface boundaries on the simple boards than on the plain board. (Top) The distributions of the field edge lengths within the boundary zone. The distributions of the field edge lengths collected from the simple boards are represented by black bars, with the mean values denoted by the solid lines; and the distributions of the plain board control are represented by white bars, with the mean values denoted by the dash lines. (Bottom) The permutation test of the edge length difference. For the permutation tests, the denotations are as described in Figure 5-10B.

tape-shift board (Figure 5-14B; two-tailed Mann-Whitney U test, n is the number of fields, and m is the median of the contour lengths: leather-standard, $n_{texture} = 41$, $n_{plain} = 40$, $m_{texture} = 30$, $m_{plain} = 22$, $U = 461.5$, $p < 0.001$; leather-shift, $n_{texture} = 26$, $n_{plain} = 38$, $m_{texture} = 28$, $m_{plain} = 22$, $U = 289.0$, $p = 0.003$; tape-standard, $n_{texture} = 43$, $n_{plain} = 35$, $m_{texture} = 25$, $m_{plain} = 22$, $U = 400.5$, $p < 0.001$; tape-shift, $n_{texture} = 22$, $n_{plain} = 33$,

$m_{texture}$ = 25, m_{plain} = 22, U=320.0, p=0.232. α = 0.05 with Bonferroni correction for 4 comparisons). The edge length analysis excluded place fields that did not overlap with the boundary zones. Thus, in the 2-dimensional environments, we observed higher field edge density differences than chance levels because the place fields close to the cue boundaries extended along the boundaries and therefore increased the length of the field edge aligned with the cue boundaries.

5.2.4 Population activity changes more rapidly across, rather than along, the boundary

The structures of the place field distributions described in the previous section suggested that the PVs at adjacent locations would be more similar when the animal moved along uniform surfaces than when it crossed the boundaries. To examine this hypothesis, for each location we calculated the movement direction along which the PVs changed most (Figure 5-15A; see Section 5.1.9 *Population vector direction of change analyses*). For all but the tape-shift board, the changes in PVs were the largest in the direction perpendicular (or near perpendicular) to the cue boundaries for most locations within the boundary zone; for the non-boundary zone, the directions varied at different locations and were more divergent (Figure 5-15B). To test this difference statistically, we first tested whether the directions of maximal PV difference were more concentrated in the cue-boundary zone than the non-boundary

zone. We computed the difference between the mean vector lengths (MVL) of the directional distributions of the two zones. When the rate maps were normalized by the peak firing rates before the construction of the PVs, bootstrapped distributions were significantly larger than zero for the leather boards but not for the tape boards (Figure 5-15C, bootstrap confidence intervals with significance level $\alpha = 0.05$, Bonferroni corrected for 4 comparisons: leather-standard, [0.180, 0.505]; leather-shift, [0.404, 0.781]; tape-standard, [-0.017, 0.333]; tape-shift, [-0.025, 0.326]). When the population vectors of firing rates were constructed based on the raw firing-rate maps, the bootstrapped distributions were significantly larger than zero for all but the tape-shift board (Figure 5-16)

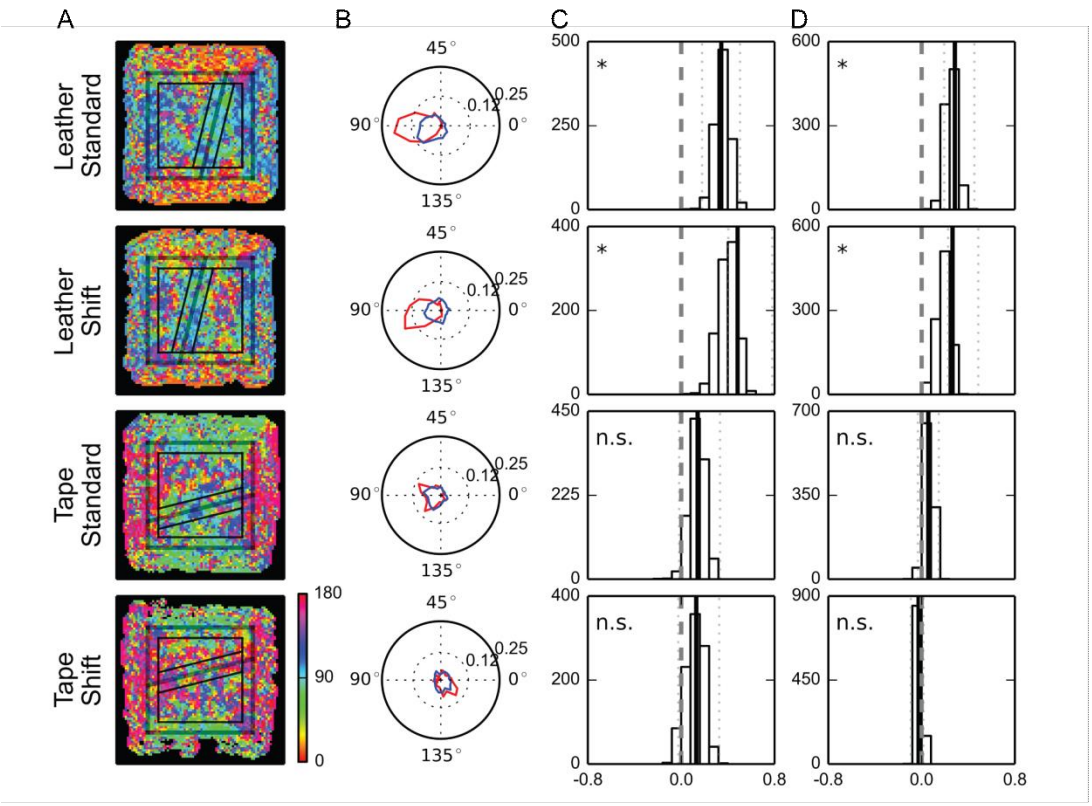

Figure 5-15 Population activity changes more rapidly across, rather than along, the surface boundary

(A) Visualizations of the movement directions at which the PVs changed most rapidly. Color red represents direction parallel to the surface boundary and color blue represents direction perpendicular to the boundary. The denotations of the lines are as described in Figure 5-10A. (B) The Rayleigh plot of the movement directions observed within the boundary zone (red) and the non-boundary zone (blue). The movement direction ranged from 0° to 180°, 0° when parallel with the cue boundary and 90° when perpendicular to the cue boundary. (C) The bootstrap distributions of the MVL differences. (D) The bootstrap distributions of the spatial bin proportion difference. For (C)(D) the denotations are as described in Figure 5-10B.

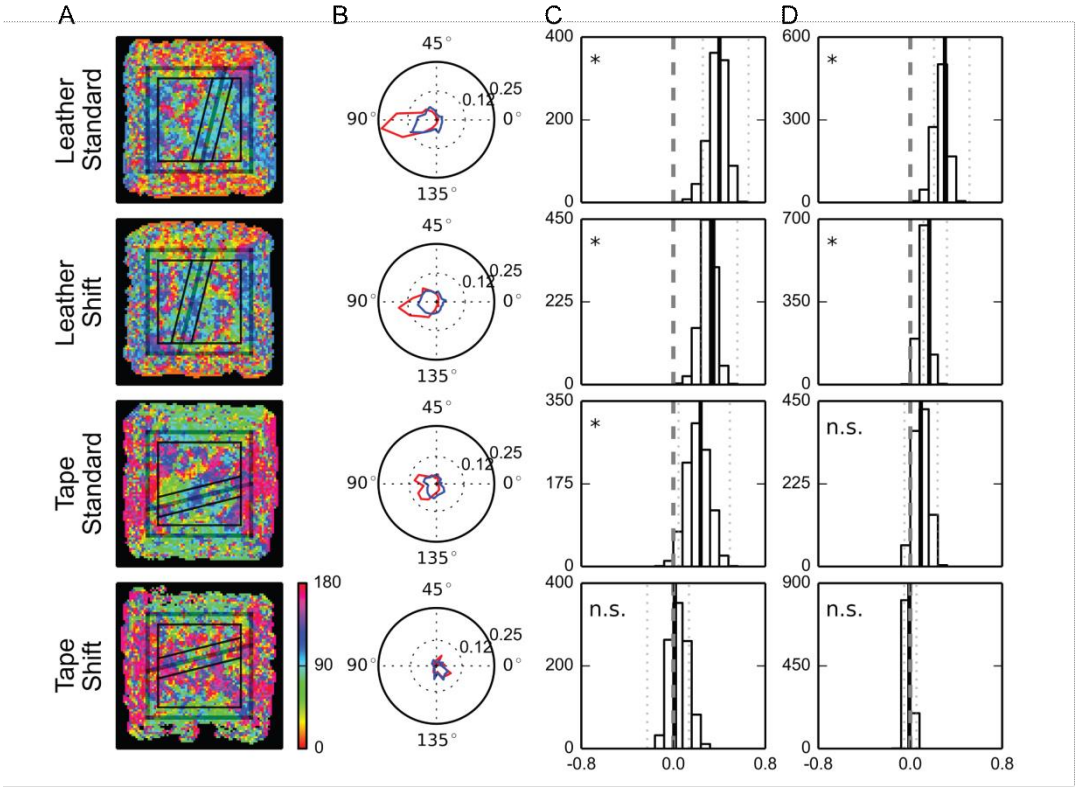

Figure 5-16 Non-normalized population activity change analyses

The same plots as described in Figure 5-15 except that the firing-rates were not normalized.

To determine whether the direction bias was preferentially perpendicular to the direction of the cue boundary, we calculated the proportion of spatial bins in which the movement directions were ±15° from the angle perpendicular to the cue boundary. Bootstrapped distributions of the difference in this proportion between the

boundary and non-boundary zones were significantly larger than zero for the leather boards; a similar trend was observed for the tape-standard board but was not significant (Figure 5-15D, bootstrap confidence intervals with significance level $\alpha = 0.05$, Bonferroni corrected for 4 comparisons: leather-standard, [0.206, 0.516]; leather-shift, [0.114, 0.319]; tape-standard, [-0.051, 0.238]; tape-shift, [-0.053, 0.054]). These results suggested that for the leather boards, the directions of maximal population decorrelation were significantly more consistent and perpendicular to the cue-boundaries when the animals were near the boundaries than when the animals were away from the boundaries.

5.2.5 Cue-boundary shifts triggered place cell remapping

For the simple board foraging task, the animal experienced two standard sessions followed by one shift session, and then one more standard session on each recording day (Figure 5-2). During the shift sessions, the cue boundaries shifted to new locations and induced context changes. Inconsistencies between firing-rate maps were observed when comparing the rate maps recorded in the standard sessions to the rate map of the same cell collected during the shift session. Among 28 place cells collected from the leather boards, 1 cell (3.57%) developed a field only in the shift session, and 6 cells (21.43%) had field(s) in the first two standard sessions but the field(s) disappeared in the shift session. For the tape boards, among 19 place cells

collected, 2 cells (10.53%) had field(s) appearing in the shift session, and 3 cells (15.79%) had field(s) disappearing in the shift session. (combined: 47 place cells, 3 (6.38%) appeared, 9 (19.15%) disappeared) A small proportion of fields demonstrated a strong boundary-modulation effect in that they either shifted with the cue boundary, or expanded or shrank correspondingly to the new boundary locations (Figure 5-17A).

To examine whether the place field remapped at a population level when the cue boundary shifted, we calculated the cross-correlation coefficients between the rate maps collected from the first two standard sessions, and compared that to the correlations between rate maps collected from the second standard session and the shift session (Figure 5-17B). The standard-shift correlations were significantly smaller than the standard-standard correlations (two-tailed p values reported. leather boards: paired t test, $p=0.003$; Wilcoxon signed-rank test, $p=0.003$. tape boards: paired t test, $p=0.007$; Wilcoxon signed-rank test, $p=0.005$. combined: paired t test, $p<0.001$; Wilcoxon signed-rank test, $p<0.001$), indicating that place cell remapping was triggered by the shift of the cue boundaries.

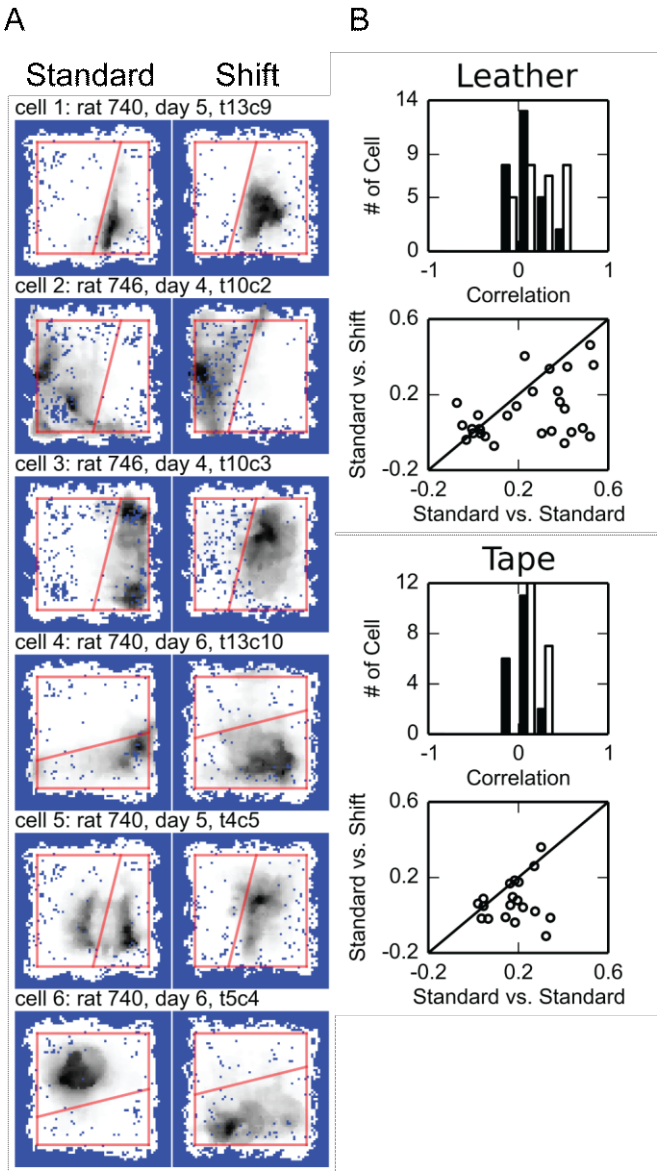

Figure 5-15 Shift of cue boundary triggered place cell remapping

Examples of place field changes when the cue boundary was shifted to a new location. Each row represents the data collected from the same cell in the standard session (Left) and the following shift session (Right). During the shift session, there were fields with edges that followed the boundary (cells 1-4), fields separated by the cue boundary merging into one field (cell 5), or fields flipping along the cue boundary (cell 6). (B) Remapping was observed between the standard and the shift session for the leather board. (Top) The distributions of the correlations between firing-rate maps from different sessions. The standard vs. standard correlation coefficients are denoted by the black bars, and the standard vs. shift correlation coefficients by the white bars. (Bottom) The scatter plots of the correlation coefficient pairs. The abscissa of the scatter plot is the correlation coefficient between two standard sessions and the ordinate is the correlation coefficient between the standard and the shift session. Most points were below the diagonal line, indicating that for most units the correlation coefficients were larger when comparing between the standard sessions than comparing between the standard and the shift session.

Chapter 6: Discussion

Previous studies have shown that the presence of boundaries can modulate the cognitive map and alter the perception of space. However, few studies strived to explain the underlying neural mechanism of the distorted spatial perception based on physiological data. In this current work, we focused on boundaries constructed by 2-D surface cues, which provide no obstruction to the movement and vision of an animal, and investigated the neural representation of such boundaries in the place field map with tetrode recordings. Enhanced decorrelation of the population neural activity was observed near the cue boundaries, which can be a potential physiological mechanism explaining an anisotropic representation of a compartmentalized space.

6.1 Neural representation of space decorrelated near the cue boundary because of concentration of field edges

We first examined place cell activity while rats ran counterclockwise on a 1-D circular track. The edges of the place fields concentrated near the local-cue boundaries (the transitions between different surface textures on the track), and this tendency produced an enhanced decorrelation of the population representations of different sides of the boundary. While salient global cues were also present in the

environment, place field edges did not seem to concentrate near the global-cue boundaries when they were not overlapped with the local-cue boundaries. Because place field properties can differ in 1-D and 2-D environments, we further scrutinized the field edge distributions on 2-D open fields with inhomogeneous flat surface cues. The field edges concentrated near the cue boundaries between different surface textures, and a weaker effect was observed near tape line markings. Abrupt decorrelation of the population vector (PV) of firing rates was observed near the cue boundary, and the PV changed most rapidly in the direction perpendicular to the boundary (most slowly in parallel with the boundary). When the cue boundary was shifted to another location, global remapping was observed, in that ~1/4 of the fields appeared or disappeared in the shift session, and complicated behaviors were seen for the rest of the fields.

In both 1-D and 2-D environments, our results suggest that the presence and location of the surface cue boundary can be retrieved from the place field map. The locations of the boundaries appeared to be encoded at the population level by a more rapid decorrelation of the ensemble representation of space as the rat crossed the boundary, compared to when it moved an equivalent distance in the center of a texture segment or along a boundary. A downstream structure able to decode the rate of change of the neural representation would thus be able to detect the presence of

the boundary. This neural coding scheme may result in a psychological perception that the mental distance between two locations across a surface cue boundary might be elongated.

6.2 Concentration of field edges may elongate the mental distance across a boundary

At a local scale, the magnitude of correlation between the hippocampal representations of different locations reflects the physical distance between the locations. In an environment where the place fields are homogeneously distributed, if two locations are not farther apart than the average size of place fields (i.e., the spatial scale factor), the distance between them would be negatively correlated with the similarities between their neural representations (McNaughton, 1998). However, if the distribution of place fields is inhomogeneous, such that the correlation between population firing rate vectors of neighboring locations can vary, the mental distance between these locations might vary accordingly. In our data, the surface cue boundaries were encoded by a concentration of place field edges, and this representation decreased the correlation between the population firing rate vectors across the boundaries. We therefore hypothesize that a ‘mental gap’ would be inserted in the animal’s perception of distance traveled whenever an animal moved across or mentally traversed through the boundary.

The insertion of mental gaps may also elongate the perceived distance between locations at a more global scale. When two locations are sufficiently far apart, such that there is no longer any overlap in the population of place cells encoding the locations, the representations are maximally decorrelated with no further relationship to longer distances. However, the brain may estimate distance between two remote locations by integrating distances between neighboring points connecting these locations. The mental distance between any two locations across the surface texture boundary may thus be elongated, since they would be connected by paths including the mental gap. It has been shown in other sensory systems that a local change near the boundary can elicit a global perceptual effect. For example, the Cornsweet Illusion (Cornsweet, 1970. Figure 6-1) demonstrates that when two areas of equal brightness are separated by two local illumination gradients at the border, the entire areas are perceived as having different brightnesses defined by the strong contrast that exists only at the border. The perception of spatial segregation might similarly be mediated by neural mechanisms that can extend the mental gaps generated at the boundaries to regions farther from the border, creating a global percept of greater distance across the entire environment.

The ‘mental gap’ hypothesis may help explain certain phenomena from the human literature regarding distorted representations of space. When requested to

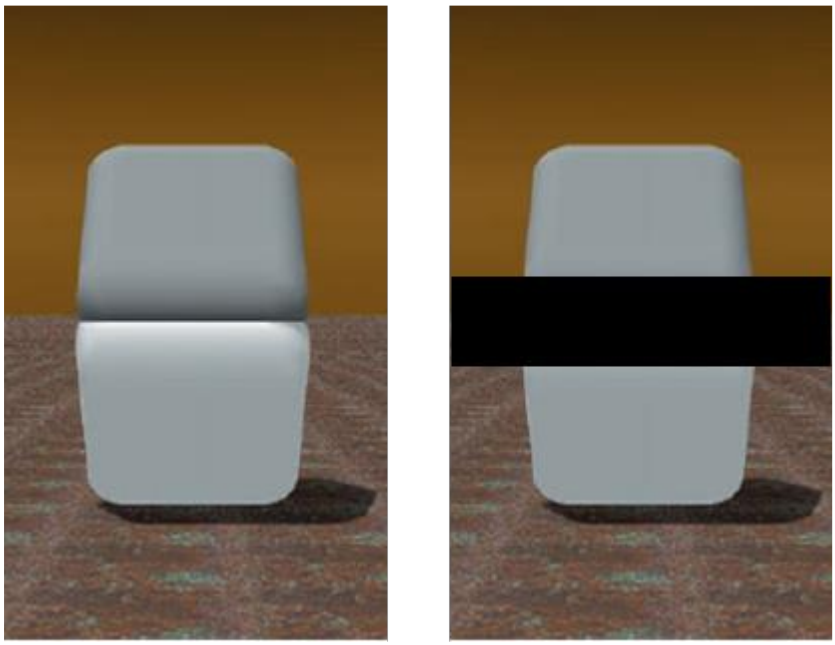

Figure 6-1 The Cornsweet illusion

The Cornsweet illusion (Cornsweet, 1970) demonstrates how a local change of illumination can affect the perception of the entire area. On the left hand side is a gray surface, with local illumination gradients near the middle line. The upper part of the surface seems to be slightly darker than the lower part, even though they actually share the same brightness. The equivalence is obvious when the central band with gradients is hidden (right). The colors of the upper and the lower parts appear to be identical with the presence of the black band. The figures are modified from Purves *et al.*, 1999

memorize the locations of objects or landmarks in a compartmented environment, people tend to underestimate distances between targets within the same spatial compartment and overestimate distances between targets in different compartments (Allen, 1981; Hirtle & Jonides, 1985; Kosslyn *et al.*, 1974; McNamara, 1986; McNamara *et al.*, 1989; Newcombe & Liben, 1982). Similarly, judgment errors in relative spatial relationships increase when two objects are located in different spatial compartments (Greenauer & Waller, 2010; Han & Becker, 2014). Even when there are not explicit boundaries (i.e., physical barriers, markings, or discrete

transitions in context) in an environment, subjects tend to exaggerate the distance between two locations if the locations are in two conceptually distinct regions connected by a smooth transition (e.g. woods gradually changing into a field) (Allen, 1981; Hirtle & Jonides, 1985). The systematic errors in estimating angles or distance suggest that the psychological representation of space is not isomorphic to physical space, and our results might provide insight into the underlying physiological mechanisms instantiating local anisotropies or other distortions of the mental representation.

6.3 Alternative hypotheses accounting for the concentration of field edges

Although the potential association between neural decorrelation and surface boundary matches well with the human literature, there are alternative hypotheses explaining why the field edge concentrated near the cue boundaries. One possibility is that a proportion of the 'place fields' was actually driven by the local sensory features of specific surface textures, rather than encoding the abstract concept of space. Such fields would start and end at the texture boundary simply because the cells were activated when the animal was on their preferred textures, and inactivated when the animal left the textures. As a result, more fields than expected by chance would be observed to fill up one or multiple surface texture patches, and have both

of their edges near the texture boundaries. The influence of these texture-driven fields can be excluded by examining the distribution of field edges only for the fields with a single edge (start or end) near the local-cue boundary (i.e., by removing all fields in which both start and end edges correspond to texture boundaries). However, in a more complicated situation, in which a cell might be simultaneously driven by animal position and local non-spatial features, thus potentially producing fields with none or only one edge at the texture boundary, it would be nearly impossible to identify these fields. Therefore, we cannot dissociate the boundary-related and texture-related causations of the field edge concentration effect if such complex conjunctive firing activity exists.

There has been evidence demonstrating that some hippocampal complex-spike cells are driven by specific surface texture cues (Shapiro *et al.*, 1997; Young *et al.*, 1994). These cells have firing fields that follow the displacement of a single surface texture cue even when the manipulation altered the topological relationships between cues. When rats were performing a non-spatial task on a plus maze with interchangeable surface texture inserts on each arm, about 20% of the cells had firing patterns attached to the texture encountered by the animal but not to the location of the texture on the maze, and about half of the fields only fired when a specific texture was presented at a specific location (Young *et al.*, 1994). On a similar maze,

when rats were performing a foraging task with no fixed reward location, about 10% of the fields were observed to follow specific texture cues when the texture patches on different arms were scrambled (Shapiro *et al.*, 1997). The firing fields of these cells did not necessarily cover the entire surface texture patch, which implies a conjunction effect of animal location and local sensory input. These results support the hypothesis that there might be potential confounds caused by texture-driven activity.

Nevertheless, our data indicate that this is unlikely to be the case at least for the 2-D environment. On the tape-standard board, field edges concentrated near the tape boundary which segregated two subareas sharing the same surface texture, and this effect cannot be explained by the disparity between textures across the surface boundary. The fact that the concentration effects observed on the tape boards were weaker compared to the leather boards might suggest that a combined result of boundary representation and texture-driven firing was observed on the leather boards.

The second alternative explanation is that the saliency of the surface boundary triggered behavioral inhomogeneity, which further led to concentration of place field edges. We eliminated potential artifacts caused by behavioral differences by applying different velocity and movement direction filters before the construction of the

firing-rate maps. However, there remains a remote possibility that the field edge distribution can be affected by an imbalanced head-scanning distribution. The head-scanning behavior is known to trigger the formation of new place fields near the scanning locations (Monaco *et al.*, 2014). Since the rat scanned the environment more often when it was near the local-cue boundaries in our 1-D environment, the field edge concentration effect may be a consequence of preferential head-scanning behavior. While we showed that the prevalence of head-scanning within the boundary window was not correlated with the prevalence of place field edges within the window across animals, we cannot examine nor exclude potential historical effects caused by the head-scanning behavior that happened during the training stage before recordings started.

In the 2-D environments, there is indirect evidence against the notion that the field edge concentration effect is related to scanning-triggered field formation. The freedom to move at arbitrary directions in a 2-D environment hindered us from successfully segregating lateral head movements from forward movements, let alone isolating the head-scanning event from the epochs of lateral movements. Therefore, the influence of the head-scanning behavior could not be examined directly on the open fields. However, based on the observation that similar proportions of fields were observed near the surface boundary locations for most of the simple boards

compared to the plain board, we concluded that there was not a significant field number difference near the boundary. This result indirectly precludes the possibility that the field edge concentration effect was primarily caused by the accumulation of new place fields recruited by head-scanning behavior.

Overall, our results argue against the alternative explanations and suggest that the field edges concentrated to encode the cue boundaries. Neither texture-driven sensory inputs nor inhomogeneous head-scanning distribution seemed to be the determining factor which led to the concentration of field edges. However, they might have further increased this tendency. Even if the field edge concentration effect is indeed a side effect of texture-driven firing or scanning-triggered potentiations, the mental distance across the boundary might still be elongated based on the mental gap hypothesis. In other words, the perception of spatial segregation could be passively generated upon experiencing local contextual changes or visiting preferred head-scanning locations, even though the internal boundary itself was not actively encoded by the cognitive map.

6.4 A universal neural coding mechanism for representing boundaries

There are a number of well-studied, neural coding mechanisms that the hippocampus might have used to represent the surface cue boundaries in our

experiments. First, the hippocampus might have overrepresented the boundary by developing a larger number of place fields along the boundary, similar to the overrepresentation previously shown for the peripheral borders of an environment (Hetherington & Shapiro, 1997), starting sites (Ainge *et al.* 2007; Grieves *et al.*, 2016) or goal locations (Hollup *et al.*, 2001; Kobayashi *et al.*, 1997). However, our analyses of place field locations provided little evidence for a disproportionate number of place fields located at the texture boundaries. Second, the place cells might have fired at a higher or lower mean rate at the boundaries than in the middle of the textures. Again, our analyses showed little evidence of such rate coding of the boundaries. Instead, our results emphasize the importance of the exact contour of a place field, and suggest a novel mechanism that the surface boundaries are encoded by accelerating the decorrelation rate of neural representation near the boundary.

A subsequent question is whether such a neural coding scheme is generally adopted upon encountering separating boundaries, that is, whether decorrelation of neural representations has been, or is expected to be, observed when different types of internal boundaries were presented. Tall and opaque walls have been widely used to construct experimental chambers and to segregate environments, and place fields are known to over-represent the periphery but not the center of a chamber encompassed by such walls (Hetherington & Shapiro, 1997). In a compartmentalized

environment, if a similar over-representation phenomenon was observed within each spatial compartment, and the place fields were confined within individual compartments, then we would expect to see a high prevalence of place field edges near the internal wall as well. Although it would be impossible for an animal to cross the boundary (i.e. wall) directly in the physical world, the mental distance across the boundary might still increase when the animal mentally transversed through these boundaries. If the proposed neural activity pattern is observed in such wall-separated environments, we can assume that the mental gap theory is also applied to opaque, movement-restricting internal segregations.

Prior studies of hippocampal correlates of spatial segmentation focused on how place cells distinguish similar, connected environments (Fuhs *et al.*, 2005; Grieves *et al.*, 2017; Grieves *et al.*, 2016; Singer *et al.*, 2010; Skaggs & Mcnaughton, 1998; Spiers *et al*., 2015). In these studies, a significant number of place cells repeated their firing patterns in geometrically corresponding locations across perceptually similar compartments with high walls oriented in the same direction. Analogous repeating firing patterns were also seen in grid cell maps when rats ran through a hairpin maze (Derdikman *et al.*, 2009) or on early exposure to an environment consisting of two visually identical boxes connected by an external corridor (Carpenter *et al.*, 2015). However, when the compartments were oriented differently,

place cells were able to distinguish the compartments and did not repeat their firing fields, presumably because the head direction cell system was able to discriminate the orientation of the boundaries across the compartments (Fuhs *et al.*, 2005; Grieves *et al.*, 2016). The distributions of place field edges were not reported in these studies since it was irrelevant to the question being investigated. Hence, it is still unclear whether the decorrelation effect was observed across opaque walls that segregate an environment.

The observation made by Spiers *et al.* (2015) might indirectly support the idea that rapid decorrelation of neural activity is a generalized neural coding mechanism for representing spatial segregation. In daily life, we tend to segregate a space by the presence of doorways (Radvansky & Copeland, 2006). While the distribution of the place field edges was not examined, Spiers *et al.* (2015) reported that place fields clustered near doorways as the rats foraged between four perceptually similar boxes, which were connected to an exterior corridor through doorways. If the place fields were flanking the doorways and accumulating field edges, the correlations between the PVs across the doorways would presumably decrease, and the perception of spatial segregations might thus be triggered by doorways.

The mental gap hypothesis was developed based on the observation that spatial proximity breeds similarity in neural representations, and the same trend was also

observed along the temporal axis. Episodic memory is composed of a series of concatenated events. While the temporal flow is always continuous, discrete contextual changes can often be observed and used to segregate individual temporal events (DuBrow & Davachi, 2013). For example, the sensory changes that occur upon entering a coffee shop might denote the onset of a conversation event that happened in the coffee shop. Analogous to the distorted perception of distance in a compartmentalized space, the judgement of temporal proximity between two time points is affected by contextual segregation of different events. In the work presented by Ezzyat and Davachi (2014), a series of image pairs were sequentially displayed to the human subjects. Each image pair was composed of an object or a famous face, accompanied by an outdoor scene. The subjects were requested to imagine the object or the celebrity located within the scene. The series of image pairs constructed a temporal sequence, and the subjects tended to classify two objects/faces as temporally distant if they were paired with different background scenes, and temporally close if the contexts were the same. Interestingly, when two objects/faces were paired with different scenes, the estimation of temporal proximity between them could be predicted by the hippocampal pattern similarity in BOLD activity. This work demonstrates that segregation induces distorted representation also in the temporal domain, and suggests that the similarity between neural signals reflects the

temporal distance between the corresponding time points being represented.

Terada *et al.*(2017) further showed that the linkage between segregating boundaries and decorrelation of neural signals can be observed along the temporal axis. In rats, the onset of a temporal event (i.e. the delivery of an odor stimulus) was marked by transient shifts of firing rates and theta phases of CA1 complex-spike cells. Some of these cells exhibited such temporal and rate coding only when the preferred odor stimulus was preceded by a specific auditory stimulus and followed by a specific behavioral response. The authors concluded that such cells encoded the onset of a unique event rather than being driven by bottom-up sensory inputs. As a consequence of the rapid rate changes of the cell population, decorrelation of neural activity was observed at the event boundary. These results suggest that the same neural coding scheme might be used to encode the concept of a boundary across both the temporal and the spatial dimensions.

6.5 Interpretation of the geometric module studies on 2-D boundaries

The observed neural representation of flat surface cue boundaries might appear to be contradictory to the geometric module studies. As mentioned in Chapter 2, human children and chickens failed to use flat surface cue boundaries to reorient themselves (Lee & Spelke, 2011; Lee *et al.*, 2012). One might thus conclude that

boundaries constructed by such cues were undetected by the cognitive mapping system, thereby precluding the influence of the geometric module. Our results demonstrated, however, that even when the spatial compartments were segregated by flat surface cues, the demarcation information was present in the cognitive map. Therefore, information about the presence of geometric boundaries may be dissociated from the use of this geometric information for orientation. Although the influence of environmental geometry on head direction cell tuning is influenced by complex factors (Clark *et al.*, 2012; Dudchenko & Zinyuk, 2005; Knight *et al.*, 2011), it is nonetheless possible that the geometry-controlled reorientation phenomenon is caused in large part by geometric control over these cells. In turn, the head direction cells can reorient downstream grid cells and place cells by virtue of their close coupling (Knierim *et al.*, 1995; Knierim *et al.*, 1998; Sargolini *et al.*, 2006). Alternatively, the reorientation may be largely dependent on boundary-selective neurons (Lever *et al.*, 2009; Savelli *et al.*, 2017; Savelli *et al.*, 2008; Solstad *et al.*, 2008), which may not respond to the floor texture boundaries of the present study. In any case, the reported inability of organisms to reorient to geometric boundaries defined by flat surfaces does not necessarily imply that the spatial representations of these shapes are not encoded.

6.6 Local cues modulate the underlying distributions of place fields

Another substantial implication of the current work is that local sensory cues can modulate the cognitive map by defining the contours of the place fields. It was not until recently that the importance of local cues in modulating the cognitive map had been appraised. Previous studies have demonstrated that surface texture cues can be used as reference points to anchor the cognitive maps or trigger remapping when the cue configuration were conflicting with other sensory cues in the environment (Shapiro et al., 1997; Brown & Skaggs, 2002; Knierim, 2002; Knierim and Hamilton, 2011). It has also been shown that when associated with rewards, the presence of local cues can attract place fields and cause inhomogeneity in the place field map (Gothard *et al.*, 1996). However, no studies have examined whether local cues that are task-irrelevant and have neutral valence can also trigger such over-representation of place fields. Our task did not require the rats to remember the surface boundary location, and the boundary was not associated with rewards or given valence. Even so, inhomogeneity in the place field map was observed, and the boundary cue locations were represented by the concentration of the field edges, not of the centers of mass of the fields. These results demonstrate a novel way that the local cues can modulate the cognitive map.

In our 1-D environment, the field edges concentrated near the local-cue boundaries but not the global-cue boundaries. This finding seconds the idea that the local cues can dominate in controlling the cognitive map even in the presence of salient global cues. However, it is worth noting that the global and local cues used in the experiment were perceptually different in many aspects, and such differences might have affected the interpretations of the results. In our double rotation experiment, the global cues were visually salient objects placed at a distance from the rats, and the local cues were multi-modal surface markings which were immediately accessible to the rats. While the local-cue boundaries could be unambiguously mapped onto specific locations on the track and immediately sensed by the animals upon traversal, the distances to the global cues, together with the widths of the global cues, abolished such possibilities for the global-cue boundaries. The rat might have projected the same global-cue boundaries to various locations on each lap, and smeared out the field edge concentration effect near the global-cue boundaries. Also, it seems more intuitive to segregate an environment based on a demarcating line (the transition between different texture surfaces) than a reference point (object). Therefore, the dominant role of the local-cue boundaries observed in our experiment might be challenged if the local and global cues were more comparable.

The influence of the local cues over the cognitive map is also reflected in the remapping of place fields triggered by the movement of the surface boundary. It had been previously published that in the double rotation task, a significant amount of place fields globally remapped (i.e., the place field appeared, disappeared, or translocated to a random location) when the local cues and the global cues rotated in opposite directions (the MIS sessions). In the 2-D environments, a small number of fields had field edges that followed the translocation of the surface boundary, and global remapping was observed at the population level in the shift session. However, instead of shifting the surface cues of the same board, a different experimental board with a corresponding surface pattern was used during the shift session. Hence there is a slight possibility that the subtle differences between experiment boards, but not the shift of surface boundary, might have triggered the remapping.

In sum, the current work demonstrates a potential novel neural coding scheme representing local surface cue boundaries. The results broaden our understanding of the potential features essential for constituting a boundary, and possess psychological implications that explain certain perceptual distortions caused by spatial segregation. The results also suggest that task-irrelevant local features can trigger inhomogeneity in place field distribution by shaping the contours of the fields. This thesis sheds light on understanding how the perception of spatial segregation can be formed.

However, there is no direct evidence showing that an organism would perceptually segregate the environment based on these surface cue boundaries, and further work needs to be done to investigate this possibility.

Chapter 7: Future Work

Although the current results imply the possibility that the perception of spatial segregation can be triggered by flat surface boundaries, there was no direct evidence verifying this hypothesis. The possibility remains that the segregation-irrelevant features associated with the boundary, such as its saliency or the elongated nature, triggered the concentration of place field edges. Here we specify two potential directions to examine this possibility. First, a surface cue boundary would not be regarded as a demarcation line segregating the space, at least not intuitively, if it is part of a continuous pattern. For example, while multiple boundaries can be observed in a stripe pattern, none of them would be recognized as a separating line because of the continuity of the global pattern across the boundary. In Figure 7-1 (Experiment A) we demonstrate an example experiment board design instantiating this idea. In this experiment setup, the two right-most surface texture patches are identical across boards, and constitute two comparable surface boundaries on different boards. However, only on the test board does the boundary seem to divide the environment into distinct spatial compartments, and we predict that the field edges would only concentrate near the surface cues on the test board as the animal forages on the board.

The second direction utilizes the concept of enclosure. Theoretically, a spatial compartment is formed when a subarea is enclosed by boundaries (perhaps with small gaps such as doorways) and becomes isolated from the rest of the environment. We can thus evaluate the necessity for the boundary to segregate an environment by comparing two sets of boundaries, one that constitutes an enclosure and one that does not. We can use two rectangular boards that are identical in size and surface texture, but marked by different tape linings serving as internal surface boundaries (Figure 7-1, Experiment B). The internal boundaries on the two boards are identical except for their orientations. On the test board, the internal boundary is parallel with the short edges of the board and contacts the rim of the board at both ends and thus segregates the board into two subareas; on the control board, the internal boundary is perpendicular to the short edges and does not intersect with the rim of the board nor form a spatial enclosure. While in this example the orientation of the surface cue is not controlled, the potential interference caused by orientation change can be easily ruled out by applying the same experimental design onto two square boards (enclosures would be formed on both square boards) and see if the edge concentration effect is observed on both square boards regardless of the orientation of the internal boundary.

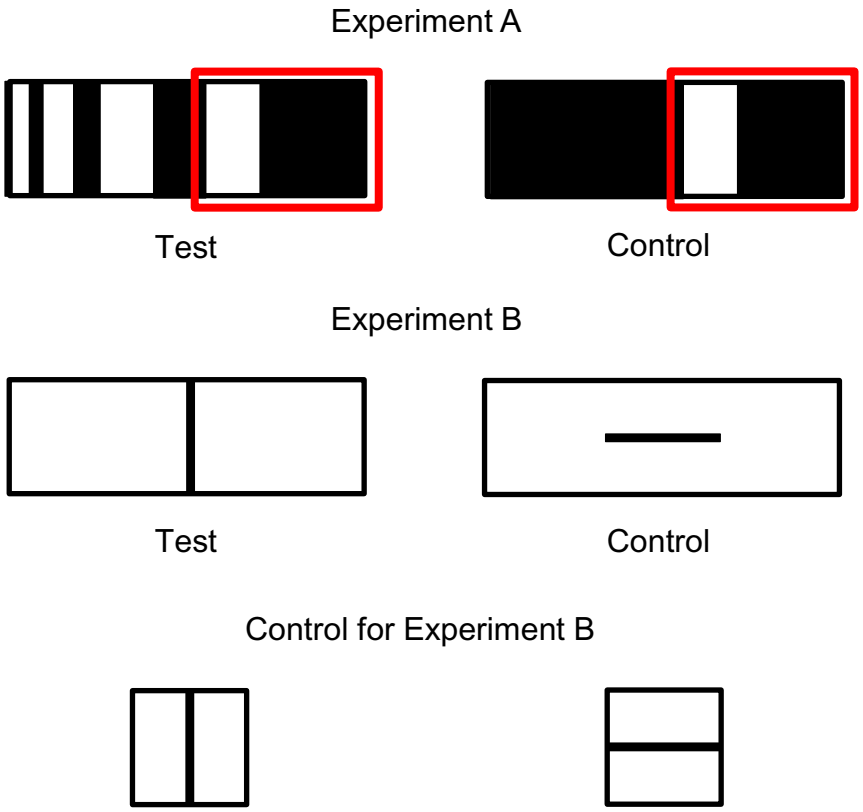

Figure 7-1 Schematic cartoons of experiment designs

The top-down view of the arena used in two different experiments which are designed to examine whether the place field edge concentration effect is only observed when the surface boundary segregates the space. The black and white patches in experiment A denote different surface textures. The subareas encompasses by the red rims are identical across the two boards, and thus the texture boundaries are comparable across boards. The thick black lines in experiment B denote tape linings

We can also seek behavioral evidence demonstrating perception of spatial segregation with the presence of a surface boundary. The distance estimation task used in the human literature quantifies how much the mental representation of space is distorted and can serve as an appropriate task to evaluate the influence of a surface boundary. However, modifications are required in order to apply the descriptive task to nonverbal animals. In the counterpart of the distance estimation task, the animal can be trained to reach and wait inside a reward zone after leaving the start zone to

receive rewards. Both the reward zone and the start zone are unmarked areas on a circular track placed in an environment with no deliberate polarizing cues. During the training phase, the reward zone and the start zone is separated by a surface cue boundary. Once the animal has an accurate estimation of how far it needs to move from the start site to get rewards and can successfully perform the task, the probe phase starts in which the animal performs the same task with the surface cues removed. It is worth noting that during the probe phase the animal cannot use the boundary as a reference point, and needs to depend on idiothetic cues to identify the location of the reward zone. We predict that the animal would tend to overestimate the distance between the start and reward zone and go beyond the reward zone during the probe phase. An alternative explanation of the overestimation of distance is that the animal solves the task by learning the distance between the boundary and the reward zone, and tends to keep moving forwards until it has passed the boundary. A control experiment with the surface cue boundary remaining present during the probe phase, but shifted towards the starting zone can be used to exclude this possibility. The animal is expected to underestimate the distance between the start and reward zone if its estimation is based on the location of the boundary.

Another fundamental question related to the current work is the origin of the field edge concentration effect. Within the hippocampus, the major connection

circuit guides the information flow from the DG to CA3 and then CA1. We recorded place cells from CA1 in both 1-D and 2-D environments, and from CA3 only in the 1-D environment. In all cases the field edge concentration effect was observed, suggesting that the boundary information is encoded by the place field map as early as CA3. However, it is still unclear whether the representation of environmental boundary already arises at DG, or if it is not until the CA3 region that the information starts to show. Different types of boundaries have been shown to activate the boundary vector cells (BVCs) in subiculum and the border cells in MEC. Both brain areas send outputs to the CA areas, and place cells may receive boundary information from these cells. It is still unknown whether a flat surface cue can trigger the BVC and border cells like other traditionally defined boundaries (e.g. walls, apparatus edges, etc.). Also, it has been hypothesized that the place cell firing pattern arises from combined grid cell inputs (Solstad *et al.*, 2006). Thus it is important to examine whether and how the grid fields are modulated by the surface boundaries in order to understand the underlying mechanism of the field edge concentration phenomenon.

In the current work, we focused on analyzing the firing rates of the place cells, but did not examine whether the boundary information is also represented by theta-related coding mechanisms. The activity of hippocampal complex-spike cells is

entrained to the theta oscillation, and it has been shown that information can be encoded by the phase of theta at which a place cell fires. For example, the onset of a temporal event can be represented by a swift shift of the theta phases (Terada *et al.*, 2017). It is possible that a universal coding mechanism is used to represent boundaries in both temporal and spatial domains, and similar theta phase transitioning might also be observed near a surface boundary.

The boundary information might also be reflected in the spike sequences observed during a theta cycle. When a rat is moving in an environment, place cells are activated in sequence reflecting the order of the place fields the animal has passed through (Foster & Wilson, 2007). The firing sequence repeats itself in a time-compressed manner within individual theta cycle, and this firing pattern is called the 'theta sequence' (Foster & Wilson, 2007). Each theta sequence corresponds to a physical path denoted by the locations of the activated place fields. When a rat was trained to run in a modified figure-8 maze, the corresponding path of the theta sequence extended to the turning points of the track, as if the sequence was representing different spatial segments of the track (Gupta *et al.*, 2012). In our data, the theta sequence might also extend to the surface boundaries and signify the spatial segregation defined by these boundaries.

At the end of this dissertation, we proposed a few potential research directions

to help further understand how a segregated space can be perceived and represented by the cognitive map system. More general, we hope the current work informs future studies of the functional role played by the hippocampus in spatial representation, navigation, and the formation of episodic memory.

Appendix A

The firing rates of different place cells formed the population vector of firing rate $\vec{r}$, which is a function of the physical location of the animal:

$$\vec{r}(x,y) = [r_1(x,y), r_2(x,y), \cdots r_n(x,y)]^T,$$

where $r_i(x,y)$ is the smoothed mean firing rate of the i^{th} place cell.

When the animal moved from (x_0, y_0) to (x_1, y_1) on the experiment board, there would be a corresponding change in the population vector

$$\begin{aligned}\Delta\vec{r} &= [r_1(x_1,y_1), r_2(x_1,y_1), \cdots r_n(x_1,y_1)]^T - [r_1(x_0,y_0), r_2(x_0,y_0), \cdots r_n(x_0,y_0)]^T \\ &= [r_1(x_1,y_1) - r_1(x_0,y_0), r_2(x_1,y_1) - r_2(x_0,y_0), \cdots r_n(x_1,y_1) - r_n(x_0,y_0),]^T\end{aligned}$$

For any point (x,y) close to (x_0,y_0), $\vec{r}(x,y)$ can be linearly approximated by its tangent plane $T(x,y)$ at (x_0,y_0):

$$\vec{r}(x,y) \approx T(x,y)$$

Similarly, $\Delta\vec{r}$ can be approximated by the corresponding change on the tangent plane:

$$\Delta\vec{r} \approx \Delta T = T(x,y) - T(x_0,y_0)$$

In order to compute $T(x,y)$, for each spatial bin we calculated the Jacobian matrix:

$$\mathrm{J}(x,y) = \begin{bmatrix} \frac{\partial r_1}{\partial x} & \frac{\partial r_1}{\partial y} \\ \vdots & \vdots \\ \frac{\partial r_n}{\partial x} & \frac{\partial r_n}{\partial y} \end{bmatrix}$$

The Jacobian matrix at (x_0,y_0) transforms a point close to (x_0,y_0) to its corresponding location on the tangent plane $T(x,y)$. In other words, we can linearly

approximate $\vec{r}(x, y)$ near (x_0, y_0) by calculating the Jacobian matrix $J(x_0, y_0)$, and

$$T(x, y) = J(x_0, y_0) \cdot \begin{bmatrix} x - x_0 \\ y - y_0 \end{bmatrix} + T(x_0, y_0)$$

Therefore,

$$\Delta\vec{r} \approx J(x_0, y_0) \cdot \begin{bmatrix} x - x_0 \\ y - y_0 \end{bmatrix}$$

We quantify $\Delta\vec{r}$ by the Euclidean distance between two population vectors ($\|\Delta\vec{r}\|$). The heading direction on the x-y plane that led to the strongest change in the population vector of firing rates would thus be the same direction that led to the longest displacement on the tangent plane. In other words, we were looking for the heading direction $[x - x_0,\ y - y_0]^T = [\cos\omega\,, \sin\omega]^T$ that maximized $\|\Delta\vec{r}\|$, and solving $\underset{\omega}{\operatorname{argmax}}\|\Delta\vec{r}\|$ is equivalent to solving

$$\underset{\omega}{\operatorname{argmax}} \left\| J(x_0, y_0) \cdot \begin{bmatrix} \cos\omega \\ \sin\omega \end{bmatrix} \right\|$$

The solution ω can range from 0° to 360°, however, given the linearity of function ΔT

$\|\Delta T(\cos(\omega + \pi)\,, \sin(\omega + \pi))\|$

$= \|\Delta T(-\cos\omega\,, -\sin\omega)\| = \|-\Delta T(\cos\omega\,, \sin\omega)\| = \|\Delta T(\cos\omega\,, \sin\omega)\|$

We thus restricted ω to range from 0° to 180°.

References

Ainge, J. A., Tamosiunaite, M., Woergoetter, F., &Dudchenko, P. A. (2007). Hippocampal CA1 Place Cells Encode Intended Destination on a Maze with Multiple Choice Points. *Journal of Neuroscience*, *27*(36), 9769–9779. https://doi.org/10.1523/JNEUROSCI.2011-07.2007

Allen, G. L. (1981). A developmental perspective on the effects of "subdividing" macrospatial experience. *Journal of Experimental Psychology: Human Learning and Memory*, *7*(2), 120–132. https://doi.org/10.1037/0278-7393.7.2.120

Alvarez, P., Zola-Morgan, S., &Squire, L. R. (1994). The animal model of human amnesia: long-term memory impaired and short-term memory intact. *Proceedings of the National Academy of Sciences of the United States of America*, *91*(12), 5637–5641. Retrieved from http://www.ncbi.nlm.nih.gov/pubmed/8202540

Amaral, D., &Lavenex, P. (2007). Hippocampal neuroanatomy. In P.Anderson, R.Morris, D.Amaral, T.Bliss, &J.O'Keefe (Eds.), *The Hippocampus Book* (First Edit, p. 37). New York: Oxford University Press.

Andersen, P. (1975). Organization of Hippocampal Neurons and Their Interconnections. In *The Hippocampus* (pp. 155–175). Boston, MA: Springer US. https://doi.org/10.1007/978-1-4684-2976-3_7

Aronov, D., Nevers, R., &Tank, D. W. (2017). Mapping of a non-spatial dimension by the hippocampal-entorhinal circuit. *Nature*, *543*(7647), 719–722. https://doi.org/10.1038/nature21692

Attneave, F., B., M., &Hebb, D. O. (1950). The Organization of Behavior; A Neuropsychological Theory. *The American Journal of Psychology*. https://doi.org/10.2307/1418888

Barry, C., Hayman, R., Burgess, N., &Jeffery, K. J. (2007). Experience-dependent rescaling of entorhinal grids. *Nature Neuroscience*, *10*(6), 682–684. https://doi.org/10.1038/nn1905

Barry, C., Lever, C., Hayman, R., Hartley, T., Burton, S., O'Keefe, J., …Burgess, N. (2006). The boundary vector cell model of place cell firing and spatial memory. *Reviews in the Neurosciences*, *17*(1–2), 71–97. Retrieved from http://www.ncbi.nlm.nih.gov/pubmed/16703944

Bittner, K. C., Grienberger, C., Vaidya, S. P., Milstein, A. D., Macklin, J. J., Suh, J., …Magee, J. C. (2015). Conjunctive input processing drives feature selectivity in hippocampal CA1 neurons. *Nature Neuroscience*, *18*(8), 1133–1142. https://doi.org/10.1038/nn.4062

Brown, J. E., &Skaggs, W. E. (2002). Concordant and Discordant Coding of Spatial Location in Populations of Hippocampal CA1 Pyramidal Cells. *Journal of Neurophysiology*, *88*(4), 1605–1613. https://doi.org/10.1152/jn.2002.88.4.1605

Buckland, S. T., Davison, A. C., &Hinkley, D.V. (2006). Bootstrap Methods and Their Application.

Biometrics. https://doi.org/10.2307/3109789

Bunsey, M., &Eichenbaum, H. (1996). Conservation of hippocampal memory function in rats and humans. *Nature*, *379*(6562), 255–257. https://doi.org/10.1038/379255a0

Carpenter, F., Manson, D., Jeffery, K., Burgess, N., &Barry, C. (2015). Grid cells form a global representation of connected environments. *Current Biology*, *25*(9), 1176–1182. https://doi.org/10.1016/j.cub.2015.02.037

Cheng, K. (1986). A purely geometric module in the rat's spatial representation. *Cognition*, *23*(2), 149–178. https://doi.org/10.1016/0010-0277(86)90041-7

Clark, B. J., Harris, M. J., &Taube, J. S. (2012). Control of anterodorsal thalamic head direction cells by environmental boundaries: comparison with conflicting distal landmarks. *Hippocampus*, *22*(2), 172–187. https://doi.org/10.1002/hipo.20880

Clark, R. E., West, A. N., Zola, S. M., &Squire, L. R. (2001). Rats with lesions of the hippocampus are impaired on the delayed nonmatching-to-sample task. *Hippocampus*, *11*(2), 176–186. https://doi.org/10.1002/hipo.1035

Cohen, N. J., &Eichenbaum, H. (2008). Memory, Amnesia and the Hippocampal System. *Journal of Neurology, Neurosurgery & Psychiatry*, *58*(1), 128–128. https://doi.org/10.1136/jnnp.58.1.128-a

Corkin, S. (1984). Lasting Consequences of Bilateral Medial Temporal Lobectomy: Clinical Course and Experimental Findings in H.M. *Seminars in Neurology*, *4*(02), 249–259. https://doi.org/10.1055/s-2008-1041556

Correll, R. E., &Scoville, W. B. (1965a). Effects of medial temporal lesions on visual discrimination performance. *Journal of Comparative and Physiological Psychology*, *60*(2), 175–181. https://doi.org/10.1037/h0022290

Correll, R. E., &Scoville, W. B. (1965b). Performance on delayed match following lesions of medial temporal lobe structures. *Journal of Comparative and Physiological Psychology*, *60*(3), 360–367. https://doi.org/10.1037/h0022549

Cressant, A., Muller, R. U., &Poucet, B. (1997). Failure of centrally placed objects to control the firing fields of hippocampal place cells. *The Journal of Neuroscience : The Official Journal of the Society for Neuroscience*, *17*(7), 2531–2542. Retrieved from http://www.ncbi.nlm.nih.gov/pubmed/9065513

Derdikman, D., Whitlock, J. R., Tsao, A., Fyhn, M., Hafting, T., Moser, M. B., &Moser, E. I. (2009). Fragmentation of grid cell maps in a multicompartment environment. *Nature Neuroscience*, *12*(10), 1325–1332. https://doi.org/10.1038/nn.2396

Doeller, C. F., &Burgess, N. (2008). Distinct error-correcting and incidental learning of location relative to landmarks and boundaries. *Proceedings of the National Academy of Sciences*, *105*(15), 5909–5914. https://doi.org/10.1073/pnas.0711433105

DuBrow, S., &Davachi, L. (2013). The influence of context boundaries on memory for the sequential order of events. *Journal of Experimental Psychology: General*, *142*(4), 1277–1286.

https://doi.org/10.1037/a0034024

Dudchenko, P. A., &Zinyuk, L. E. (2005). The formation of cognitive maps of adjacent environments: Evidence from the head direction cell system. *Behavioral Neuroscience*, *119*(6), 1511–1523. https://doi.org/10.1037/0735-7044.119.6.1511

Ekstrom, A. D., Kahana, M. J., Caplan, J. B., Fields, T. A., Isham, E. A., Newman, E. L., &Fried, I. (2003). Cellular networks underlying human spatial navigation. *Nature*, *425*(6954), 184–188. https://doi.org/10.1038/nature01964

Ezzyat, Y., &Davachi, L. (2014). Similarity Breeds Proximity: Pattern Similarity within and across Contexts Is Related to Later Mnemonic Judgments of Temporal Proximity. *Neuron*, *81*(5), 1179–1189. https://doi.org/10.1016/j.neuron.2014.01.042

Felleman, D. J., &VanEssen, D. C. (1991). Distributed hierarchical processing in the primate cerebral cortex. *Cerebral Cortex*, *1*(1), 1–47. https://doi.org/10.1093/cercor/1.1.1

Ferrara, K., &Park, S. (2016). Neural representation of scene boundaries. *Neuropsychologia*, *89*, 180–190. https://doi.org/10.1016/j.neuropsychologia.2016.05.012

Foster, D. J., &Wilson, M. A. (2007). Hippocampal theta sequences. *Hippocampus*, *17*(11), 1093–1099. https://doi.org/10.1002/hipo.20345

Fuhs, M. C., VanRhoads, S. R., Casale, A. E., McNaughton, B., &Touretzky, D. S. (2005). Influence of Path Integration Versus Environmental Orientation on Place Cell Remapping Between Visually Identical Environments. *Journal of Neurophysiology*, *94*(4), 2603–2616. https://doi.org/10.1152/jn.00132.2005

Gabrieli, J. D., Milberg, W., Keane, M. M., &Corkin, S. (1990). Intact priming of patterns despite impaired memory. *Neuropsychologia*, *28*(5), 417–427. Retrieved from http://www.ncbi.nlm.nih.gov/pubmed/2377287

Gaffan, D. (1972). Loss of recognition memory in rats with lesions of the fornix. *Neuropsychologia*, *10*(3), 327–341. Retrieved from http://www.ncbi.nlm.nih.gov/pubmed/4628086

Gaffan, D. (1974). Recognition impaired and association intact in the memory of monkeys after transection of the fornix. *Journal of Comparative and Physiological Psychology*, *86*(6), 1100–1109. Retrieved from http://www.ncbi.nlm.nih.gov/pubmed/4209603

Georgopoulos, A. P., Schwartz, A. B., &Kettner, R. E. (1986). Neuronal population coding of movement direction. *Science (New York, N.Y.)*, *233*(4771), 1416–1419. Retrieved from http://www.ncbi.nlm.nih.gov/pubmed/3749885

Greenauer, N., &Waller, D. (2010). Micro- and Macroreference Frames: Specifying the Relations Between Spatial Categories in Memory. *Journal of Experimental Psychology: Learning Memory and Cognition*, *36*(4), 938–957. https://doi.org/10.1037/a0019647

Grieves, R. M., Duvelle, É., Wood, E. R., &Dudchenko, P. A. (2017). Field repetition and local mapping in the hippocampus and the medial entorhinal cortex. *Journal of Neurophysiology*, *118*(4), 2378–2388. https://doi.org/10.1152/jn.00933.2016

Grieves, R. M., Jenkins, B. W., Harland, B. C., Wood, E. R., &Dudchenko, P. A. (2016). Place field

repetition and spatial learning in a multicompartment environment. *Hippocampus*, *26*(1), 118–134. https://doi.org/10.1002/hipo.22496

Grieves, R. M., Wood, E. R., &Dudchenko, P. A. (2016). Place cells on a maze encode routes rather than destinations. *ELife*, *5*(JUNE2016), 1–24. https://doi.org/10.7554/eLife.15986

Gupta, A. S., van derMeer, M. A. A., Touretzky, D. S., &Redish, A. D. (2012). Segmentation of spatial experience by hippocampal theta sequences. *Nature Neuroscience*, *15*(7), 1032–1039. https://doi.org/10.1038/nn.3138

Hafting, T., Fyhn, M., Molden, S., Moser, M.-B., &Moser, E. I. (2005). Microstructure of a spatial map in the entorhinal cortex. *Nature*, *436*(7052), 801–806. https://doi.org/10.1038/nature03721

Han, X., &Becker, S. (2014). One spatial map or many? Spatial coding of connected environments. *Journal of Experimental Psychology: Learning Memory and Cognition*, *40*(2), 511–531. https://doi.org/10.1037/a0035259

Hartley, T., Burgess, N., Lever, C., Cacucci, F., &O'Keefe, J. (2000). Modeling place fields in terms of the cortical inputs to the hippocampus. *Hippocampus*, *10*(4), 369–379. https://doi.org/10.1002/1098-1063(2000)10:4<369::AID-HIPO3>3.0.CO;2-0

Hartley, T., Lever, C., Burgess, N., &O'Keefe, J. (2014). Space in the brain: how the hippocampal formation supports spatial cognition. *Philosophical Transactions of the Royal Society of London. Series B, Biological Sciences*, *369*(1635), 20120510. https://doi.org/10.1098/rstb.2012.0510

Hartley, T., Trinkler, I., &Burgess, N. (2004). Geometric determinants of human spatial memory. *Cognition*, *94*(1), 39–75. https://doi.org/10.1016/j.cognition.2003.12.001

Hermer, L., &Spelke, E. S. (1994). A geometric process for spatial reorientation in young children. *Nature*, *370*(6484), 57–59. https://doi.org/10.1038/370057a0

Hetherington, P. A., &Shapiro, M. L. (1997). Hippocampal place fields are altered by the removal of single visual cues in a distance-dependent manner. *Behavioral Neuroscience*, *111*(1), 20–34. https://doi.org/10.1037/0735-7044.111.1.20

Hirtle, J; Jonides, J. C. (1985). Evidence of hierarchcies in cognitive maps. *Memory and Cognition*, *13*(3), 208–217. https://doi.org/10.3758/BF03197683

Hollup, S. a, Molden, S., Donnett, J. G., Moser, M. B., &Moser, E. I. (2001). Accumulation of hippocampal place fields at the goal location in an annular watermaze task. *The Journal of Neuroscience*, *21*(5), 1635–1644. https://doi.org/21/5/1635 [pii]

Horner, A. J., Bisby, J. A., Wang, A., Bogus, K., &Burgess, N. (2016). The role of spatial boundaries in shaping long-term event representations. *Cognition*, *154*, 151–164. https://doi.org/10.1016/j.cognition.2016.05.013

Horner, A. J., Bisby, J. A., Zotow, E., Bush, D., &Burgess, N. (2016). Grid-like Processing of Imagined Navigation. *Current Biology : CB*, *26*(6), 842–847. https://doi.org/10.1016/j.cub.2016.01.042

Jacobs, J., Weidemann, C. T., Miller, J. F., Solway, A., Burke, J. F., Wei, X.-X., …Kahana, M. J. (2013). Direct recordings of grid-like neuronal activity in human spatial navigation. *Nature*

Neuroscience, *16*(9), 1188–1190. https://doi.org/10.1038/nn.3466

Julian, J. B., Keinath, A. T., Muzzio, I. A., &Epstein, R. A. (2015). Place recognition and heading retrieval are mediated by dissociable cognitive systems in mice. *Proceedings of the National Academy of Sciences*, *112*(20), 6503–6508. https://doi.org/10.1073/pnas.1424194112

Keinath, A. T., Epstein, R. A., &Balasubramanian, V. (2018). Environmental deformations dynamically shift the grid cell spatial metric. *ELife*, *7*. https://doi.org/10.7554/eLife.38169

Keinath, A. T., Julian, J. B., Epstein, R. A., &Muzzio, I. A. (2017). Environmental Geometry Aligns the Hippocampal Map during Spatial Reorientation. *Current Biology*, *27*(3), 309–317. https://doi.org/10.1016/j.cub.2016.11.046

Kimble, D. P. (1963). The effects of bilateral hippocampal lesions in rats. *Journal of Comparative and Physiological Psychology*, *56*(2), 273–283. https://doi.org/10.1037/h0048903

Kneisler, T. B., &Dingledine, R. (1995). Synaptic input from CA3 pyramidal cells to dentate basket cells in rat hippocampus. *The Journal of Physiology*, *487*(1), 125–146. Retrieved from http://www.ncbi.nlm.nih.gov/pubmed/7473243

Knierim, J. J. (2002). Dynamic interactions between local surface cues, distal landmarks, and intrinsic circuitry in hippocampal place cells. *The Journal of Neuroscience : The Official Journal of the Society for Neuroscience*, *22*(14), 6254–6264. https://doi.org/20026608

Knierim, J. J., &Hamilton, D. A. (2011). Framing Spatial Cognition: Neural Representations of Proximal and Distal Frames of Reference and Their Roles in Navigation. *Physiological Reviews*, *91*(4), 1245–1279. https://doi.org/10.1152/physrev.00021.2010

Knierim, J. J., Kudrimoti, H. S., &McNaughton, B. L. (1995). Place cells, head direction cells, and the learning of landmark stability. *The Journal of Neuroscience : The Official Journal of the Society for Neuroscience*, *15*(3 Pt 1), 1648–1659. Retrieved from http://www.ncbi.nlm.nih.gov/pubmed/7891125

Knierim, J. J., Kudrimoti, H. S., &McNaughton, B. L. (1998). Interactions Between Idiothetic Cues and External Landmarks in the Control of Place Cells and Head Direction Cells. *Journal of Neurophysiology*, *80*(1), 425–446. https://doi.org/10.1152/jn.1998.80.1.425

Knierim, J. J., &Rao, G. (2003). Distal landmarks and hippocampal place cells: effects of relative translation versus rotation. *Hippocampus*, *13*(5), 604–617. https://doi.org/10.1002/hipo.10092

Knight, R., Hayman, R., Lin Ginzberg, L., &Jeffery, K. (2011). Geometric cues influence head direction cells only weakly in nondisoriented rats. *The Journal of Neuroscience : The Official Journal of the Society for Neuroscience*, *31*(44), 15681–15692. https://doi.org/10.1523/JNEUROSCI.2257-11.2011

Kobayashi, T., Nishijo, H., Fukuda, M., Bures, J., &Ono, T. (1997). Task-Dependent Representations in Rat Hippocampal Place Neurons. *Journal of Neurophysiology*, *78*(2), 597–613. https://doi.org/10.1152/jn.1997.78.2.597

Kosslyn, S. M., Pick, H. L., Fariello, G. R., &Fariello, G. R. (1974). Cognitive Maps in Children and Men. *Child Development*, *45*(3), 707. https://doi.org/10.2307/1127837

Krupic, J., Bauza, M., Burton, S., Barry, C., &O'Keefe, J. (2015). Grid cell symmetry is shaped by environmental geometry. *Nature*, *518*(7538), 232–235. https://doi.org/10.1038/nature14153

Krupic, J., Bauza, M., Burton, S., &O'Keefe, J. (2018). Local transformations of the hippocampal cognitive map. *Science*, *359*(6380), 1143–1146. https://doi.org/10.1126/science.aao4960

Kubie, J. L., &Ranck J.B., J. (1983). Sensory-behavioral correlates in individual hippocampal neurons in three situations: space and context. In W.Seifert (Ed.), *Neurobiology of the Hippocampus* (pp. 433–447). London: Academic Press.

Kuwahara, M., Hachimura, K., Eiho, S., &Kinoshita, M. (1976). Processing of RI-Angiocardiographic Images. In *Digital Processing of Biomedical Images* (pp. 187–202). Boston, MA: Springer US. https://doi.org/10.1007/978-1-4684-0769-3_13

Lashley, K. S. (1950). In search of the engram. In *Symposia of the society for experimental biology*. https://doi.org/10.1097/00008877-199204001-00015

Lawrence, Z., &Peterson, D. (2016). Mentally walking through doorways causes forgetting: The location updating effect and imagination. *Memory*, *24*(1), 12–20. https://doi.org/10.1080/09658211.2014.980429

Learmonth, A. E., Nadel, L., &Newcombe, N. S. (2002). Children's Use of Landmarks: Implications for Modularity Theory. *Psychological Science*, *13*(4), 337–341. https://doi.org/10.1111/j.0956-7976.2002.00461.x

Learmonth, A. E., Newcombe, N. S., &Huttenlocher, J. (2001). Toddlers' Use of Metric Information and Landmarks to Reorient. *Journal of Experimental Child Psychology*, *80*(3), 225–244. https://doi.org/10.1006/jecp.2001.2635

Lee, H., Wang, C., Deshmukh, S. S., &Knierim, J. J. (2015). Neural Population Evidence of Functional Heterogeneity along the CA3 Transverse Axis: Pattern Completion versus Pattern Separation. *Neuron*, *87*(5), 1093–1105. https://doi.org/10.1016/j.neuron.2015.07.012

Lee, I., &Knierim, J. J. (2007). The relationship between the field-shifting phenomenon and representational coherence of place cells in CA1 and CA3 in a cue-altered environment. *Learning & Memory (Cold Spring Harbor, N.Y.)*, *14*(11), 807–815. https://doi.org/10.1101/lm.706207

Lee, I., Rao, G., &Knierim, J. J. (2004). A Double Dissociation between Hippocampal Subfields. *Neuron*, *42*(5), 803–815. https://doi.org/10.1016/j.neuron.2004.05.010

Lee, I., Yoganarasimha, D., Rao, G., &Knierim, J. J. (2004). Comparison of population coherence of place cells in hippocampal subfields CA1 and CA3. *Nature*, *430*(6998), 456–459. https://doi.org/10.1038/nature02739

Lee, S. A., Miller, J. F., Watrous, A. J., Sperling, M. R., Sharan, A., Worrell, G. A., …Jacobs, J. (2018). Electrophysiological Signatures of Spatial Boundaries in the Human Subiculum. *The Journal of Neuroscience : The Official Journal of the Society for Neuroscience*, *38*(13), 3265–3272. https://doi.org/10.1523/JNEUROSCI.3216-17.2018

Lee, S. A., &Spelke, E. S. (2011). Young children reorient by computing layout geometry, not by

matching images of the environment. *Psychonomic Bulletin & Review*, *18*(1), 192–198. https://doi.org/10.3758/s13423-010-0035-z

Lee, S. A., Spelke, E. S., &Vallortigara, G. (2012). Chicks, like children, spontaneously reorient by three-dimensional environmental geometry, not by image matching. *Biology Letters*, *8*(4), 492–494. https://doi.org/10.1098/rsbl.2012.0067

Lee, S. A., Vallortigara, G., Flore, M., Spelke, E. S., &Sovrano, V. A. (2013). Navigation by environmental geometry: the use of zebrafish as a model. *Journal of Experimental Biology*, *216*(19), 3693–3699. https://doi.org/10.1242/jeb.088625

Lever, C., Burton, S., Jeewajee, A., O'Keefe, J., &Burgess, N. (2009). Boundary vector cells in the subiculum of the hippocampal formation. *The Journal of Neuroscience : The Official Journal of the Society for Neuroscience*, *29*(31), 9771–9777. https://doi.org/10.1523/JNEUROSCI.1319-09.2009

Lorente de No, R. (1934). Studies on the structure of the cerebral cortex II. Continuation of the study of the Ammonic system. *J Psychol Neurol*, *46*, 113–177.

MacDonald, C. J., Lepage, K. Q., Eden, U. T., &Eichenbaum, H. (2011). Hippocampal "time cells" bridge the gap in memory for discontiguous events. *Neuron*, *71*(4), 737–749. https://doi.org/10.1016/j.neuron.2011.07.012

Malamut, B. L., Saunders, R. C., &Mishkin, M. (1984). Monkeys with combined amygdalo-hippocampal lesions succeed in object discrimination learning despite 24-hour intertrial intervals. *Behavioral Neuroscience*, *98*(5), 759–769. https://doi.org/10.1037/0735-7044.98.5.759

Marchette, S. A., Ryan, J., &Epstein, R. A. (2017). Schematic representations of local environmental space guide goal-directed navigation. *Cognition*, *158*, 68–80. https://doi.org/10.1016/j.cognition.2016.10.005

Markus, E. J., Qin, Y. L., Leonard, B., Skaggs, W. E., McNaughton, B. L., &Barnes, C. A. (1995). Interactions between location and task affect the spatial and directional firing of hippocampal neurons. *The Journal of Neuroscience : The Official Journal of the Society for Neuroscience*, *15*(11), 7079–7094. Retrieved from http://www.ncbi.nlm.nih.gov/pubmed/7472463

McNamara, T. P. (1986). Mental representations of spatial relations. *Cognitive Psychology*, *18*(1), 87–121. https://doi.org/10.1016/0010-0285(86)90016-2

McNamara, T. P., Hardy, J. K., &Hirtle, S. C. (1989). Subjective Hierarchies in Spatial Memory. *Journal of Experimental Psychology: Learning, Memory, and Cognition*, *15*(2), 211–227. https://doi.org/10.1037/0278-7393.15.2.211

McNaughton, B. L. (1998). The neurophysiology of reminiscence. In *Neurobiology of Learning and Memory* (Vol. 70, pp. 252–267). Academic Press. https://doi.org/10.1006/nlme.1998.3851

Milner, B. (1962). Les troubles de la mémoire accompagnant des lésions hippocampiques bilatérales. In *Physiologie de l'hippocampe* (pp. 257–272).

Milner, B., Corkin, S., &Teuber, H.-L. (1968). Further analysis of the hippocampal amnesic

syndrome: 14-year follow-up study of H.M. *Neuropsychologia*, *6*(3), 215–234. https://doi.org/10.1016/0028-3932(68)90021-3

Mishkin, M., &Delacour, J. (1975). An analysis of short-term visual memory in the monkey. *Journal of Experimental Psychology. Animal Behavior Processes*, *1*(4), 326–334. Retrieved from http://www.ncbi.nlm.nih.gov/pubmed/811754

Monaco, J. D., Rao, G., Roth, E. D., &Knierim, J. J. (2014). Attentive scanning behavior drives one-trial potentiation of hippocampal place fields. *Nature Neuroscience*, *17*(5), 725–731. https://doi.org/10.1038/nn.3687

Moser, E. I., Kropff, E., &Moser, M.-B. (2008). Place Cells, Grid Cells, and the Brain's Spatial Representation System. *Annual Review of Neuroscience*, *31*(1), 69–89. https://doi.org/10.1146/annurev.neuro.31.061307.090723

Mountcastle, V. B. (1997). The columnar organization of the neocortex. *Brain : A Journal of Neurology*, *120 (Pt 4)*, 701–722. Retrieved from http://www.ncbi.nlm.nih.gov/pubmed/9153131

Muller, R. U., &Kubie, J. L. (1987). The effects of changes in the environment on the spatial firing of hippocampal complex-spike cells. *Journal of Neuroscience*, *7*(7), 1951–1968. https://doi.org/10.1523/JNEUROSCI.07-07-01951.1987

Neunuebel, J. P., &Knierim, J. J. (2014). CA3 Retrieves Coherent Representations from Degraded Input: Direct Evidence for CA3 Pattern Completion and Dentate Gyrus Pattern Separation. *Neuron*, *81*(2), 416–427. https://doi.org/10.1016/j.neuron.2013.11.017

Neunuebel, J. P., Yoganarasimha, D., Rao, G., &Knierim, J. J. (2013). Conflicts between Local and Global Spatial Frameworks Dissociate Neural Representations of the Lateral and Medial Entorhinal Cortex. *Journal of Neuroscience*, *33*(22), 9246–9258. https://doi.org/10.1523/JNEUROSCI.0946-13.2013

Newcombe, N., &Liben, L. S. (1982). Barrier effects in the cognitive maps of children and adults. *Journal of Experimental Child Psychology*, *34*(1), 46–58. https://doi.org/10.1016/0022-0965(82)90030-3

Nitz, D. A. (2011). Path shape impacts the extent of CA1 pattern recurrence both within and across environments. *Journal of Neurophysiology*, *105*(4), 1815–1824. https://doi.org/10.1152/jn.00573.2010

O'Keefe, J. (1976). Place units in the hippocampus of the freely moving rat. *Experimental Neurology*, *51*(1), 78–109. https://doi.org/10.1016/0014-4886(76)90055-8

O'Keefe, J., &Burgess, N. (1996). Geometric determinants of the place fields of hippocampal neurons. *Nature*, *381*(6581), 425–428. https://doi.org/10.1038/381425a0

O'Keefe, J., &Conway, D. H. (1978). Hippocampal place units in the freely moving rat: why they fire where they fire. *Experimental Brain Research*, *31*(4), 573–590. Retrieved from http://www.ncbi.nlm.nih.gov/pubmed/658182

O'Keefe, J., &Dostrovsky, J. (1971). The hippocampus as a spatial map. Preliminary evidence from

unit activity in the freely-moving rat. *Brain Research*, *34*(1), 171–175. https://doi.org/10.1016/0006-8993(71)90358-1

O'Keefe, J., &Nadel, L. (1978). *The hippocampus as a cognitive map*. Oxford University Press.

Olypher, A. ., Lánský, P., Muller, R. ., &Fenton, A. . (2003). Quantifying location-specific information in the discharge of rat hippocampal place cells. *Journal of Neuroscience Methods*, *127*(2), 123–135. https://doi.org/10.1016/S0165-0270(03)00123-7

Orbach, J., Milner, B., &Rasmussen, T. (1960). Learning and Retention in Monkeys After Amygdala-Hippocampus Resection. *Archives of Neurology*, *3*(3), 230–251. https://doi.org/10.1001/archneur.1960.00450030008002

Overman, W. H., Ormsby, G., &Mishkin, M. (1990). Picture recognition vs. picture discrimination learning in monkeys with medial temporal removals. *Experimental Brain Research*, *79*(1), 18–24. Retrieved from http://www.ncbi.nlm.nih.gov/pubmed/2311695

Pecchia, T., &Vallortigara, G. (2012). Spatial reorientation by geometry with freestanding objects and extended surfaces: A unifying view. *Proceedings of the Royal Society B: Biological Sciences*, *279*(1736), 2228–2236. https://doi.org/10.1098/rspb.2011.2522

Postle, B. R., &Corkin, S. (1998). Impaired word-stem completion priming but intact perceptual identification priming with novel words: evidence from the amnesic patient H.M. *Neuropsychologia*, *36*(5), 421–440. Retrieved from http://www.ncbi.nlm.nih.gov/pubmed/9699950

Radvansky, G. A., &Copeland, D. E. (2006). Walking through doorways causes forgetting: Situation models and experienced space. *Memory & Cognition*, *34*(5), 1150–1156. https://doi.org/10.3758/BF03193261

Radvansky, G. A., Krawietz, S. A., &Tamplin, A. K. (2011). Walking through doorways causes forgetting: Further explorations. *Quarterly Journal of Experimental Psychology*, *64*(8), 1632–1645. https://doi.org/10.1080/17470218.2011.571267

Radvansky, G. A., Tamplin, A. K., &Krawietz, S. A. (2010). Walking through doorways causes forgetting: Environmental integration. *Psychonomic Bulletin & Review*, *17*(6), 900–904. https://doi.org/10.3758/PBR.17.6.900

Ringo, J. L. (1991). Memory decays at the same rate in macaques with and without brain lesions when expressed in d′ or arcsine terms. *Behavioural Brain Research*, *42*(2), 123–134. https://doi.org/10.1016/S0166-4328(05)80003-8

Rudy, J. W., &Sutherland, R. J. (1995). Configural association theory and the hippocampal formation: An appraisal and reconfiguration. *Hippocampus*, *5*(5), 375–389. https://doi.org/10.1002/hipo.450050502

Sargolini, F., Fyhn, M., Hafting, T., McNaughton, B. L., Witter, M. P., Moser, M.-B., &Moser, E. I. (2006). Conjunctive representation of position, direction, and velocity in entorhinal cortex. *Science (New York, N.Y.)*, *312*(5774), 758–762. https://doi.org/10.1126/science.1125572

Savelli, F., Luck, J., &Knierim, J. J. (2017). Framing of grid cells within and beyond navigation

boundaries. *ELife*, *6*. https://doi.org/10.7554/eLife.21354

Savelli, F., Yoganarasimha, D., &Knierim, J. J. (2008). Influence of boundary removal on the spatial representations of the medial entorhinal cortex. *Hippocampus*, *18*(12), 1270–1282. https://doi.org/10.1002/hipo.20511

Scoville, W. B. (1954). The Limbic Lobe in Man. *Journal of Neurosurgery*, *11*(1), 64–66. https://doi.org/10.3171/jns.1954.11.1.0064

Scoville, W. B., &Milner, B. (1957). Loss of recent memory after bilateral hippocampal lesions. *Journal of Neurology, Neurosurgery, and Psychiatry*, *20*(1), 11–21. Retrieved from http://www.ncbi.nlm.nih.gov/pubmed/13406589

Shapiro, M. L., Tanila, H., &Eichenbaum, H. (1997). Cues that hippocampal place cells encode: dynamic and hierarchical representation of local and distal stimuli. *Hippocampus*, *7*(6), 624–642. https://doi.org/10.1002/(SICI)1098-1063(1997)7:6<624::AID-HIPO5>3.0.CO;2-E

Siegel, J. J., Neunuebel, J. P., &Knierim, J. J. (2008). Dominance of the proximal coordinate frame in determining the locations of hippocampal place cell activity during navigation. *Journal of Neurophysiology*, *99*(1), 60–76. https://doi.org/10.1152/jn.00731.2007

Singer, A. C., Karlsson, M. P., Nathe, A. R., Carr, M. F., &Frank, L. M. (2010). Experience-Dependent Development of Coordinated Hippocampal Spatial Activity Representing the Similarity of Related Locations. *Journal of Neuroscience*, *30*(35), 11586–11604. https://doi.org/10.1523/JNEUROSCI.0926-10.2010

Skaggs, W. E., &Mcnaughton, B. L. (1998). Spatial Firing Properties of Hippocampal CA1 Populations in an Environment Containing Two Visually Identical Regions. *The Journal of Neuroscience*, *18*(20), 8455–8466. https://doi.org/10.1523/JNEUROSCI.18-20-08455.1998

Skaggs, W. E., McNaughton, B. L., Gothard, K. M., &Markus, E. J. (1992). An Information-Theoretic Approach to Deciphering the Hippocampal Code. *Advances in Neural Information Processing Systems*, *5*, 1030–1037. https://doi.org/10.1109/PROC.1977.10559

Solstad, T., Boccara, C. N., Kropff, E., Moser, M.-B., &Moser, E. I. (2008). Representation of geometric borders in the entorhinal cortex. *Science (New York, N.Y.)*, *322*(5909), 1865–1868. https://doi.org/10.1126/science.1166466

Solstad, T., Moser, E. I., &Einevoll, G. T. (2006). From grid cells to place cells: A mathematical model. *Hippocampus*, *16*(12), 1026–1031. https://doi.org/10.1002/hipo.20244

Spiers, H. J., Hayman, R. M. A., Jovalekic, A., Marozzi, E., &Jeffery, K. J. (2015). Place field repetition and purely local remapping in a multicompartment environment. *Cerebral Cortex*, *25*(1), 10–25. https://doi.org/10.1093/cercor/bht198

Squire, L. R. (2004). Memory systems of the brain: A brief history and current perspective. *Neurobiology of Learning and Memory*, *82*(3), 171–177. https://doi.org/10.1016/j.nlm.2004.06.005

Striedter, G. F. (1997). The Telencephalon of Tetrapods in Evolution; pp. 179–194. *Brain, Behavior and Evolution*, *49*(4), 179–194. https://doi.org/10.1159/000112991

Tanila, H., Shapiro, M. L., &Eichenbaum, H. (1997). Discordance of spatial representation in ensembles of hippocampal place cells. *Hippocampus*, *7*(6), 613–623. https://doi.org/10.1002/(SICI)1098-1063(1997)7:6<613::AID-HIPO4>3.0.CO;2-F

Taube, J. S., Muller, R. U., &Ranck, J. B. (1990). Head-direction cells recorded from the postsubiculum in freely moving rats. I. Description and quantitative analysis. *The Journal of Neuroscience : The Official Journal of the Society for Neuroscience*, *10*(2), 420–435. https://doi.org/10.1523/JNEUROSCI.10-02-00420.1990

Teng, E., Stefanacci, L., Squire, L. R., &Zola, S. M. (2000). Contrasting effects on discrimination learning after hippocampal lesions and conjoint hippocampal-caudate lesions in monkeys. *The Journal of Neuroscience : The Official Journal of the Society for Neuroscience*, *20*(10), 3853–3863. https://doi.org/10.1523/JNEUROSCI.20-10-03853.2000

Terada, S., Sakurai, Y., Nakahara, H., &Fujisawa, S. (2017). Temporal and Rate Coding for Discrete Event Sequences in the Hippocampus. *Neuron*, *94*(6), 1248–1262.e4. https://doi.org/10.1016/j.neuron.2017.05.024

Tolman, E. C. (1948). Cognitive maps in rats and men. *Psychological Review*, *55*(4), 189–208. https://doi.org/10.1037/h0061626

Tosches, M. A., Yamawaki, T. M., Naumann, R. K., Jacobi, A. A., Tushev, G., &Laurent, G. (2018). Evolution of pallium, hippocampus, and cortical cell types revealed by single-cell transcriptomics in reptiles. *Science (New York, N.Y.)*, *360*(6391), 881–888. https://doi.org/10.1126/science.aar4237

Tukey, J. W. (John W. (1977). *Exploratory data analysis*. Addison-Wesley Pub. Co.

Yoganarasimha, D., Yu, X., &Knierim, J. J. (2006). Head Direction Cell Representations Maintain Internal Coherence during Conflicting Proximal and Distal Cue Rotations: Comparison with Hippocampal Place Cells. *Journal of Neuroscience*, *26*(2), 622–631. https://doi.org/10.1523/JNEUROSCI.3885-05.2006

Young, B. J., Fox, G. D., &Eichenbaum, H. (1994). Correlates of hippocampal complex-spike cell activity in rats performing a nonspatial radial maze task. *The Journal of Neuroscience : The Official Journal of the Society for Neuroscience*, *14*(11 Pt 1), 6553–6563. https://doi.org/10.1523/JNEUROSCI.14-11-06553.1994

Yu, X., Yoganarasimha, D., &Knierim, J. J. (2006). Backward Shift of Head Direction Tuning Curves of the Anterior Thalamus: Comparison with CA1 Place Fields. *Neuron*, *52*(4), 717–729. https://doi.org/10.1016/j.neuron.2006.10.003

Zola-Morgan, S., Squire, L. R., &Amaral, D. G. (1989). Lesions of the hippocampal formation but not lesions of the fornix or the mammillary nuclei produce long-lasting memory impairment in monkeys. *The Journal of Neuroscience : The Official Journal of the Society for Neuroscience*, *9*(3), 898–913. Retrieved from http://www.ncbi.nlm.nih.gov/pubmed/2494309

CURRICULUM VITAE

The Johns Hopkins University School of Medicine

Chia-Hsuan Wang May 30th, 2019

Educational History:

Ph.D. expected	2019	Program in Neuroscience Mentor: James J. Knierim, Ph.D.	Johns Hopkins School of Medicine
B.S.	2010	Department of Computer Science and Information Engineering	National Taiwan University
		Department of Biochemical Science and Technology	National Taiwan University

Other Professional Experience:

Research Rotation	2011-2012	Lab of Charles E. Connor	Johns Hopkins School of Medicine
Research Rotation	2012-2012	Lab of James J. Knierim	Johns Hopkins School of Medicine
Research Rotation	2011-2011	Lab of Ernst Niebur	Johns Hopkins School of Medicine
Post-bac research	2010-2011	Lab of Visual Neurophysiology and Neuroengineering PI: Chou-Po Hung	National Yang Ming University
Undergraduate and post-bac Research	2009-2011	Lab of Computational Learning PI: Husan-Tien Lin	National Taiwan University
Undergraduate and post-bac Research	2008-2011	Lab of Fu-Shan Jaw	National Taiwan University
Undergraduate Research	2007-2007	Lab of Che-Kun James Shen	Academia Sinica

Conference Papers and Abstracts:

Wang, C.; Rao, G. and Knierim, J. J. (2017) Surface texture boundaries alter firing rates of CA1 place cells in 2-dimensional environments. *Society for Neuroscience (SfN) Conference*, Washington, DC, 2017.

Wang, C.; Monaco, J. D.; Rao, G.; Deshmukh, S. S. and Knierim, J. J. (2016) CA1 place fields respect local surface texture boundaries. *Society for Neuroscience (SfN) Conference*, San Diego, 2016.

Wang, C.; Rao, G.; Monaco, J. D.; Deshmukh, S. S. and Knierim, J. J. (2014) Potentiation of place fields along the CA1 transverse axis by investigatory head-scanning behavior. *Society for Neuroscience (SfN) Conference*, Washington, DC, 2014.

Kao, Y.; **Wang, C.** and Jaw, F. (2008) Utilizing Cross Correlation Coefficient for Estimation the Detection

Range of Michigan Probe, poster session, *The 10th International Conference on Cognitive Neuroscience*, Bodrum, Turkey, 2008.

Lo, H.; Chang, K.; Chen, S.; Chiang, T.; Ferng, C.; Hsieh, C.; Ko, Y.; Kuo, T.; Lai, H.; Lin, K.; **Wang, C.**; Yu, H.; Lin, C.; Lin, H.; Lin, S. (2009) An Ensemble of Three Classifiers for KDD Cup 2009: Expanded Linear Model, Heterogeneous Boosting, and Selective Naıve Bayes", *The 15th ACM SIGKDD Conference on Knowledge Discovery and Data Mining*, Paris, France, 2009.